THESIS

DO MESENCHYMAL STROMAL CELLS ABROGRATE THE IMMUNE RESPONSE IN MASSIVE CORTICAL ALLOGRAFT RECIPIENTS?

Submitted by

Kaitlyn Louise McNamara

Department of Clinical Sciences

In partial fulfillment of the requirements

For the Degree of Master of Science

Colorado State University

Fort Collins, Colorado

Summer 2015

Master's Committee:

Advisor: Nicole Ehrhart
Co-Advisor: Steven Dow

Seth Donahue
Colleen Duncan
Ross Palmer
Rodney Page

ABSTRACT

DO MESENCHYMAL STROMAL CELLS ABROGATE THE IMMUNE RESPONSE IN MASSIVE CORTICAL ALLOGRAFT RECIPIENTS?

OBJECTIVE: To evaluate the humoral and cellular immune response against bone associated antigens when delivered in a vaccine, and to evaluate the immunomodulation on the aforementioned immune response with the addition of adipose-derived mesenchymal stromal cells (AD-MSCs).

ANIMALS: 68 C57BL/6 mice

PROCEDURES: Femur fragments harvested from Balb/C or C57BL/6 mice were resuspended in PBS and cationic liposomal DNA complexes (CLDC) to create an allograft or autograft vaccine, respectively. A positive control vaccine was created utilizing bovine alkaline phosphatase (ALP) resuspended in PBS and CLDC. Twenty C57BL/6 mice were divided into four treatment groups: non-vaccinated (n=5), ALP vaccine recipients (n=5), allograft bone vaccine recipients (n=5), or autograft bone vaccine recipients (n=5). Forty-eight C57BL/6 mice were divided into the same 4 vaccine treatment groups (n=16), and received either intravenous AD-MSCs (n=8) or a subcutaneous injection of AD-MSCs (n=8). All mice received an initial vaccine on Day 1 and a booster vaccine on Day 7, followed by euthanasia on Day 21. Blood was collected on Day 1 and Day 7 just prior to vaccination, and on Day 21 just prior to euthanasia. Serum was subjected to an antibody detection ELISA to

evaluate the humoral response. Spleens were collected and flow cytometry was used to evaluate T cell proliferation as an indicator of the cellular immune response.

RESULTS: The bone vaccines did no elicit a detectable humoral immune response to the total bone antigen vaccine used in this model. The addition of AD-MSCs had no effect on the lack of a detectable humoral immune response. The T cell response towards a bone antigen was dampened in mice previously vaccinated with a bone vaccine. This effect was most pronounced when looking at the T cell response towards an allograft bone antigen in mice previously vaccinated with an allograft bone vaccine, particularly with the addition of AD-MSCs.

CONCLUSIONS AND CLINICAL RELEVANCE: The bone vaccine model used in this study allowed evaluation of the humoral and cellular immune response towards bone associated antigens. The model suggests that recipients of an allograft bone vaccine will dampen the T cell proliferation seen upon second exposure to the bone antigens. This model could be used in future vaccine studies looking at the effect of vaccinating mice with a bone vaccine prior to undergoing a limb-salvage procedure. If efficacious, the bone vaccine model may provide a new treatment option for decreasing the risk of transplant rejection following massive limb reconstruction.

DEDICATION

I want to first and foremost dedicate this work to my family. I would never have been able to make it through these last couple years without the love and support of my dad, Roger, my mom, Cindy, and my brother, Collin. Of course, a big thank you to my four-legged partner in crime, Kayenne, for keeping me grounded and reminding me why I do this work.

Thank you so much to my advisor, Dr. Nicole Ehrhart, for your mentorship and guidance. The opportunities and experiences you have given me are invaluable and have been instrumental in guiding my career as a scientist. Thank you to my co-advisor, Dr. Steve Dow, for your expertise and for furthering my understanding of the wonderful world of immunology. Thank you to my committee, Drs. Colleen Duncan, Seth Donahue, Rod Page, and Ross Palmer. Thank you to the members of the Laboratory of Comparative Musculoskeletal Oncology and Traumatology – Ruth, Morgan, Megan, Lily, and Callie.

I have truly enjoyed my time as a Master's student in the Flint Animal Cancer Center at Colorado State University and I look forward to many more experiences the brilliant people that make working here a truly wonderful experience.

TABLE OF CONTENTS

ABSTRACT……ii
DEDICATION……iv
1.CHAPTER 1……1
2. CHAPTER 2……19
3. CHAPTER 3……38
4. CHAPTER 4……51
5. REFERENCES……55
6. APPENDICES……59

CHAPTER 1

INTRODUCTION

Osteosarcoma

Osteosarcoma is the most common primary malignant bone tumor in both human and canine patients, making up 85% of all skeletal malignancies (20). It has a bimodal age distribution with an average onset occurring during the teenage years or over 60 in humans, and a median age of 7 in canines (14, 20). The majority of osteosarcoma tumors arise in the appendicular skeleton near the metaphysis of long bones; a region characterized by abundant levels of trabecular bone and decreased levels of cortical bone, as compared to the adjacent diaphysis. The onset of osteosarcoma is associated with rapid bone turnover and increased osteoblastic activity. The 5-year survival rate for human patients with localized osteosarcoma ranges from 60-70% when treatment includes chemotherapy. The 5-year survival decreases to 20% when metastatic disease is present due to limited efficacy of current treatment protocols in controlling the progression of the disease (22). The median survival for dogs treated with both chemotherapy and surgery is nine to eleven months, with a 20% 2-year survival rate (8). Micro-metastasis is present in 90-95% of canine patients at the time of diagnosis and one-third of human patients will develop metastatic disease (2, 8). Without chemotherapy, 90% of canine patients will develop metastatic disease by 1 year, and 80% of humans will develop metastatic disease by 2 years, with the lung being the primary metastatic location for both species (20).

Current protocols for treating osteosarcoma in dogs include both palliative and curative-intent therapies.

Palliative therapies are aimed at increasing the quality of life of the patient, but have no effect on survival time. Common palliative protocols include amputation or radiation therapy, and most commonly target bone cancer pain. Radiation therapy is considered the most effective palliative treatment and is used to alleviate the osteolytic bone pain that accompanies osteosarcoma. Osteosarcoma bone pain is attributed to the high density of nociceptors, or pain receptors, present at the periosteal surface and in the medullary cavity. Chemical mediators released from tumor cells with invasive malignant osteoblast growth can stimulate the nociceptors, causing intense pain for the patient (4). Furthermore, the positive modulation of neurotrophins, a group of proteins aimed at increasing development and function of neurons, can result in nociceptor sensitization to outside stimuli. The dysregulated osteoclast activity present in primary or metastatic bone disease can induce an increase in acidity within the bone, causing the sensitized nociceptors to increase expression of acid-sensing receptors, leading to activation of the nociceptors and severe pain within the bone (7, 20). Radiation therapy is known to induce apoptosis of diseased osteoblasts and osteoclasts (20). It has been hypothesized that the inhibition of osteoclast activity by radiation and other palliative therapies such as bisphosphonates will increase the pH of the bone microenvironment, thereby decreasing the stimulation of the acid-sensing receptors on nociceptors and reducing overall bone cancer pain (4). Of the canine patients presenting with osteosarcoma, 74-96% tend to experience a median pain-free time interval of 53-130 days following a standard 2 to 4 treatment fraction protocol, with each treatment delivering 6 to 10 Grey fractions of

radiation (11, 20). While palliative therapies can be successful at managing bone cancer pain and increasing quality of life, they are not able to control progression of the metastatic disease. The delivery of chemotherapy in conjunction with radiation therapy has been shown to delay the onset of metastatic disease, but this combination does not function as a curative-intent therapy. Radiation therapy alone in canine patients yields a mean survival time of 4.1-10.4 months (11).

Curative-intent therapies target the local tumor, as well as the systemic disease in the hopes of prolonging survival time for the patient. The standard protocol for curative–intent therapy is amputation or limb salvage of the affected limb to remove the local tumor, followed by chemotherapy to target the micrometastasic disease. Surgery alone will rid the patient of the primary tumor, however is not considered a curative-intent therapy. Human patients have a survival rate of 5 to 23% at 5 years following amputation alone, and a study looking at the outcome of amputation alone in 19 canines showed a mean survival time of 218 days (10). Canine patients are able to rapidly compensate with three limbs as long as no preexisting orthopedic or neurologic conditions that could severely impact ambulation are present (20). Human patients respond well to amputation and are able to walk with the use of prosthetics. An inefficient gait and alteration of ideal mechanical and anatomical alignment due to loss of the knee joint can be seen in human patients having an above-the-knee amputation as opposed to a below-the-knee amputation, however an overall rapid compensation to limb loss is observed (9). While amputation is still a prevalent treatment for patients with osteosarcoma, limiting factors such as severe pre-existing orthopedic disease or a lack of social acceptance towards amputation requires the need for a different therapeutic procedure targeting the local tumor.

Limb-Salvage Procedure

The limb-salvage procedure was developed as an alternative to amputation, and can employ segmental bone autograft or allograft, massive endoprostheses or combinations. In canine patients, ideal candidates for the limb-salvage procedure include patients presenting with osteosarcoma that is confined to the limb and less than 50% of the bone is affected. Furthermore, an ideal candidate would also present without pathologic fracture of the bone (20). Commonly, a fresh-frozen allograft is harvested from a donor, and is cut to fit the defect during surgery. Once placed, the graft is stabilized with a dynamic compression plate. (20). Recovery after a limb-spare procedure is rapid, and good limb use can be seen within 10 days post-operatively for canine patients and 6-8 weeks for human patients. While not widely recognized, the use of an allograft is accompanied with the presence of transplantation immunity, which can be a contributing factor to allograft failure (5). While the allograft limb-salvage procedure does prevent the need for amputation, massive allograft reconstruction is accompanied with a high failure rate of 60% at 10 years for human patients and 50% at 2 years for canine patients. Furthermore, 30% of human patients and 50% of canine patients will develop complications within the first 1-3 years post surgery, including infection, local recurrence, and implant failure (9,20). Canines have an infection rate of 40-50%, despite the intra-operative use of antibiotics (20).

An autograft can be used in the limb-salvage procedure, and is obtained from the same individual undergoing the procedure. This is most commonly seen in an ulna

transposition limb salvage procedure performed in canines, in which the ipsilateral distal ulna is used to reconstruct a distal radial defect. Due to the use of autologous bone, the chance of infection and transplantation immunity is negated, and the healing period is accelerated as compared to patients receiving an allograft. However, the transposed ulna is smaller in size compared to the surrounding radius, so the risk of biomechanical failure is increased with this procedure (20).

Biologic Response to Allografts and Autografts

In order to better understand the factors contributing to massive allograft failure, Sharon Stevenson conducted a study to evaluate the recipient biologic response to allografts and autografts in canine patients (5). A successful graft will induce osteogenesis, or the formation of new bone that will allow graft incorporation into host bone. This process of forming new bone can be referred to as osteoinduction, and involves bone morphogenic protein (BMP)- stimulated differentiation of mesenchymal cells into osteoblasts. Results from the study by Stevenson, et al show that BMP is present in both fresh autografts and modified allografts, but is eliminated with heat treatment, such as autoclaving the graft. Massive cortical grafts undergo incorporation into host bone, which is characterized by a multi-phase process involving inflammation, osteogenesis and remolding, and development of a mechanically efficient bone, however the cortical allograft will forever remain a mix of necrotic, non-viable bone and host bone. The initial inflammatory phase of the graft incorporation process is due to the host immune system launching an acute inflammatory response to the trauma caused by surgery, regardless of

the type of graft placed. This acute inflammatory response will subside over the first week post-operation and allow for an increase in osteoclastic activity to repair bone. The osteoinduction process will continue for several weeks, and it is during this time that the host immune system will recognize foreign antigens present on the donor allograft bone (5).

Stevenson, et. al compared the rate of bone incorporation between massive cortical autografts and allografts in a canine model. They found that resorption of cortical bone grafts is dictated by the presence of osteoclasts and will increase for 6 weeks post-operation and undergo a gradual decline afterwards. Massive allograft transplants have a higher risk of poor revascularization and host-graft incorporation as compared to an autograft. These investigators hypothesized that poorer incorporation seen with massive cortical allograft transplant as compared to autograft transplant is in part due the host immune response mounted against the foreign donor antigens present on the allograft. The delayed incorporation results in a significantly weaker bone construct as compared to an autograft, construct and contributes to a rapid failure rate. In attempts to eliminate the host immune response against an allograft, Stevenson, et. al looked at the effect of freezing on allograft incorporation and immune response, and found that, while the initial immune response was dampened in groups receiving the frozen allograft compared to the groups receiving a fresh cortical allograft, bone formation was still significantly delayed in patients receiving a frozen graft and bone strength was considerably weaker for longer periods of time when compared to autograft (5). While the best outcome of host-graft incorporation is seen following the transplant of a cortical autograft, clinically, massive cortical allografts are more readily available in the form of cadaveric bone, and more feasible for large

reconstructive surgeries. While freezing of the allograft bone diminishes the immune response, it does not completely eliminate the host immune response to donor bone antigens. Therefore, modulation of allograft immunogenecitiy could be useful to increase the success of allograft use in limb-salvage procedures.

Transplant Rejection

Transplant rejection is a well-described phenomenon in whole organ transplantation, however, the same processes occur with fresh tissue grafts. Transplant rejection occurs when the host immune system recognizes alloantigens present on the donor tissue. These alloantigens are proteins that vary between individuals and are therefore recognized by the immune system as being foreign to the recipient. Foreign pathogens are internalized by host cells, which will modify the pathogen protein into peptide fragments, or alloantigens, through a method known as antigen processing. Specialized glycoproteins known as major histocompatibility complex (MHC) molecules bring these fragments to the cell surface for circulating T cells to recognize (12).

MHC molecules are encoded for in the host genome major histocompatibility gene complex, and play a major role in the immune response towards transplanted tissues. The MHC complex is high polymorphic, resulting in multiple gene variants present in one population. In humans, the MHC genes are referred to as the human leukocyte antigen, or HLA genes. These genes can vary between individuals, which is why the donor and recipient must be MHC matched before a transplant. Differences in HLA genes between

donor and recipient result in rapid transplant rejection due to host T cells recognizing the donor MHC molecules as being foreign, a phenomenon known as an alloreaction (12).

An alloreaction is the T cell recognition of a foreign MHC molecule by the allelic polymorphism present. While it was first believed that the foreign MHC molecule was enough to elicit a T cell response, studies now show that the T cells recognize the foreign peptide:foreign MHC complex through the cross-reactivity of the T cell receptor (TCR) to the foreign peptide:MHC complex. While host T cells undergo positive selection in the thymus to prevent reaction with self-MHC molecules, they are inadvertently primed to cross-react with any type of MHC molecule that varies from the self-MHC. Furthermore, TCRs are genetically encoded to inherently recognize an MHC complex, which increases the frequency of alloreactions. TCRs have evolved to recognize foreign peptide:MHC complexes through two different methods: peptide dependent and peptide independent recognition. Peptide dependent recognition occurs when the foreign peptide fits well in the TCR peptide-binding groove, causing binding to occur even if the foreign MHC molecule does not fit well with the receptor. Peptide independent recognition occurs with the foreign MHC molecule fits well with the TCR, so binding occurs regardless of the foreign peptide present in the MHC:peptide complex. Both of these recognition methods can play a part in the alloreactivity of a foreign tissue transplant, and will result in an immune response being mounted against the transplant that eventually leads to transplant rejection (12,15). T cells are only able to elicit an immune response towards the transplant once they recognize a foreign alloantigen, so the MHC:peptide complex is crucial. MHC molecules are divided into two different classes, MHC Class I and Class II. These classes dictate the type of foreign peptide that will bind to the MHC molecules, and they determine the type of T cell

that will be activated. MHC Class I molecules bind foreign peptides made in the cytosol and will activate host CD8+ T cells. MHC Class II molecules will bind foreign peptides from intracellular vesicles, and will activate CD4+ T cells. In the case of foreign antigens released from a transplant, the host circulating antigen-presenting cells (APCs) will engulf the foreign antigen and degrade the protein into peptides in the intracellular vesicle system. MHC Class II molecules will bind these peptides and activate CD4+ T cells. These peptides can also bind to MHC Class I molecules through cross-presentation, a process that transplants antigens from the vesicular system of the cell to the cytosol through retrotranslocation. Once in the cytosol, the peptides can bind to MHC Class I molecules and activate CD8+ T cells.

While common protocol in major organ transplant procedures include the matching of donor and recipient for the major histocompatibility complex, this protocol is not considered essential for massive cortical bone transplants. This is primarily because cortical allografts are considered to be acellular. Nonetheless, research suggests that MHC matching of donor and recipient does impact allo-osseous integration. Strong, et. al looked at the effect of MHC matching of osseous allograft transplants in a human model after previous animal models suggested that there is a correlation between graft outcome and "the degree of genetic disparity between donor and recipient" at the MHC locus (18). He found that the use of an allograft resulted in a recipient sensitization towards the MHC molecules on the graft bone, as measured by anti-HLA Class I antibodies present in the serum. Higher levels of anti-donor HLA antibodies present were correlated to poorer graft outcome, as previously seen in animal models and with major organ transplants in humans. (18). Despite these findings, current clinical practice does not involve MHC matching of

massive cortical bone allograft between donor and recipient. This is partly because of the limited availability of allograft bone, and partly because massive cortical allografts are frozen prior to implantation which has previously been shown to diminish host immune response to donor bone. The lack of access to readily available technologies to better match allografts with recipients is also a limitation to the use of routine graft typing. However, as previously shown by Stevenson et al. , frozen cortical allografts heal more slowly and with less new bone formation than autograft. Thus, new approaches to allow better control of the allograft rejection process could significantly improve the overall utility of allografts for reconstruction of bony defects or limb amputations.

Immunosuppressive Therapy following Allograft Transplant

Modulation of the immune system to improve allograft healing following a massive bone transplant may improve allograft-host bone incorporation. This concept seems logical especially when one considers is that even patients receiving matched grafts can experience a transplant rejection. Welter, et. al showed that, while MHC matched allografts have higher levels of remodeling and revascularization compared to MHC mismatched allografts, graft rejection is still possible through the presence of mismatched minor histocompatibility antigens. These antigens are a result of differences in genetic loci besides the MHC loci between donor and recipient. The loci encoding for the minor histocompatibility antigens can produce proteins containing polymorphic peptides that are recognized by the recipient as a minor histocompatibility antigen. The recipient T cells will mount an immune response against all cells expressing these minor histocompatibility

antigens, which will effectively target and destroy all the cells present in the graft. Due to only identical twins being considered to have both matched major and minor histocompatibility antigens, the use of potent immunosuppressive drugs following transplants are a necessity (5).

Welter, et.al further examined the use of Cyclosporin A, a potent immunosuppressive drug, with a mismatched allograft in a canine model. This was a short-term study using nonvascularized cortical grafts. Purpose-bred beagles were all typed for both MHC Class I and Class II antigens at the dog leukocyte antigen (DLA) loci, and were either considered matched for both or mismatched for both. Dogs received either a sham operation; an autograft; an allograft that was DLA Class I and Class II matched; an allograft that was DLA Class I and Class II mismatched; or an allograft that was DLA Class I and Class II mismatched, as well as cyclosporin for 30 days beginning at one day pre-operation. Dogs were euthanized at 3 months post-operation, and resorption scores, bone strength and stiffness, and histology, were evaluated. There was no difference seen in resorption scoring between the group receiving an autograft and the group receiving mismatched allografts and cyclosporin with all animals having slight to moderate erosion. The groups receiving matched allografts or mismatched allografts saw a resorption score of severe erosion to resorbed areas, with no difference between the two groups. Bone strength and stiffness were evaluated by mechanical testing of with a material testing machine that twisted the bones to failure. Autografts and the mismatched allografts treated with cyclosporin had the similar outcomes of high strength and stiffness. Mismatched allografts were weaker than the autografts, and a small difference ($p=0.07$) in strength and stiffness was noted between the autograft and the matched allograft. Of the four groups, the autograft had the highest

area of bone and the lowest level of porosity on histological findings. The autografts were also completely re-vascularized. The matched allografts had extensive levels of resorption and bone remodeling, some level of blood vessels being visible in all vascular spaces, but also had high levels of porosity. The mismatched allografts were largely resorbed with high porosity and fragmentation of the graft. Furthermore, a large amount of fibrous tissue surrounded the graft, and there was delayed blood vessel presence. The mismatched allografts treated with cyclosporin were histologically similar in appearance to the autografts, and experienced full revascularization, although higher levels of porosity compared to the autograft were seen.

This study hypothesized that the addition of cyclosporin increased the efficacy of incorporation and outcome of allografts by either dampening the immune response long enough to allow for incorporation of the graft to reach a level that would sequester the alloantigens away from circulating T cells, or the immune system was dampened to the point of allowing for tolerance of the graft. However, future studies showed that antibodies against the graft were made after discontinuation of cyclosporin treatment. Furthermore, the effects of cyclosporin on bone resorption were reversed within days of finishing treatment. This study illustrates the fact that the immune system does play a role in successful allograft incorporation but brings to light a clinical dilemma that still exists. Chronic immunosuppression with potent drugs such as cyclosporin is not ideal. Other immunomodulators that could provide the same level of local immunosuppression would be ideal for improving the outcome of allograft transplants (19).

Mesenchymal Stromal Cells

Mesenchymal stromal cells (MSCs) are a population of adult stromal cells that have differentiated past the level of embryonic stem cells (1). These are multipotent cells characterized by their ability to differentiate down osteogenic, chondrogenic, and adipogenic lineages. While originally isolated from bone marrow, MSCs can be isolated from a variety of tissues, including adipose tissue. Mesenchymal stromal cells have been frequently referred to as 'mesenchymal stem cells', resulting in Horwitz et al to publish a paper in 2005 clarifying the correct nomenclature for MSCs. They declared the plastic adherent cells isolated from the stromal compartment of tissues, such as adipose, bone marrow, etc. should be referred to as 'mesenchymal stromal cells', a term which indicates the general cell type being described, and infers a heterogeneous cell population. Furthermore, Horwitz et al acknowledged that certain subsets of mesenchymal stromal cells may be termed 'mesenchymal stem cells' as long as they were a homogeneous cell population with stem cell activity (6). The National Institutes of Health describe stem cells to be a population of unspecialized cells that are capable of self-renewal, and can be induced to differentiate down a specific cell lineage (17). The Mesenchymal and Tissue Stem Cell Committee of the International Society for Cellular Therapy defined mesenchymal stromal cells to be cells fulfilling three major criteria: 1. They must be plastic-adherent in standard culture conditions, 2. They must contain a specific cell marker profile, including expression of specific markers such as CD73 and lacking specific markers such as CD14, and 3. They must be able to differentiate into osteoblasts, adipocytes, and chondroblasts in vitro (3).

MSCs possess potent immunomodulatory abilities, and are able to partially avoid allorecognition by the host immune system. They can alter both the innate and adaptive immune response by inducing either anti-inflammatory or pro-inflammatory effects depending on signals they receive from the surrounding environment (1). Within hours of an initial inflammatory response towards a pathogen or in response to tissue injury, toll-like receptors (TLRs) recognize non-self molecular patterns on infected or damaged cells, and initiate the release of inflammatory mediators (12). These mediators will recruit macrophages and neutrophils to the site of infection or injury, resulting in a localized inflammatory environment. These TLRs can also activate resident MSCs, which, upon activation, will increase secretion of growth factors and chemokines necessary to recruit more neutrophils and lymphocytes and propagate the pro-inflammatory response. Studies have shown that in the presence of pro-inflammatory cytokines such as interferon-gamma (IFN-γ), tumor necrosis factor (TNF), and interleukin-1β (IL-1β), MSCs will increase the expression of specific TLRs that sensitize them to the pro-inflammatory environment. Initial exposure to TLRs that support a pro-inflammatory response, like TLR 4, cause MSCs to adopt a proinflammatory phenotype known as MSC 1. This MSC 1 subset will allow an increase of T cell proliferation by lowering levels of nitric oxide (NO) secretion and by increasing secretion of chemokines needed to attract lymphocytes to the local inflammatory environment and increase the overall response in early-stage inflammation (1).

Prolonged interaction with the pro-inflammatory TLR ligands, however, will cause a decrease in expression of TLR4, and an increase in expression of TLR3, an anti-inflammatory propagator. MSCs primed with TLR3 will adopt an anti-inflammatory

phenotype known as MSC 2. MSC 2 cells will secrete factors such as tumor growth factor-β (TGF- β) that promote regulatory T cells (Tregs) to dampen the pro-inflammatory response, and MSC 2 cells will increase levels of NO, further inhibiting T cell proliferation. While the exact stimuli and mechanism by which MSCs can switch between an MSC 1 and MSC 2 phenotype are not completely understood, it is hypothesized that expression of specific TLRs and levels of NO play a key role (1).

Additionally, studies have shown interferon-gamma (IFN-γ) augments the immunosuppressive capabilities of MSCs by directly or indirectly altering the T cell response. Upregulation or deregulation of MSC inhibitory factors by IFN- γ results in decreased T cell activation and will induce T cells to switch from a pro-inflammatory to an anti-inflammatory phenotype. Additionally, a substantial increase in Tregs and T cell negative signaling is observed with high concentrations of IFN- γ. However, some conflicting data has shown that allogeneic MSC may have increased immunogenicity properties in the presence of IFN- γ, which would promote a pro-inflammatory environment. Therefore, it is imperative to look at differing properties between allogeneic and autologous MSCs in the presence of cytokines such as IFN- γ to determine their immunomodulatory effects and explore their potential use in therapeutics (16).

Bernardo et. al used a murine graft-versus-host disease (GvHD) model to look at the effect of delivering MSCs at varying time points after a bone marrow transplant. MSCs delivered the same day as the transplant had no effect on suppressing the GvHD, whereas MSCs delivered 3, 8, or 20 days after transplant successfully dampened the GvHD progression and decreased symptoms associated with the disease. Furthermore, MSCs that were pretreated with IFN-γ before administration prevented GvHD fatalities. These results

suggest that the level of pro-inflammatory cytokine exposure play a role in whether MSCs take on a pro-inflammatory or anti-inflammatory phenotype (1).

Mesenchymal Stromal Cells and Allograft Incorporation

Due to their ability to differentiate down an osteogenic lineage into osteoblasts, emerging studies continue to look at the benefit of mesenchymal stem cells on allograft incorporation. Nather, et al. looked at the effect of autogenous bone marrow derived mesenchymal stem cells (BM-MSCs) on the level of host-graft union, resorption, new bone formation, and osteocyte production in an allograft using a rabbit model. Rabbits received either a non-vascularized autograft, a frozen allograft, or a frozen allograft seeded with BM-MSCs. They found that at 12 weeks, union at both host-graft junctions was seen in all animals receiving an autograft transplant, but union was not seen in any animals receiving an allograft transplant. Host-graft union for the animals receiving an allograft was seen in 50% of the animals at 16 weeks, and in all animals at 24 weeks. However, this delayed union response was diminished in animals receiving an allograft loaded with MSCs; complete host-graft union for these animals was seen at 12 weeks. There was no significant difference in the level of bone resorption at 12 weeks between animals receiving an autograft and animals receiving an allograft seeded with MSCs. The animals receiving an allograft alone had a significant increase in resorption levels compared to the other two groups. The autograft recipients had the highest level of new bone formation at 12 weeks, and had identical levels of formation at weeks 16 and 24 as those seen in the recipients of allografts loaded with MSCs. Recipients of allografts alone had significantly lower levels of

new bone formation as compared to the other groups. The highest level of osteocytes, which indicate fully formed bone, was significantly higher in the recipients of the allograft loaded with MSCs as compared to both the allograft and autograft recipients at 12, 16, and 24 weeks (13). Results of this study suggest the addition of mesenchymal stem cells to allografts will increase graft incorporation by helping increase new bone formation, yield higher levels of osteocytes in a faster manner, and will aid in the host-graft union.

Project Rationale

Aforementioned studies show that the success of allograft transplantation is dependent of levels of host-graft incorporation, new bone formation, and revascularization of the graft. However, a host immune response directed towards the alloantigens present on a MHC mismatched allograft can impede successful incorporation, contributing to eventual graft failure. The addition of immunosuppressive drugs following a mismatched allograft transplant result in incorporation, new bone formation, and revascularization levels nearly identical to those seen in a matched MHC autograft transplant, suggesting that immunomodulation may be an important determinant of allograft transplant success. Clinically, it is not ideal to place a patient on chronic immunosuppressive medication. The immunomodulatory agent is one that could effectively modulate the local immune response towards the transplant without causing systemic immunosuppression. Additionally, an immunomodulator that could have a potent, long term effect without having to be administered chronically would increase the quality of life of the patient, and would decreased added health risks of being on chronic immunosuppressives.

Mesenchymal stem cells can influence the immune system through various signaling and activation pathways. Moreover, MSCs have been shown to increase the incorporation and success of a mismatched allograft. The research described in the following chapters was initiated to begin to address the question of whether or not the increased success when using local administration of MSCs with a cortical allograft is due, at least in part, to the immunomodulation of the host immune system by the mesenchymal stem cells. This body of work describes 1) an experiment utilizing a novel bone vaccine that suggests adipose derived mesenchymal stem cells have no detectible effect on the humoral immune response towards total bone antigen delivered in a vaccine, 2) the effect of mesenchymal stem cells on the cellular immune response towards an allograft or autograft bone vaccine and whether the route of administration (intravenous or local) influences this effect, and 3) the effect of mesenchymal stem cells on the cellular immune response towards a massive cortical allograft or autograft transplant.

This goal of this research was to evaluate the influence on the host immune response elicited by an allograft or autograft either alone or when accompanied with mesenchymal stem cells. Understanding how mesenchymal stem cells influence the immune system following an allograft transplant will aid in future studies looking for the most efficacious treatment to allow for successful allograft incorporation.

CHAPTER 2

The Effect of Adipose Derived Mesenchymal Stromal Cells and Vaccines Prepared from Allogeneic Bone Tissues On The Humoral and Cellular Host Immune Responses Against Donor Bone Antigens

INTRODUCTION

Massive bone allografts are utilized to reconstruct large bone defects after tumor resection or trauma. Traditionally, allografts are obtained from deceased, non-related tissue donors, sterilely harvested, stripped of soft tissues and frozen to diminish antigenicity. Due to lack of availability of matched tissue and the paucity of cellular material on the allograft, massive cortical bone allografts are not are not matched for major histocompatibility antigens with the recipient. Limb-salvage treatments utilizing massive allografts have a 60% failure rate at 10 years in human patients and a 50% failure rate at one year for canine patients (9). Studies performed by Sharon Stevenson in the 1980's evaluated healing outcome in canines receiving either a matched or mismatched vascularized and nonvascularized frozen large cortical grafts, and found that there was improved graft incorporation when the graft donor and host were matched for major histocompatibility antigens. In 1990, Welter, et.al investigated whether modulation of the immune system would improve allograft healing following a massive cortical allograft transplant and allow for better incorporation. They found that recipients of a mismatched allograft treated daily with a potent immunosuppressant (Cyclosporin A) resulted in higher levels of new bone formation and lower levels of fracture and resorption compared to

recipients of a mismatched allograft alone. These positive results changed with the discontinuation of Cyclosporin A resulting in decreased new bone formation and increased levels of fracture and resorption. Based up on previous work, it is known that the poor healing seen after mismatched large frozen cortical allograft transplants are partly immune-mediated, and can be contributed to T cell recognition of graft alloantigens (7,8).

The use of mesenchymal stromal cells (MSCs) following major organ transplantation had been widely investigated in the hope of finding a new standard of immunosuppressive treatment. While current immunosuppressive drugs greatly decrease the risk of graft rejection, long-term use is not advantageous. Mesenchymal stromal cells are not only able to avoid recognition by the host immune response due to low surface levels of major histocompatibility complex (MHC) Class I molecules and absent levels of MHC Class II molecules, but they are able to modulate T cell proliferation to propagate either a pro-inflammatory and anti-inflammatory response based on the environment they are introduced to (1). Furthermore, the regulation of the immune system can be highly specific due to the ability of MSCs to home to sites of injury and inflammation.

The objective of this study was to evaluate the humoral and cellular immune response against allograft bone versus autograft bone when delivered as a vaccine, to determine whether or not the addition of adipose-derived mesenchymal stromal cells (AD-MSCs) would dampen the immune response towards an allograft bone vaccine. A secondary objective was to determine if there was a difference in the level of immunosuppression observed in mice receiving intravenously delivered MSCs as compared to mice receiving subcutaneously injected MSCs. To accomplish these objectives we developed a murine bone vaccine model to mimic the immune response seen following

a limb-salvage procedure. We hypothesized that: 1) An allograft-derived bone vaccine would elicit a greater humoral immune response as compared to an autograft-derived bone vaccine in a murine model; 2) An adipose-derived mesenchymal stromal cells (AD-MSCs) would dampen the recipient humoral immune response against donor bone-associated antigens, with intravenously administered MSCs having a more potent immunomodulatory effect than a subcutaneous delivery of MSCs; and 3) T cell proliferation would be suppressed in mice receiving a vaccine with AD-MSCs compared to mice a receiving a vaccine alone.

MATERIALS AND METHODS

Animals

All animals were obtained from the National Cancer Institute (NCI) or National Institute of Health (NIH). Female BALB/C mice and female C57B/6 mice arrived at 6-8 weeks of age, and were allowed to acclimate for one week before use. The handling, treatment, and euthanasia of mice followed a Colorado State University Institutional Animal Care and Use Committee (IACUC) approved protocol.

Allograft and Autograft Collection

Bones used for the allograft vaccine were obtained from the femurs of BALB/C mice. Femurs were collected under sterile conditions in a laminar flow hood immediately following humane euthanasia. All instruments used were sterilized prior to use. Femurs

were collected, scraped with a scalpel blade to remove all periosteum, and placed into cryovials. Cryovials were immediately placed into a container with liquid nitrogen to flash-freeze the bones. Bones were stored at -80°C for a minimum of one week before further processing. Bones used in the autograft vaccine were obtained from C57Bl/6 mice in the same manner as described for the allograft bone collection.

Bone Vaccine Preparation

The donor femurs were removed from the -80°C storage and were immediately placed into a liquid nitrogen container. A mortar and pestle were placed in ethanol for 10 minutes and used to smash the bones into a powder. The final concentration of bone powder in the vaccine was 10µg/mL.

The bone powder and freshly made cationic liposomal DNA complex (CLDC) adjuvant was re-suspended in sterile PBS and stored at -20°C until use (9). Final bone vaccines contained bone dust of the allograft (BALB/C) bone or an autograft (C57Bl/6) bone; a CLDC adjuvant; and sterile PBS.

The allograft and autograft treatment groups were compared against a positive control vaccine containing alkaline phosphatase (ALP) (Phosphatase, Alkaline from bovine intestinal mucosa, Sigma-Aldrich P7640-500MG). The final ALP concentration in the vaccine was 10µg/mL, and was re-suspended in sterile PBS and CLDC adjuvant.

Serum Collection

Serum (0.1 ml) was collected from the tail vein on days 1 and 7 before administration of the vaccine. On Day 21, mice were anesthetized, and blood was collected via cardiac puncture just prior to euthanasia. Blood was placed into serum separator tubes

(BD Microtainer® Serum Separator Tubes, REF 365956), which were spun down in a micro-centrifuge (Fisher Scientific accuSpin Micro 17) at 7 x 1,000g for 5 minutes. Serum was pipetted into Ependorf tubes and stored at -20°C.

Vaccine Injection

C57Bl/6 mice (n=20) were treated with an initial vaccine injection on Day 1, followed by a booster vaccine injection on Day 7. Mice were randomly assigned to receive an ALP vaccine (n=5), an allograft vaccine (n=5), an autograft vaccine (n=5), or were non-vaccinated (n=5). Mice were anesthetized, and a 0.1mL vaccine was injected subcutaneously through a 14gauge needle.

Mice (n=48) were randomly assigned to receive a vaccine with either intravenously delivered (IV) MSCs (n=24) or with subcutaneous MSCs (n=24). Recipients within each MSC delivery group received an ALP vaccine (n=8), an allograft vaccine (n=8), an autograft vaccine (n=8), or were non-vaccinated (n=8).

Adipose Tissue Harvest for Preparation of MSC

Adipose tissue was collected from the abdominal fat pads of C57BL/6 mice using sterile instruments under a laminar flow hood. Fat was isolated, minced, and resuspended in 1mg/mL of collagenase with an antibiotic/antimycotic solution. Cells were incubated at 37°C for 30 minutes before MSC media (antibiotic/antimycotic solution, 15% FBS, MEM vitamins, and MEM nonessential amino acids) was added. Cells were washed, resuspended in MSC media, and plated in flasks that were stored at 37°C.

Adipose-Derived Mesenchymal Stem Cell Collection and Storage

Cells were allowed to incubate at 37°C until reaching a minimum of 80% confluency. Cells were washed and trypsinized before being transferred to a 50mL conical tube. The cells were resuspended in PBS-Heparin (0.1mL Heparin in 9.9mL sterile PBS) with a final volume of $5x10^5$ cells/100µL PBS-Heparin. MSCs in unused flasks were frozen and stored for later use Cells in flasks that were not used for treatment were washed, trypsinized, and spun like mentioned before, and were resuspended in freeze media (20% DMSO, 40% growth media, 40% FBS). Cells were transferred to cyrovials and stored at -80°C.

Ad-MSC Injection

During injections, the MSC-PBS-Heparin suspension was stored in a 37°C water bath. For mice receiving an intravenous Ad-MSC injection, mice were placed under a heat lamp for 20 minutes, placed into a restrainer and 0.1mL of the MSC-PBS/Heparin solution was injected into the tail vein using an insulin needle. Mice received two tail vein injections of $5x10^5$ MSCs/0.1mL 48 hours apart beginning on Day 1, and two injections 48 hours apart beginning on Day 7. The injections on Day and Day 7 were given immediately after vaccination.

Mice that received a subcutaneous injection of MSCs received one subcutaneous injection of $1x10^6$ MSCs/0.1mL PBS-Heparin on Day 1 and one injection on Day 7. A 0.1mL injection of MSCs was delivered subcutaneously between the shoulder blades using an insulin needle immediately following vaccination.

Bone Protein Extraction

Bone protein from C57BL/6 mice was isolated using TRIzol Reagent (TRIzol Reagent, Life Technologies 15596-026) and used as the antigen in the antibody detection ELISA. Femurs were collected from C57BL/6 mice in a sterile manner and stored at -80°C prior to use. Femurs were immediately placed into liquid nitrogen, freeze fractured, and crushed into a powder. TRIzol reagent was added at 1mL/50mg of protein, and the sample was homogenized using a power homogenizer (Fisher Scientific PowerGen 1000). The homogenized sample was incubated for 5 minutes at room temperature and chloroform (Chloroform, 99.9+%, A.C.S. HPLC grade, Aldrich Chemical Co, Inc. 67-66-3) was added at 0.2mL per 1mL of TRIzol Reagent, and then centrifuged in a Hermle Labnet Z-383K High Performance Centrifuge at 12,000 x g for 15 minutes at 4°C. The upper aqueous phase was removed, and 0.3mL of 100% ethanol per 1mL of TRIzol Reagent was added. The sample was spun at 2,000xg for 5 minutes at 4°C, and the supernatant was transferred to a new tube. Isopropanol (2-Propanol HPLC Grade, Fisher Scientific A451-4) was added to the supernatant at 1.5mL isopropanol per 1mL TRIzol Reagent and the sample was incubated for 10 minutes at room temperature, spun at 12,000 x g for 10 minutes at 4°C, and the supernatant was removed. The protein pellet was washed with 2mL of a 0.3M guanidine hydrochloride in 95% ethanol wash solution per 1mL of TRIzol Reagent, incubated for 20 minutes at room temperature and then spun at 7500 x g for 5 minutes at 4°C. The wash solution was removed and 2mL of 100% ethanol was added to the protein pellet. The solution was vortexed and then incubated at room temperature for 20 minutes. The sample was spun at 7500 x g for 5 minutes at 4°C, the ethanol wash was removed, and the protein

pellet air-dried for 10 minutes before 200µL of 1% SDS was added. The solution was pipetted up and down until the pellet was resuspended, spun at 10,000 x g for 10 minutes at 4°C and the supernatant containing the protein was transferred to a new tube. The protein yield was determined with a BCA Protein Assay Kit (Pierce 23225). The protein yield from the TRIzol extraction method was determined with a BCA Protein Assay Kit (Pierce 23225). The protein concentration was determined to be 5mg/mL.

Spleen Collection

Immediately after euthanasia, spleens were collected under sterile conditions in a laminar flow hood for the purpose of evaluating the cellular immune response to total bone antigens by measuring T cell proliferation present in the spleen cells. Spleens were placed into petri dishes containing 1-2mL HBSS media (HBSS, 1x with calcium and magnesium, CORNING cellgro REF 21-020-CV) and subjected to a single-cell suspension protocol. Briefly: the spleen and media were pushed through a cell strainer; spun in a centrifuge (Beckman Coulter Allegra™ 6R) at 1200 rpm for 5 minutes; resuspended in 2mL of ACK Lysing Buffer (Lonza BioWhittaker® Catalog No: 10-548E) for 5 min; resuspended in HBSS and spun at 1200 rpm for 5 minutes; and cells were resuspended in 1mL of freeze media and stored at -80°C.

Serum Analysis for IgG Antibody Levels

Serum samples were subjected to an antibody-detection ELISA. Briefly: a Nunc-Immuno Maxisorp 96-well plate (Nunc #442404, Fisher 12-565-135) was coated with

C57BL/6 bone protein suspended in carbonate buffer at 5 µg/mL. The plate was covered and incubated overnight at 4°C. A 5% PBS-milk blocking buffer was used and the plate was incubated at room temperature for 60 minutes. Serial dilutions of the samples from 1:10 to 1:10,000 were performed. Blanks were 3% BSA-PBS with no sample. An anti-IgG detection antibody (ImmunoPure® Goat Anti-Mouse IgG (H+L), Pierce Prod# 31430) was diluted 1:500 in 5% PBS-Milk and added before the plate was incubated at room temperature for 60 minutes in the dark. A TMB substrate (3, 3', 5, 5'-Tetra Methylbenzidine (TMB) Liquid Substrate System for ELISA, Sigma-Aldrich T0440-1L) was brought to room temperature during the 60-minute incubation time, and was added to each well. Color was allowed to develop in the dark for two minutes, and a 1N HCl stop solution was then added to each well. The plate was immediately read at 450nm in a BioTek Synergy HT plate reader. Absorbance readings were analyzed with Gen5 2.00 Software.

Statistical Analyses

The raw optical density (OD) values of the 1:10 dilution in the antibody detection ELISA were analyzed to look at differences in antibody production between treatment groups. Differences in T cell proliferation levels between different treatment groups were also analyzed. All analyses were performed with a 2-way ANOVA followed by a Bonferroni post-test. A p-value of less than 0.05 was considered statistically significant for all analyses, and raw p-values are reported. Statistical analyses were performed using GraphPad Prism Version 5 for Windows.

RESULTS

Antibody Response

Among animal receiving vaccines (no Ad-MSCs) recipients of an ALP vaccine had a significantly higher antibody response on Day 21 compared to recipients of an autograft bone vaccine (Figure 2.1). No other differences were noted.

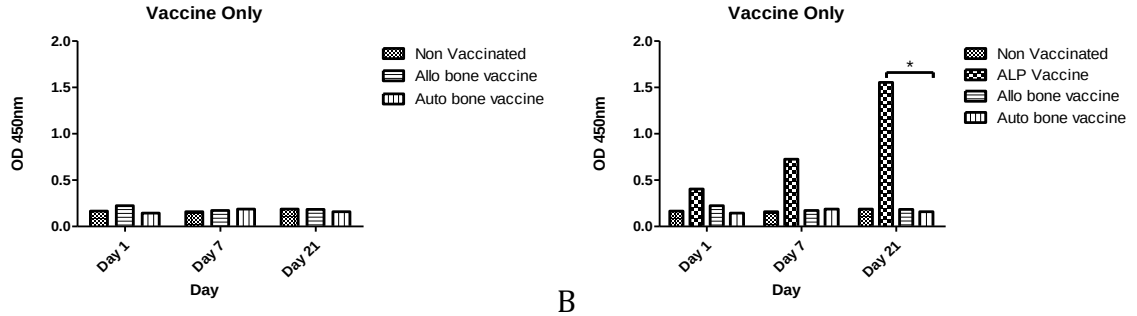

A. B

Figure 2.1 Antibody Response Towards Bone Antigen in Vaccine Recipients. Graph A depicts the antibody response towards a bone antigen in recipients of an allograft or autograft bone vaccine compared to a non-vaccinated mouse. Graph B depicts the differences in antibody response seen between non-vaccinated animals and recipients of an ALP vaccine, an allograft vaccine, or an autograft vaccine.
*p-value<0.05

Among mice receiving both a vaccine and intravenously –delivered Ad-MSCs, there were no significant differences in ALP antibody response observed between treatment groups on Day 1 or Day 7. On Day 21, mice receiving both ALP vaccine and intravenously –delivered Ad-MSCs had greater antibody production when compared to recipients of an allograft or autograft vaccine with Ad-MSCs, the non-vaccinated group with IV MSCs, and the non-

vaccinated group that did not receive MSCs. The same trend was noted in recipients of subcutaneous MSCs (Figure 2.2).

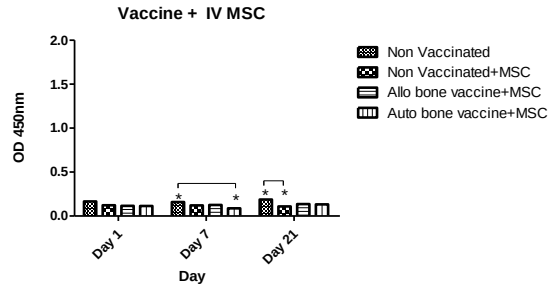

A.

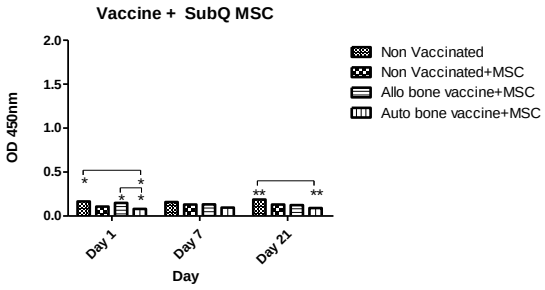

B.

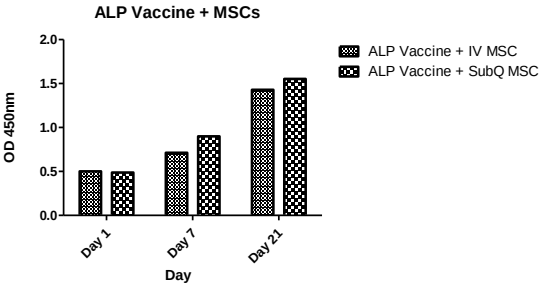

C.

Figure 2.2 Antibody Response in Vaccine Recipients With the Addition of MSCs. Graph A depicts the antibody response towards a total bone antigen in recipients of IV delivered MSCs with the various treatment groups. Graph B depicts the antibody response in recipients of subcutaneous MSCs with the various treatment groups. Graph C shows the antibody response towards total bone antigen in recipients of the ALP (positive control) vaccine.

Differences in antibody response within each treatment group receiving a vaccine were evaluated to examine any immunomodulatory effect of MSC administration with the different vaccines, as well as to evaluate if there was any MSC immunomodulatory effect on non-vaccinated mice in order to ascertain the non-vaccine induced MSC effect on the immune system. On Day 21, non-vaccinated recipients had a significantly more robust antibody response compared to non-vaccinated recipients that received MSCs. On Day 1, recipients of an allograft bone vaccine co-administered with IV MSCs had a significantly

less robust antibody response ($p < 0.05$) compared to recipients of an allograft bone vaccine alone. No differences were observed (Figure 2.3)

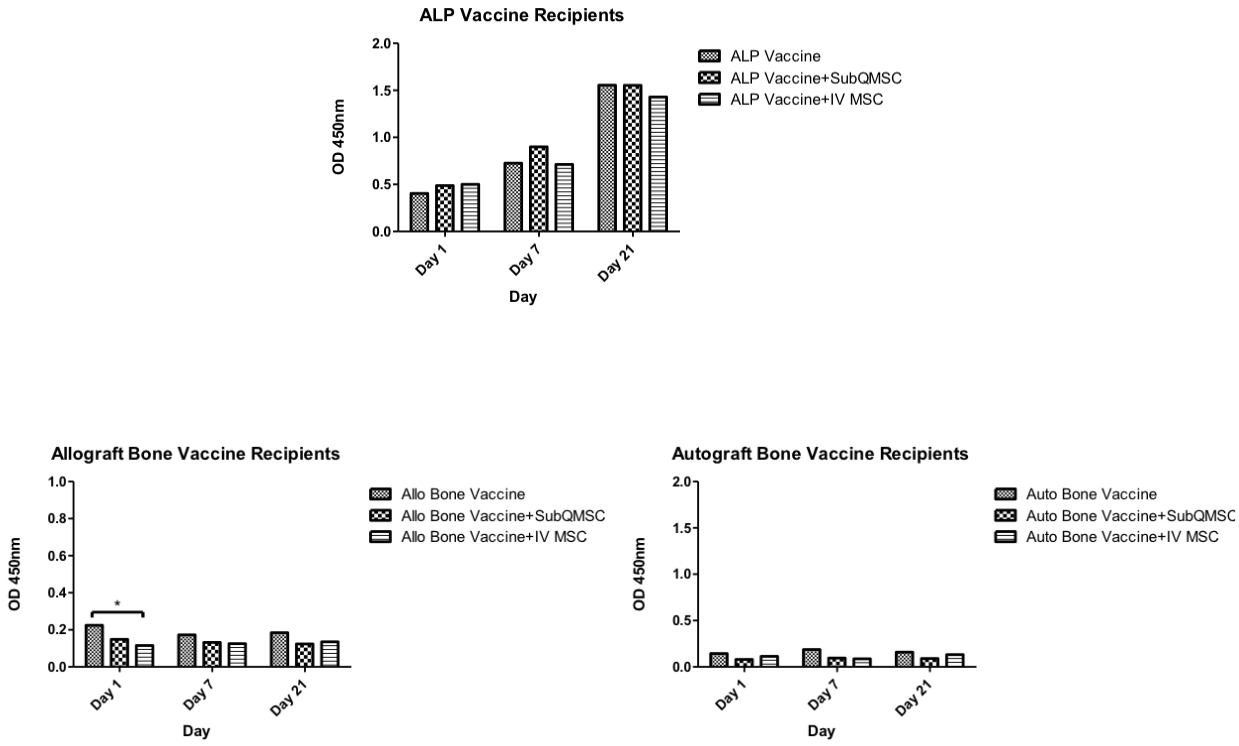

Figure 2.3 Antibody Responses Within ALP Vaccine, Allograft Bone Vaccine, and Autograft Bone Vaccine Treatment Groups Recipients of an allograft bone vaccine with IV MSCs had a significantly less robust antibody response on Day 1 compared to recipients of an allograft bone vaccine alone. No other differences within treatment groups were reported. *p-value<0.05

T Cell Proliferation

T cell proliferation in response to a negative control, an allograft bone antigen, and an autograft bone antigen were evaluated in recipients of an ALP vaccine (n=5), an allograft vaccine (n=5), an autograft vaccine (n=5), non-vaccinated mice (n=5), and recipients of the

aforementioned treatment groups with IV MSCs (n=8 per group) and with subcutaneous MSCs (n=8 per group).

Recipients of an allograft bone vaccine with IV MSCs and with subcutaneous MSCs had a significantly less potent T cell proliferation response to an allograft bone antigen compared to the amount of proliferation found in non-vaccinated animals. No differences in T cell proliferation were observed between recipients of an allograft bone vaccine upon exposure to an autograft bone antigen (Figure 2.4).

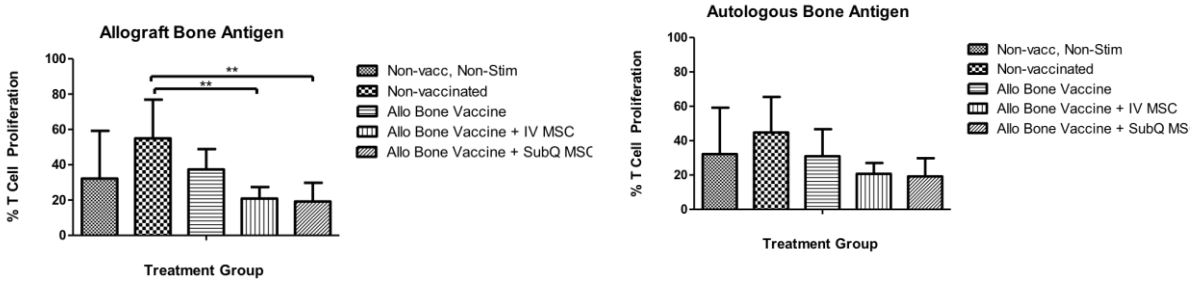

Figure 2.4 T Cell Proliferation in Recipients of an Allograft Bone Vaccine. The first graph depicts T cell proliferation response upon in vivo re-exposure to allograft bone protein in recipients of an allograft bone vaccine. This response is compared against the response in a non-vaccinated mouse after in vivo re-exposure to an allograft bone protein, as well as the response in non-vaccinated mice that are not re-exposed in vivo to any bone protein. A significantly less potent T cell proliferation response to an allograft bone protein is observed in recipients of an allograft bone vaccine with IV MSCs and with subcutaneous MSCs compared to non-vaccinated mice. No differences in T cell proliferation in response to an autograft bone protein were observed. Error bars depict SD. **p-value<0.01

No differences in T cell proliferation were noted in recipients of an autograft bone vaccine with IV MSCs and with subcutaneous MSCs in response to an allograft bone antigen compared to the response found in non-vaccinated animals. The same result was observed in response to an autograft antigen (Figure 2.5).

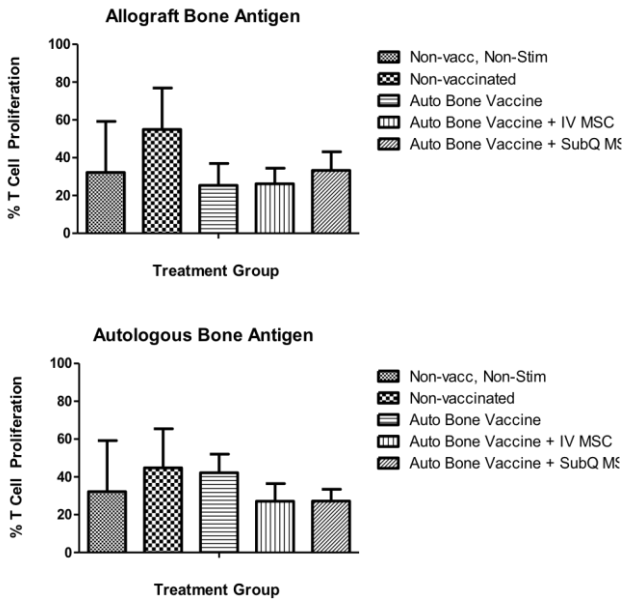

Figure 2.5 T Cell Proliferation in Recipients of an Autograft Bone Vaccine. The first graph depicts T cell proliferation upon exposure to an allograft bone antigen in recipients of an autograft bone vaccine. This response is compared against the response in a non-vaccinated mouse after exposure to an allograft bone antigen, as well as in non-vaccinated mice that are not exposed to any antigen. No significant differences in T cell proliferation in response to an allograft bone antigen or an autograft bone antigen were observed. Error bars depict SD.

DISCUSSION

The role of T-cells in acute graft rejection, as well as the effect of the initial, antigen-independent, inflammatory response present after a transplant, have been examined as key players in amplifying and propagating the graft-specific adaptive immune response (7). Studies using T-cell deficient mice that received mismatched skin or cardiac allografts looked at the effect of adoptive T cell transfer after grafts were allowed to heal. With the

addition of T cells, acute rejection of the graft was seen, even in mismatch grafts that were considered well-healed, with normal histological appearance (1, 4, 7).

The T cell immune response can be stimulated either through a direct pathway or an indirect pathway of antigen presentation. In the direct stimulation of T cells, the polymorphic donor's MHCs present on the graft are recognized by host T cells thereby stimulating naïve T cell activation and proliferation into effector T cells targeted against the graft. The indirect pathway of antigen presentation T cell occurs when donor graft cells with intact MHCs are secreted into the periphery, internalized by host antigen presenting cells, and presented to naïve T-cells, which results in increased activation and proliferation of T cells (4). While cross-over of pathway activation can occur during an immune response, there is no doubt that the antigen presentation by MHCs is essential for activation of T cell proliferation.

As part of the primary immune response, T cells are activated against a specific antigen, and divide into CD4+ and CD8+ subsets to effectively target and kill infected cells while activating B cells to produce antibodies against the foreign antigen. The primary immune response will also induce the production of memory T cells, which are primed against the foreign antigen, and are capable of mounting a faster and greater immune response upon second exposure to the specific antigen (5).

The antigen-independent proinflammatory events that occur in response to trauma and/or surgery may propagate the T-cell response towards the graft. Inflammatory mediators are partly responsible for the expression of toll-like receptors (TLRs) that, once stimulated by a foreign peptide, will increase production of proinflammatory cytokines and chemokines, as well as increase antigen presentation to T cells (6, 7). A pro-inflammatory

environment induces upregulation of MHC molecules on antigen presenting cells, thereby increasing the opportunity for T cells to encounter a MHC molecule presenting peptide from the graft (2).

Allograft rejection can be due to a collaborative response between the host immune system and the transplant site environment. The allograft itself is capable of stimulating a T-cell immune response by antigen activation of T-cells through either a direct or indirect pathway. The direct pathway of T cell activation involves recipient T cells recognizing intact, donor MHC:peptide complexes present on donor cells. T cells can also recognize antigen via an indirect pathway in which recipient antigen presenting cells will process donor MHC molecules into peptides, and present the MHC:peptide complex to recipient T cells (4). The antigen presentation is enhanced by the TLRs present in response to surgery-induced inflammation at the allograft transplant site.

The novel bone vaccine model used in this study was an attempt to mimic the immune response seen in a clinical setting following massive cortical allograft transplantation in order to investigate the humoral and cellular immune response towards a bone antigen. The overall increase in antibody production observed in response to the ALP vaccine support the concept of a vaccine model to evaluate the humoral immune system toward a single bone antigenic protein. However, the lack of statistically significant differences in antibody response towards a bone vaccine was unexpected. It is possible that the amount of complex bone antigen delivered in the allograft and autograft bone vaccines was not sufficient to elicit a strong humoral immune response. Each mouse received 0.1μg of bone in the vaccine; so future studies looking at increasing this concentration might yield more detectable differences. Nonetheless, these data suggest

little to no humoral response towards the total bone antigen mixture delivered in the vaccines. Additionally, the administration of Ad-MSCs, whether delivered subcutaneously or intravenously, did not alter this outcome.

Evaluation of the Ad-MSC immunomodulation of the cellular immune response did reveal a suppressive effect on T cell proliferation levels in recipients of a vaccine with MSCs. This effect was most pronounced in recipients of an allograft bone vaccine and Ad-MSCs when spleen cells were exposed to an allograft bone antigen. T cell proliferation suppression by Ad-MSCs was less pronounced when cells were exposed to an autograft bone antigen. Additionally, this suppression was not as pronounced in recipients of an autograft vaccine when exposed to an allograft bone antigen or an autograft bone antigen. When considered as a whole, these data support the hypothesis that Ad-MSCs do suppress cellular immunity towards allograft bone antigens.

An additional unexpected observation was noted during the analysis of the T cell proliferation following re-exposure to the bone antigens. Wherein one would normally expect re-exposure to an antigen via vaccine to enhance the immune response to a particular antigen, we noted that T cell proliferation towards the allograft bone antigen was dampened in animals previously vaccinated with an allograft bone vaccine. This effect was most profound when the allograft bone vaccine was given with MSCs. This suggests that vaccinating against a total allograft bone antigen may in fact decrease the immune response to the allograft, especially with the addition of MSCs. The high failure rate associated with massive cortical allograft transplants is partly immune mediated, and previous studies have shown this immune response is in part due to T cells activated by the host immune system to target the non-self mismatched major histocompatibility complex

molecules present on the donor bone. However, recipients of a bone vaccine had a dampened T cell response upon re-exposure to the bone antigen. These findings provide an avenue to explore future methods aimed at dampening the immune response against a massive cortical allograft transplant. Investigating whether vaccination with a bone vaccine prior to a massive cortical allograft transplant could lead to novel ways of dampening the host immune response towards the donor bone and lead to overall higher allograft transplant success.

CONCLUSION

The employment of a massive cortical allograft for limb-salvage is widely performed in clinical settings with little concern for the matching of donor and recipient MHC complexes. Failure of an allograft to incorporate into host bone is partly immune-mediated. We developed a novel vaccine model to mimic the immune response seen towards a massive cortical allograft in a clinical setting. We have shown that the administration of ad-MSCs modulate the cellular immune response to allograft bone antigen has little effect on the humoral immune response in this model. However, there is some immunomodulation of the cellular immune response with the addition of MSCs as seen in the T cell proliferation response to an antigen. Lastly, data presented herein suggests a possible new avenue to explore to diminish immune response following massive allograft transplant through prior vaccination of the patient with the allograft. A future vaccine study looking at this potential mechanism is needed to determine if the suppression of T cell proliferation present in vaccinated animals is related to clinically improved graft incorporation. If

successful, vaccination with an allograft bone antigen could yield a potential new therapeutic for increasing the success of a massive cortical allograft transplant.

CHAPTER 3

Massive Cortical Allograft Transplants Result in Increased Antigen Presentation and T Cell Proliferation

INTRODUCTION

Mesenchymal stem cell (MSCs) modulation of the host immune response is partly dependent on the cytokine profile of the surrounding environment. Initial exposure to pro-inflammatory cytokines such as interferon-gamma (IFN-ϒ) will activate MSCs to up-regulate expression of specific toll-like receptors (TLRs) that are involved in maintaining an inflammatory immune response through the increased proliferation of T cells. However, the MSC immune modulation is equipped with a self-regulatory mechanism to prevent a hyperimmune response. With extended exposure to pro-inflammatory cytokines, MSCs will decrease expression of pro-inflammatory TLRs and increase expression of anti-inflammatory TLRs (7).

A pro-inflammatory, primary cell-mediated immune response is characterized by increased T cell proliferation into CD4+ and CD8+ T cells. CD4+ T cells are involved in the humoral immune response that results in increased macrophage and neutrophil migration to sites of infection or injury, as well as the activation of B cells to produce antibodies against a foreign antigen. CD8+ T cells are involved in the cellular immune response that targets and kills infected cells (4).

An anti-inflammatory immune response involves a decrease in pro-inflammatory cytokines and the increased expression of CD4+ T regulatory cells (T_{reg} cells) that are responsible for dampening and eventually eliminating the immune response (5).

Mesenchymal stem cells have been shown to suppress T cell proliferation both in vivo and in vitro; however, the level of suppression is dependent on the environment surrounding the MSC-T cell interaction. Interferon-gamma (IFN-γ) is a regulatory protein that is produced in response to T cell activation by an alloantigen. High levels of IFN-γ in an inflammatory environment have been shown to induce the production of indoleamine 2,3-dioxygenase (IDO) as a self-regulatory mechanism to prevent a hyperinflammatory response. IDO mainly functions as an enzyme to catalyze tryptophan, one of the body's essential amino acids that play a role in the induction of Foxp3+ T regulatory cells. IDO also possess a non-enzymatic, signaling function in dendritic cells (DC) that, when activated, will convert the DC phenotype to that of a regulatory DC, and tipping the immune response towards a tolerogenic response (4). MSCs exposed to high levels of IFN-γ are induced to increase production of IDO and other immunosuppressive cytokines such as tumor growth factor β (TGF-β), which may explain how MSCs help suppress the immune response seen in transplant rejection.

Santoni, et. al. looked at the effect of the addition of mesenchymal stem cells following a massive cortical allograft transplant in a murine model to evaluate new bone formation in mice receiving an allograft compared to an autograft. C57BL/6 mice received either an allograft from a Balb/C mouse; an allograft coated with a fibrin carrier; an allograft with a fibrin carried coated with adipose-derived MSCs (AD-MSCs); or an allograft followed by intravenous(IV) injection of AD-MSCs. All animals were compared against mice

receiving the same treatment with an autograft instead of an allograft. They hypothesized that the addition of AD-MSCs would decrease the immune response towards the allograft bone and allow levels of new bone formation and incorporation similar to levels seen following an autograft transplant. A pairwise analysis looking at the effect of treatment on new bone formation found that the highest level of new bone was found in groups receiving intravenous MSCs. Within the autograft treatment group, the mice receiving an autograft with IV MSCs had a significantly higher amount of new bone formation as compared to the group receiving an autograft with a fibrin carrier ($p=0.01$) and to the group receiving an autograft only ($p=0.04$). However, no statistically significant differences in new bone volume were seen in within the allograft treatment group.

The purpose of this study is to determine the MSC immunomodulation on the cellular immune response towards a massive cortical allograft transplant by evaluating T cell proliferation in the spleens collected from the study conducted by Santoni, et. al. We hypothesized that 1) Spleens from the mice receiving an allograft bone transplant will have higher levels of T cell proliferation as compared to mice receiving an autograft transplant. And 2) T cell proliferation in mice receiving an allograft or autograft transplant with MSCs will be less than that of mice receiving an allograft or autograft transplant alone, but that the autograft transplant groups will still have lower levels of T cell proliferation as compared to the allograft transplant group.

METHODS AND MATERIALS

Animals

All animals were obtained from the National Cancer Institute (NCI) or National Institute of Health (NIH). Female Balb/C mice and female C57BL/6 mice arrived at 6-8 weeks of age, and were allowed to acclimate for one week before use. The handling, treatment, and euthanasia of mice followed a Colorado State University Institutional Animal Care and Use Committee (IACUC) approved protocol.

Spleen Donors

C57BL/6 mice used in a previous study were treated with an initial vaccine injection on Day 1, a booster vaccine injection on Day 7, and were euthanized on Day 21. Mice (n=20) were randomly assigned to receive an ALP vaccine (n=5), an allograft vaccine (n=5), an autograft vaccine (n=5), or were non-vaccinated (n= 5). Mice were anesthetized, and a 0.1mL vaccine was injected subcutaneously through a 14gauge needle.

A second group of mice (n=48) were randomly assigned to receive a vaccine with either intravenously delivered (IV) MSCs (n=24) or with subcutaneous MSCs (n=24). Recipients within each MSC delivery group received an ALP vaccine (n=8), an allograft vaccine (n=8), an autograft vaccine (n=8), or were non-vaccinated (n=8).

Spleen Collection

Immediately after euthanasia, spleens were collected under sterile conditions in a laminar flow hood for the purpose of evaluating the cellular immune response to total bone

antigens by measuring T cell proliferation present in the spleen cells. Spleens were placed into petri dishes containing 1-2mL HBSS media (HBSS, 1x with calcium and magnesium, CORNING cellgro REF 21-020-CV) and subjected to a single-cell suspension protocol. Briefly: the spleen and media were placed into a cell strainer and mashed; spun in a centrifuge (Beckman Coulter Allegra™ 6R) at 1200 rpm for 5 minutes; resuspended in 2mL of ACK Lysing Buffer (Lonza BioWhittaker® Catalog No: 10-548E) for 5 min; resuspended in HBSS and spun at 1200 rpm for 5 minutes; and cells were resuspended in 1mL of freeze media and stored at -80°C.

CFSE Staining of Spleen Cells

Spleen cells were placed in a 37°C water bath to thaw, then added to warmed complete growth media and incubated for fifteen minutes. Cells were pelleted out and resuspended in PBS at a final concentration of $1x10^6$ cells/mL.

Carboxyfluorescein succinimidyl ester (CFSE) was added at 0.4µL CFSE per 1mL PBS and the cells were incubated at 37°C for ten minutes. Cells were washed with MEM media (MEM, 1x w/ Earle's salts & L-glutamine Cat. No. 10-010-Cx Cellgro), and resuspended in MEM at $4x10^5$ cells/200µL MEM for plating.

Spleen Cell Antigen Exposure

Antigens were added to a 96-well, flat-bottomed plate (Costar 9018 EIA/RIA plate 96 well flat bottom high binding certified, Corning Incorporated) at 50µL/mL MEM. All

spleen samples were co-cultured with Balb/C bone protein, C57BL/6 protein, and media. All samples were plated in triplicate. Samples were incubated at 37°C for 72 hours.

Cell Staining for Flow Cytometry

After 72 hours of incubation, plates were spun at 1800rpm for 3 minutes, the supernatant was removed and stored at -20°C., and the cell pellet was resuspended in FACS (Fluorescence-Activated Cell Sorting) buffer (1x PBS, FBS, and Sodium Azide) before being transferred to a 96-well, round bottom plate (96 well U-Bottom Plate, Tissue Culture, Treated by Vacuum Gas, Plasma Polystyrene, Non-pyrogenic REF 353077 Falcon). Non-stimulated spleen cells were plated at $4x10^5$cells/well for compensation wells. 5µL of mouse block (normal mouse serum, human IgG, FCR antibody) was added to each sample well. Antibody cocktails were made at a 1:200 dilution with 50µL/sample well, with anti-mouse CD4, CD3, and CD8 antibodies being used(Anti-mouse CD4 eFluor® 450 REF 48-0042-82 eBioscience, APC-AlexaFluor® 750 Conjugated Anti-mouse CD3e Cat #27-0032082 eBioscience, Anti-mouse CD8a (Ly-2) PE-Cy7 Cat# 25-0081-81, eBioscience). The compensation cocktail was made at a 1:200 dilution of CD3 Biotin (Biotin Conjugated Anti-mouse CD3e Cat# 13-0033-82 eBioscience) in FACs buffer. 50µL of the antibody cocktail was added to each sample well, 50µL of the compensation cocktail was added to each compensation well, and 50µL of FACs buffer was added to the blank compensation well. The plate was incubated in the dark for 20 minutes at room temperature. A 1: 500 solution of streptavidin conjugate in FACS buffer was prepared and added to the respective compensation wells at 50µL /well. The plate was incubated for 15 minutes at room

temperature in the dark before samples were resuspended in 200μL of FACs buffer and transferred to flow tubes. Samples were run on a Cyan Flow Cytometry Machine and data was analyzed using FlowJo vX0.7 for a Mac.

Statistical Analyses

Levels of T cell proliferation, CD4+ cell frequency, and CD8+ cell frequency were evaluated for all samples. Differences between groups were determined using an ANOVA and a Bonferroni multiple comparison post-test. A p-value of less than 0.05 was considered statistically significant for all analyses, and raw p-values are reported. Statistical analyses were performed using GraphPad Prism Version 5 for Windows.

Levels of T cell proliferation were evaluated for all spleen samples using FlowJo vX0.7. Populations of T cells were isolated based on the expression of the CD3 surface marker.

RESULTS

T Cell Proliferation

Levels of T cell proliferation in response to an allograft bone antigen and an autograft bone antigen were evaluated in all transplant recipients. The T cell proliferation level in all treatment groups was compared against the level found in recipients of an autograft alone. The mice in this treatment group only received self-bone and the bone transplant surgery, so they should experience the lowest levels of T cell proliferation.

Overall, the presence of AD-MSCs in an allograft transplant had no effect on T cell proliferation when exposed to an allograft bone antigen or and autograft bone antigen. Additionally, there was no significant difference in T cell proliferation levels found in allograft recipients compared to an autograft recipient.

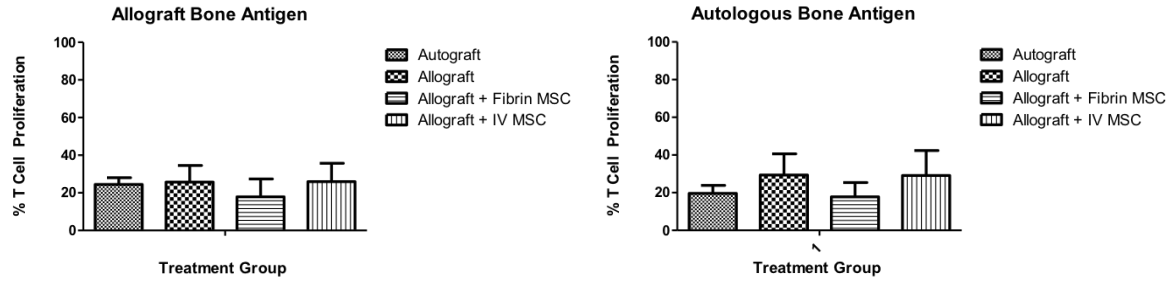

Figure 3.1 T Cell Proliferation Responses to Allograft and Autograft Bone Antigens in Recipients of an Allograft Transplant. T cell proliferation in recipients of an allograft only, an allograft with MSCs in fibrin, and an allograft with IV delivered MSCs was compared against T cell proliferation seen in recipients of an autograft**.** No significant differences in T cell proliferation levels with exposure to an allograft bone antigen or an autograft bone antigen were observed between treatment groups in recipients of a massive cortical allograft transplant.

The presence of AD-MSCs in an autograft transplant had no effect on T cell proliferation levels when exposed to an allograft bone antigen or an autograft bone antigen.

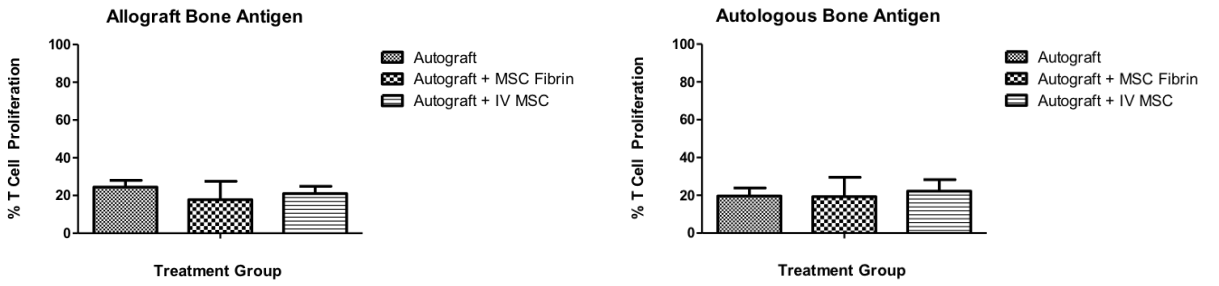

A B

Figure 3.2 T Cell Proliferation Responses to Allograft and Autograft Bone Antigens in Recipients of an Autograft Transplant. A.T cell proliferation was compared between recipients of an allograft bone vaccine, an allograft bone vaccine with MSCs delivered in fibrin, or an allograft bone vaccine with IV delivered MSCs. B.T cell proliferation was compared between recipients of an autograft bone vaccine, an autograft bone vaccine with MSCs delivered in fibrin, or an autograft bone vaccine with IV delivered MSCs.
Error Bars depict SD.

DISCUSSION

Contrary to our hypothesis, T cell proliferation in recipients of either a massive cortical allograft or autograft transplant was not affected by the presence of AD-MSCs. Data from this study suggests that the MSCs have a minimal effect on the T cell proliferation in response to a massive cortical allograft transplant. These results could also suggest that T cell proliferation is not a key player in massive cortical allograft failure. The humoral response to a transplant may have a bigger role in transplant failure in vivo. Additionally, transplant failure is normally associated with a chronic inflammatory response towards the donor tissue that prolongs over an elongated period of time (4). The immune response in this in vivo study was only measured at six weeks, so long-term immune response alterations were not evaluated. The addition of MSCs in vivo may still have

immunomodulatory effects that lead to increased bone healing, but these effects may occur immediately after transplant or over a longer period of time. However, the presence of MSCs with a transplant has been shown to increase new bone formation. These results suggest that the new bone healing in vivo promoted by the presence of MSCs is not primarily due to modulation of the T cell immune response, however this does not rule out other immunological effects. The addition of MSCs may promote new bone healing due to a local effect elicited by the MSCs.

The mechanisms of bone healing are widely studied, especially in cases of fracture repair. Fracture repair is carried out in four phases. The immediate phase involves formation of a hematoma around the fracture site. The early inflammatory phase is characterized by the recruitment of immune cells to the fracture site, and high levels of T cells and pro-inflammatory cytokines are observed. The regenerative phase is marked by the bridging of the fracture with new bone, which is then remodeled into mature bone during the final remodeling phase. Studies looking at the effects on non-steroidal anti-inflammatory drugs (NSAIDs) on fracture healing have shown that the initial pro-inflammatory phase following fracture is key for new formation and fracture healing. NSAIDs act on the cyclo-oxygenase, or COX pro-inflammatory pathway that is responsible for converting arachidonic acid into cycloendoperoxides that include prostanglandins, thromboxanes, and prostacyclin. The cycloendoperoxides are key factors needed for the pro-inflammatory immune response seen after cell membrane disruption, and are necessary for adequate fracture repair. Prostaglandin E2, one of the factors produced via the COX pathway, is known to enhance bone resorption by increasing the proliferation and activity of osteoclasts, as well as stimulating new bone formation by increasing the

replication and differentiation of osteoblasts. Interruption of this pro-inflammatory response, and more specifically, the Prostaglandin E2 response, by NSAIDs administered within the first two weeks after injury has ben shown to result in impaired fracture healing (1).

A study by Namgil, et al. looked at the effect of MSCs with NSAIDs by culturing canine bone marrow MSCs in osteogenic media to promote osteoblast differentiation of the MSCs. A COX-2 specific pro-inflammatory response was induced, and cells were treated with NSAIDs for 48 hours. At 24 hours, there was a significant drop in the Prostaglandin E2 levels, as well as a subsequent decrease in the MSC osteogenic process. However, at 48 hours, the Prostaglandin E2 levels had rebounded in the presence of MSCs, and there was a subsequent increase in the MSC osteogenic process. The researchers suggested that MSCs might have some inherent ability to compensate for the anti-inflammatory NSAID activity through regulation of Prostaglandin E2 levels to promote new bone formation (2).

The minimal effects of MSCs on T cell proliferation observed in the in vivo study differ from what was observed in the bone vaccine study. Spleen cells from recipients of a massive cortical allograft or autograft transplant experienced minimal changes in T cell proliferation with the addition of MSCs upon re-exposure to a bone antigen, whereas spleen cells from recipients of a bone vaccine with MSCs had a dampened T cell proliferation response. This would suggest that previous exposure to low levels of the bone antigen might induce tolerance towards that antigen. Mice that were vaccinated received two different exposures to the bone antigen at a low enough concentration to potentially induce a tolerogenic immune response, as compared to recipients of an allograft or autograft that could potentially induce an immune response towards the bone.

Future studies looking at the evaluation of MSC immunomodulatory effects in vivo at different time points following a massive cortical allograft transplant are needed to determine the extent of MSC effects on the cellular immune response. Additionally, future studies looking at the effects of prior exposure to a foreign bone antigen via vaccination on the overall outcome of a massive cortical allograft transplant are imperative in the search for an ideal treatment leading to improved allograft transplant success.

CONCLUSION

The addition of MSCs following a massive cortical allograft transplant has been shown to increase new bone formation. One of the potential mechanisms of this phenomenon may be attributed to the immunomodulatory properties of MSCs. The presence of MSCs may lead to new bone formation via the MSCs acting in a more local effect. MSCs will directly increase bone healing by differentiating into bone cells, and through paracrine effects. They could be enhancing the initial pro-inflammatory healing response that is seen with allograft transplant and with fracture repair, and is necessary for adequate new bone formation.

Examination of the MSC immunomodulatory effect on T cell proliferation in vivo suggest that MSCs may not modulate the immune response towards a massive cortical allograft or autograft primarily by affecting T cell proliferation. However, in the in vivo study, this response was measured at one point in time; a longitudinal study looking at the immunomodulatory effects of MSCs on T cell proliferation are needed to determine if these results are true at other time points following massive cortical allograft transplants.

Additionally, this study evaluated the effect of MSCs on the cellular immune response towards a foreign bone antigen via evaluation of T cell proliferation, so other immunological effects by MSCs cannot be ruled out. The use of MSCs in promoting new bone formation following a massive cortical transplant should continue to be explored, including other potential immunomodulatory effects of the MSCs in this environment.

CHAPTER 4

CONCLUSION AND FUTURE DIRECTIONS

CONCLUSION

The work detailed in this thesis was performed to aid in the exploration of a successful treatment protocol following the employment of a massive cortical allograft in a limb-salvage procedure. Current treatment protocols are accompanied by a high graft failure rate due to low levels of revascularization, new bone formation, and host-graft incorporation. These low levels have been deemed to be partly immune-mediated, so the use of immunosuppressives following allograft transplant are being evaluated. While immunosuppressive drugs such as Cyclosporin A effectively increase the success of an allograft, termination of the drug treatment results in eventual graft failure. Clinically, it is not advantageous to place a patient of immunosuppressives, so a different way of modulating the immune response towards the allograft is imperative.

In chapter two, we used a vaccine model to mimic the immune response seen towards an allograft as compared to an autograft in order to look at the effect of adipose-derived mesenchymal stromal cells on the humoral and cellular immune response towards the graft. We found that administration of MSCs had little to no detectable effect on the humoral immune response towards the total bone antigens delivered in the vaccine. However, the MSCs do have some effect on the cellular immune response, as observed with dampened levels of T cell proliferation in recipients of a vaccine with either IV or

subcutaneously delivered MSCs. Additionally, we found that administration of an allograft vaccine will lead to a dampened T cell proliferation level observed with exposure to an allograft bone antigen, particularly when the vaccine is given with MSCs.

In chapter three, we evaluated the effect of mesenchymal stem cells on the cellular immune response in an in vivo model to see if the results seen in the vaccine study were comparable as the results seen with an in vivo model. Answers to this question could help shed light on the increased level of new bone formation observed in recipients of a massive cortical allograft or autograft with the addition of MSCs. Contrary to our hypothesis that MSCs would dampen the cellular immune response towards the graft and thereby allow increased new bone formation, we saw little to no effect of the MSCs on the cellular immune response elicited towards a massive cortical allograft or autograft transplant. These results suggest that the new bone formation promoted by the presence of MSCs is not due primarily to immunomodulation of the T cell proliferation response by MSCs. These results could also be due to the bone antigens eliciting a low T cell response in the recipients. However, in the in vivo study, this response was measured at one point in time, so other immunological effects by MSCs cannot be ruled out. Additionally, recipients of a massive cortical allograft or autograft transplant had no prior exposure to a bone antigen, unlike recipients of a bone vaccine. This prior exposure may be a key player in the MSC immunomodulation of the T cell proliferation response seen in recipients of a bone vaccine, and may help explain why this effect was not observed in recipients of a transplant.

FUTURE DIRECTIONS

Further studies are needed to determine the effect of MSC administration following a massive cortical allograft transplant. While the MSCs had little to no effect on the T cell proliferation response in the in vivo study, other immunological effects elicited by the presence of MSCs should still be considered and explored. The effect of prior exposure to the bone antigen via a bone vaccine may play a role in the MSC immunomodulation of the T cell response, and could explain why the different results were observed in the in vivo study and in the vaccine study. In order to adequately compare these two results, an in vivo model looking at recipients of an initial vaccine with MSCs on Day 1, a booster vaccine with MSCs on Day 7, and a massive cortical allograft or autograft transplant on Day 21 compared to recipients of a transplant and MSCs alone is needed. The T cell proliferation in this model could be evaluated and correlated to levels of healing in order to determine if the prior exposure to a bone antigen and the presence of MSCs will dampen T cell proliferation in response to an allograft and autograft and allow for better levels of graft healing.

Additionally, a vaccine study is imperative in answering whether or not vaccination with an allograft bone antigen prior to a massive cortical allograft transplant will yield a better clinical outcome. While mice in this study received two vaccines, we would like to determine the number of vaccines and the time interval for administration that is most efficacious in promoting a positive clinical outcome. Timing of the first vaccination also needs to be explored. In cases of trauma patients, there is minimal time to administer the vaccine prior to a massive limb reconstruction surgery. Looking at the effects of vaccination

prior to the surgery compared to vaccination at the time of surgery could yield insights to the feasible use of this vaccination therapy in a clinical setting.

Our knowledge regarding an ideal treatment that would allow for increased massive cortical allograft success is still limited. The work described here shows that a total bone antigen is capable of inducing an immune response. The administration of MSCs has minimal to no effect on the humoral immune response in this vaccine model, however there is some effect on the cellular immune response. Unfortunately, this MSC immunomodulation of the cellular immune response is not seen in an in vivo massive cortical allograft transplant model. The work described here is a small step in understanding the response to a massive cortical allograft transplant in the hopes that one day this process will be better understood and result in a treatment protocol yielding high levels of host-graft incorporation and new bone volume, thereby increasing the overall success rate of an allograft transplant.

REFERENCES

CHAPTER 1

1. Bernardo, M., & Fibbe, W. (2013). Mesenchymal Stromal Cells: Sensors and Switchers of Inflammation. Cell Stem Cell, 13(4), 392-402.

2. Chen, X., Yang, T., Wang, W., Sun, H., Ma, B., Li, C., . . . Fan, Q. (2009). Establishment and characterization of human osteosarcoma cell lines with different pulmonary metastatic potentials. Cytotechnology, 61(1-2), 37-44.

3. Dominici, M., et al. "Minimal criteria for defining multipotent mesenchymal stromal cells. The International Society for Cellular Therapy position statement."Cytotherapy 8.4 (2006): 315-317.

4. Goblirsch, M., Zwolak, P., & Clohisy, D. (2006). Biology of Bone Cancer Pain. Clin Cancer Res, 12, 6231s-6235s.

5. Goldberg, V., & Stevenson, S. (1987). Natural History of Autografts and Allografts. Clin Orthop Relat Res, 225, 7-16.

6. Horwitz, E., Le Blanc, K., Dominici, M., Mueller, I., Slaper-Cortenbach, I., Marini, F., . . . Keating, A. (2005). Clarification of the nomenclature for MSC: The International Society for Cellular Therapy position statement. Cytotherapy, 7(5), 393-395.

7. Lozano-Ondoua, A., Symons-Liguori, A., & Vanderah, T. (2013). Cancer-induced bone pain: Mechanisms and models. Neuroscience Letters, 557(A), 52-59.

8. MacEwen, E., & Kurzman, I. (1996). Canine Osteosarcoma: Amputation and chemoimmunotherapy. Vet Clin North Am Small Anim Pract, 26(1), 123-33.

9. Marulanda, G., Henderson, E., Johnson, D., Letson, D., & Cheong, D. (2008). Orthopedic Surgery Options for the Treatment of Primary Osteosarcoma. Cancer Control, 15(1), 13-20.

10. Mauldin, G., Matus, R., Withrow, S., & Patnaik, A. (1988). Canine osteosarcoma. Treatment by amputation versus amputation and adjuvant chemotherapy using doxorubicin and cisplatin. J Vet Intern Med, 2(4), 177-80.

11. Mayer, M., & Grier, C. (2006). Palliative radiation therapy for canine osteosarcoma.Radiation Oncology, 47, 707-709.

12. Murphy, K., & Travers, P. (2008). Janeway's immunobiology (7th ed.). New York: Garland Science.

13. Nather, A., David, V., Teng, J., Lee, C., & Pereira, B. (2010). Effect of Autologous Mesenchymal Stem Cells on Biological Healing of Allografts in Critical-sized Tibial Defects Simulated in Adult Rabbits. Annals Academy of Medicine, 39(8).

14. National Cancer Institute: PDQ® Osteosarcoma and Malignant Fibrous Histiocytoma of Bone Treatment. Bethesda, MD: National Cancer Institute. Date last modified <05/22/2015>. Available at: http://www.cancer.gov/types/bone/patient/osteosarcoma-treatment-pdq. Accessed <05/24/2015>.

15. Regner, M. (2001). Cross-reactivity in T-cell antigen recognition. Immunology and Cell Biology, 79, 91-100.

16. Sivanathan, Kisha Nandini, et al. "Interferon-gamma modification of mesenchymal stem cells: implications of autologous and allogeneic mesenchymal stem cell therapy in allotransplantation." Stem Cell Reviews and Reports 10.3 (2014): 351-375.

17. Stem Cell Basics: Introduction. In Stem Cell Information [World Wide Web site]. Bethesda, MD: National Institutes of Health, U.S. Department of Health and Human Services, 2015 [cited Wednesday, July 08, 2014] Available at <http://stemcells.nih.gov/info/basics/pages/basics1.aspx>

18. Strong, D. Michael, et al. "Immunologic responses in human recipients of osseous and osteochondral allografts." Clinical orthopaedics and related research 326 (1996): 107-114.

19. Welter, J., Shaffer, J., Stevenson, S., Davy, D., Field, G., Klein, L., . . . Goldberg, V. (1990). Cyclosporin A and tissue antigen matching in bone transplantation. Fibular allografts studied in the dog. Acta Orthop Scand, 61(6), 517-27.

20. Withrow, S. (2013). Withrow & MacEwen's small animal clinical oncology (5th ed.). St. Louis, Mo.: Elsevier/Saunders.

21. Yin, Y., & Mariuzza, R. (2009). The Multiple Mechanisms of T Cell Receptor Cross-reactivity. Immunity, 31(6), 849-851.

22. Zhou, W., Hao, M., Du, X., Chen, K., Wang, G., & Yang, J. (2014). Advances in Targeted Therapy for Osteosarcoma. Discovery Medicine, 17(96), 301-7.

CHAPTER 2

1. Bunnell, Bruce A., Aline M. Betancourt, and Deborah E. Sullivan. "New concepts on the immune modulation mediated by mesenchymal stem cells."Stem Cell Res Ther 1.5 (2010): 34.

2. Cella, M., Engering, A., Pinet, V., Pieters, J., & Lanzavecchia, A. (1997). Inflammatory stimuli induce accumulation of MHC class II complexes on dendritic cells. Nature,388, 782-787.

3. Chang, S., Warner, J., Liang, L., & Fairman, J. (2009). A Novel Vaccine Adjuvant for Recombinant Flu Antigens. Biologicals, 37(3), 141-147.

4. Game, David S., and Robert I. Lechler. "Pathways of allorecognition: implications for transplantation tolerance." Transplant immunology 10.2 (2002): 101-108.

5. Murphy, K., & Travers, P. (2008). Janeway's immunobiology (7th ed.). New York: Garland Science.

6. Paulina Ruiz, Paula Maldonado, Yessia Hidalgo, et al., "Transplant Tolerance: New Insights and Strategies for Long-Term Allograft Acceptance," Clinical and Developmental Immunology, vol. 2013, Article ID 210506, 15 pages, 2013. doi:10.1155/2013/210506

7. Stevenson, Sharon. "The immune response to osteochondral allografts in dogs." The Journal of Bone & Joint Surgery 69.4 (1987): 573-582.

8.Welter, J., Shaffer, J., Stevenson, S., Davy, D., Field, G., Klein, L., . . . Goldberg, V. (1990). Cyclosporin A and tissue antigen matching in bone transplantation. Fibular allografts studied in the dog. Acta Orthop Scand, 61(6), 517-27.

9. Wheeler, Donna L., and William F. Enneking. "Allograft bone decreases in strength in vivo over time." Clinical orthopaedics and related research 435 (2005): 36-42.

CHAPTER 3

1. Bernardo, Maria Ester, and Willem E. Fibbe. "Mesenchymal stromal cells: sensors and switchers of inflammation." Cell stem cell 13.4 (2013): 392-402.

2. Dieudonne, François-Xavier, et al. "Promotion of Osteoblast Differentiation in Mesenchymal Cells Through Cbl-Mediated Control of STAT5 Activity." *Stem Cells* 31.7 (2013): 1340-1349.

3. Fischer, Uwe M., et al. "Pulmonary passage is a major obstacle for intravenous stem cell delivery: the pulmonary first-pass effect." Stem cells and development18.5 (2009): 683-692.

4. Murphy, K., & Travers, P. (2008). Janeway's immunobiology (7th ed.). New York: Garland Science.

5. Pallotta, Maria T., et al. "Indoleamine 2, 3-dioxygenase is a signaling protein in long-term tolerance by dendritic cells." Nature immunology 12.9 (2011): 870-878.

6. Polchert D, Sobinsky J, Douglas G, et al. IFN-γ activation of mesenchymal stem cells for treatment and prevention of graft versus host disease. European journal of immunology. 2008;38(6):1745-1755. doi:10.1002/eji.200738129.

7. Rodrigo Haddad and Felipe Saldanha-Araujo, "Mechanisms of T-Cell Immunosuppression by Mesenchymal Stromal Cells: What Do We Know So Far?," BioMed Research International, vol. 2014, Article ID 216806, 14 pages, 2014. doi:10.1155/2014/216806

CHAPTER 4

1. Bernardo, Maria Ester, and Willem E. Fibbe. "Mesenchymal stromal cells: sensors and switchers of inflammation." Cell stem cell 13.4 (2013): 392-402.

2. English, Karen, Anna French, and Kathryn J. Wood. "Mesenchymal stromal cells: facilitators of successful transplantation?." Cell stem cell 7.4 (2010): 431-442.

3. LaRosa, David F., Adeeb H. Rahman, and Laurence A. Turka. "The innate immune system in allograft rejection and tolerance." The Journal of Immunology178.12 (2007): 7503-7509.

4. Larsen, C. P., P. J. Morris, and J. M. Austyn. 1990. Migration of dendritic leukocytes from cardiac allografts into host spleens: a novel pathway for initiation of rejection. J. Exp. Med. 171: 307–314.

5. Matzinger, P. 1994. Tolerance, danger, and the extended family. Annu. Rev. Immunol. 12: 991–1045.

6. Murphy, K., & Travers, P. (2008). Janeway's immunobiology (7th ed.). New York: Garland Science.

7. Pallotta, Maria T., et al. "Indoleamine 2, 3-dioxygenase is a signaling protein in long-term tolerance by dendritic cells." Nature immunology 12.9 (2011): 870-878.

APPENDIX I: SOP'S

Allograft and Autograft Bone Harvest

Bones used for the allograft vaccine were obtained from Balb/C mice, with both femurs from each mouse collected. Mice were heavily anesthetized with isoflurane and oxygen, and euthanized via cervical dislocation. Femurs were collected under sterile conditions in a laminar flow hood. All instruments used were sterilized prior to use. Femurs were isolated, scraped with a fresh scalpel blade to remove all periosteum, and placed into cyrovials. Cyrovials were immediately placed into a container with liquid nitrogen to flash-freeze the bones. Bones were stored at -80°C for a minimum of one week before further processing.

Bones used in the autograft vaccine were obtained from C57BL/6 mice in the same manner as described for the allograft bone collection.

Bone Powder Collection

The donor femurs were removed from the -80°C storage and were immediately placed into a liquid nitrogen container. A mortar and pestle were placed in ethanol for 10 minutes and used to smash the bones into a powder. The bone powder was weighed and a final concentration of bone powder in the vaccine was 10μg/mL.

Donor femurs used in vaccines given to MSC recipients were removed from the -80°C storage and immediately placed into a liquid nitrogen container. Bones were placed in a sterile metal container, and a hammer was used to smash the lid and crush the bones into a powder. The bone powder was weighed and a final concentration of 10μg/mL was used in the vaccines.

Serum Collection

Mice cages were placed on a heating pad under a heat lamp for a minimum of 20 minutes before beginning the blood draws. Mice were placed in a restraining tube underneath the heat lamp, and 0.1mL of blood was collected from the tail vein on Day 1 and Day 7 before administration of the vaccine. On Day 21, mice were heavily anesthetized, and blood was collected via cardiac puncture just prior to euthanasia. Blood was placed into serum separator tubes (BD Microtainer® Serum Separator Tubes, REF 365956), which were spun down in a micro-centrifuge (Fisher Scientific accuSpin Micro 17) at 7 x 1,000g for 5 minutes. Serum was pipetted into ependorf tubes and stored at -20°C.

Vaccine Injection

C57BL/6 mice were treated with an initial vaccine injection on Day 1, followed by a booster vaccine injection on Day 7. Mice were anesthetized under oxygen and isoflurane, and a 0.1mL vaccine was injected subcutaneously through a 14gauge needle on the craniodorsal aspect between the shoulder blades.

Spleen Collection

Immediately after euthanasia, spleens were collected under sterile conditions in a laminar flow hood. Mice were sprayed with 75% ethanol, and spleens were removed with sterile instruments. Spleens were placed into petri dishes containing 1-2mL HBSS media (HBSS, 1x with calcium and magnesium, CORNING cellgro REF 21-020-CV) and subjected to a single-cell suspension protocol. A cell strainer was placed on a 15mL conical tube, and the spleen and media were dumped into the cell strainer and mashed with a 3mL syringe

plunger. The conical tubes were spun in a centrifuge (Beckman Coulter Allegra™ 6R) at 1200 rpm for 5 minutes and the cell pellet was then resuspended in 2mL of ACK Lysing Buffer (Lonza BioWhittaker® Catalog No: 10-548E) for 5 min. HBSS was added to the tube and spun at 1200 rpm for 5 minutes. Cells were resuspended in 1mL of freeze media, transferred to a cyrovial, and stored at -80°C.

Bone Protein Extraction

Bone protein from C57BL/6 mice was isolated using TRIzol Reagent (TRIzol Reagent, Life Technologies 15596-026). Femurs were collected from C57BL/6 mice in a sterile manner and stored at -80°C prior to use.

Femurs were immediately placed into liquid nitrogen, freeze fractured, and crushed into a powder. TRIzol reagent was added at 1mL/50mg of protein, and the sample was homogenized using a power homogenizer (Fisher Scientific PowerGen 1000). The homogenized sample was incubated for 5 minutes at room temperature and chloroform (Chloroform, 99.9+%, A.C.S. HPLC grade, Aldrich Chemical Co, Inc. 67-66-3) was added at 0.2mL per 1mL of TRIzol Reagent, and then centrifuged in a Hermle Labnet Z-383K High Performance Centrifuge at 12,000 x g for 15 minutes at 4°C. The upper aqueous phase was removed, and 0.3mL of 100% ethanol per 1mL of TRIzol Reagent was added. The sample was spun at 2,000xg for 5 minutes at 4°C, and the supernatant were transferred to a new tube. Isopropanol (2-Propanol HPLC Grade, Fisher Scientific A451-4) was added to the supernatant at 1.5mL isopropanol per 1mL TRIzol Reagent and the sample was incubated for 10 minutes at room temperature, spun at 12,000 x g for 10 minutes at 4°C, and the supernatant was removed. The protein pellet was washed with 2mL of a 0.3M guanidine

hydrochloride in 95% ethanol wash solution per 1mL of TRIzol Reagent, incubated for 20 minutes at room temperature and then spun at 7500 x g for 5 minutes at 4°C. The wash solution was removed and 2mL of 100% ethanol was added to the protein pellet. The solution was vortexed and then incubated at room temperature for 20 minutes. The sample was spun at 7500 x g for 5 minutes at 4°C, the ethanol wash was removed, and the protein pellet air-dried for 10 minutes before 200µL of 1% SDS was added. The solution was pipetted up and down until the pellet was resuspended, spun at 10,000 x g for 10 minutes at 4°C and the supernatant containing the protein was transferred to a new tube. The protein yield was determined with a BCA Protein Assay Kit (Pierce 23225).

BCA Protein Assay

A BCA Protein Assay Kit (Pierce 23225) was used to determine the protein concentration extracted from the TRIzol reagent protein extraction protocol. 10mL of Reagent A was added to 200µL of Reagent B to form a working reagent. Contents of an albumin standard were diluted in sterile PBS to create 8 protein standards at the following dilutions: 0, 0.125, 0.25, 0.5, 0.75, 1.0, 1.5, and 2.0mg/mL. The working reagent was added to a 96-well flat bottom plate (Costar EIA/RIA plate 96-well flat bottom high binding certified plate #90128) at 200µL/well. The standards were plated in triplicate at 25µL/well. Protein samples were added at a 1:10 and 1:25 dilution and plated in triplicate. The plate was placed on a plate shaker for 30 seconds and incubated at 37°C for 30 minutes. The plate was cooled to room temperature and read on the GenX plate reader at 562nm.

Mouse IgG2a Ready-SET-Go! ELISA

A Mouse IgG2a Ready-SET-Go! ELISA was purchased from eBioscience (Catalog #88-50420). A 96-well flat bottom plate (Costar EIA/RIA plate 96-well flat bottom high binding certified plate #90128) was used. The Coating Buffer (1x) provided was diluted at a 1:10 dilution in sterile PBS (10x). Capture antibody (250x) was diluted in the coating buffer at a 1:250 dilution. 100µL of the capture antibody: coating buffer dilution was added to each well, the plate was sealed with a plate cover, and incubated at 37°C overnight.

A blocking buffer was prepared by diluting the Assay Buffer A Concentrate (20x) in deionized water at a 1:10 dilution. The plate was washed twice with 0.05% PBS-Tween, with 1 minute of soaking time allowed for each wash. 250µL of Blocking Buffer was added to each well and the plate was incubated overnight at 4°C.

A standard was prepared by reconstituting mouse IgG2a standard in distilled water for a concentration of 50ng/mL. The standard was allowed to reconstitute for 30 minutes. The detection antibody (250x) was diluted in Assay Buffer A (1x) at a 1:250 dilution. The plate was washed twice as done in the previous wash step. Two-fold serial dilutions of the standards with Assay Buffer A were performed to make the standard curve. This was done by added 100µL of Assay Buffer A (1x) to all standard wells. 100µL of reconstituted standard was added in duplicate to well A1 and A2. Well contents were mixed via pipetting, and 100µL were transferred to wells B1 and B2, respectively. This procedure was repeated 5 times. The Assay Buffer A (1x) was added to all blank wells at 100µL/well, and added to sample wells at 50µL/well. Samples were pre-diluted I Assay Buffer A (1x) at a 1:10 dilution, and 50µL of this dilution was added to the sample well. The Detection Antibody was added to all wells at 50µL/well, and the plate was covered and incubated at room

temperature for 3 hours. The plate was washed as previously done for 4 washes. 100µL of the Substrate Solution was added to each well, and the plate was incubated at room temperature for 15 minutes. 100µL of Stop Solution was added to each well, and the plate was read at 450nm.

Antibody Detection ELISA

A Nunc-Immuno Maxisorp 96-well plate (Nunc #442404, Fisher 12-565-135) was coated with an antigen resuspended in bicarbonate buffer at 5µg/mL, with 50µL added to each well. The plate was covered with a plate sealer and incubated overnights at 4°C.

The plate was washed three times with 0.05% PBS-Tween. A 5% PBS-milk blocking buffer was made, and 250µL was added to each well. The plate was incubated for 60 minutes at room temperature. Sample dilutions were prepared by diluting samples in 3% BSA-PBS (Bovine Serum Albumin Fraction V 100g BP1605-100, Lot 067027 Catalog #9048-46-8, Fisher Scientific). The first dilution (1:10) was made by adding 6µL of sample to 54µL of 3% BSA-PBS, and samples were added to the first row of the plate. The rest of the plate was coated with 54µL of 3% BSA-PBS, and 6µL of the 1:10 dilution was transferred to the second row. Serial dilutions were performed in a similar matter and ranged from 1:10 to 1:10,000 for each sample. Tips were changed between each dilution. Blank wells contained 3% BSA-PBS. The plate was sealed and incubated at room temperature for 90 minutes. The plate was then washed three times with 0.05% PBS-Tween. An anti-IgG antibody (ImmunoPure® Antibody Goat Anti-Mouse IgG (H+L), Pierce Prod# 31430) was diluted 1:500 in 5% BSA-PBS, and 50µL was added to each well. The plate was incubated for 60 minutes and room temperature and the TMB substrate (3, 3', 5, 5'-Tetra Methylbenzidine

(TMB) Liquid Substrate System for ELISA, Sigma-Aldrich T0440-1L) was brought to room temperature during this incubation period.

The plate was washed three times with 0.05% PBS-Tween, and 50µL of the TMB substrate was added to each well. Color was allowed to develop for two minutes before 50µL of a 1N HCl stop solution was added to each well. The plates were read at 450nm.

Adipose Tissue Harvest

Adipose tissue was collected from the abdominal fat pads of C57BL/6 mice using sterile instruments under a laminar flow hood. Fat was isolated and placed in a petri dish containing HBSS. Spleens were minced with a scalpel blade, and resuspended in 1mg/mL of collagenase with an antibiotic/antimycotic solution in a 50mL conical tube. Cells were incubated at 37°C for 30 minutes before MSC media was added. Cells were spun at 2000rpm for 5 minutes, resuspended in MSC media, and spun once more. Cells were resuspended in MSC media and plated in flasks that were stored at 37°C.

Adipose-Derived Mesenchymal Stem Cell Collection

Cells were allowed to incubate at 37°C until reaching a minimum of 80% confluency, as measured by visual inspection under a microscope. Cells were washed with HBSS, and trypsin was added to the flasks and allowed to sit at room temperature for 5 minutes. The sides of the flasks were vigorously tapped to cause cells to lift off the flask, and the cell-trypsin solution was transferred to a 50mL conical tube. The tube was spun at 1220 for 5 minutes, and the cells were resuspended in PBS-Heparin (0.1mL Heparin in 9.9mL sterile

PBS) with a final volume of 500,000 cells/100µL PBS-Heparin for injection. MSCs in unused flasks were frozen and stored for later use.

Cryopreservation and Storage of MSCs

Cells in flasks that were not used for treatment were washed, trypsinized, and spun like mentioned before, and were resuspended in freeze media. Cells were transferred to cryovials and stored at -80°C.

Spleen Thawing Protocol

Cryovials containing the single-cell spleen suspension were thawed quickly in a 37°C water bath. Contents of the cyrovials were transferred to a 15mL conical tube containing 10mL of warmed complete growth media. Cells were gently mixed in the tube and incubated at 37°C for 15 minutes, with the tube lid left slightly loose. Cells were pelleted via centrifugation at 1220rpm and 25°C for 30 minutes. Media above the pellet was decanted and cells were counted and resuspended in sterile PBS at $1x10^6$cells/mL.

CFSE Staining

Conical tubes containing the spleen cells resuspended in sterile PBS at $1x10^6$cells/mL were spun at 1200g for 5 minutes. The PBS was decanted off, and cells were resuspended in 2mL of sterile PBS. Cells were counted, and resuspended in sterile PBS for a final concentration of $1x10^6$cells/mL. Carboxyfluorescein succinimidyl ester (CFSE) (CellTrace™ CFSE Cell Proliferation Kit Catalog #C34554) was added at 0.4µL CFSE per 1mL sterile PBS added to the spleen cells. The cells were incubated at 37°C for 10 minutes,

and then the conical tube was filled to 20mL with MEM. Tubes were placed on ice for 5 minutes, and then spun at 1200rpm for 5 minutes. Pellets were washed twice with MEM, and cells were counted. The cells were resuspended in MEM at $4x10^5$cells/200µL MEM for plating.

Spleen Cell Antigen Exposure

A 96-well flat bottom plate (Costar EIA/RIA plate 96-well flat bottom high binding certified plate #90128) was used for spleen cell antigen exposure. Antigens were diluted in MEM at 0.01µL/50µL. 50µL of this solution was added to all antigen-spleen sample wells. 50µL MEM was added to non-stimulated spleen sample wells. 100µL of the spleen cells was added to each well, and plates were incubated at 37°C for 72 hours.

After 72 hours, plats were spun at 1800rpm for 5 minutes, and the supernatant was transferred to cryovials and stored at -20°C. Cells were resuspended in FACS buffer and transferred to a 96-well round bottom plate (96 well U-Bottom Plate, Tissue Culture, Treated by Vacuum Gas, Plasma Polystyrene, Non-pyrogenic REF 353077 Falcon) for flow cytometry staining.

Flow Cytometry Staining

Unstained spleen cells were added to the plate for color compensation wells. One well was plated for every antibody color used, as well as one blank well for a negative compensation well. Plates were spun at 1800rpm for 3 minutes, and the FACS buffer was flicked off. 5µL of mouse block was added to each sample well, and plates were stored in a drawer. An antibody cocktail was made with a 1:200 dilution of antibody in FACS buffer.

CD3, CD4, and CD8 antibodies were used (Anti-mouse CD4 eFluor® 450 REF 48-0042-82 eBioscience, APC-AlexaFluor® 750 Conjugated Anti-mouse CD3e Cat #27-0032082 eBioscience, Anti-mouse CD8a (Ly-2) PE-Cy7 Cat# 25-0081-81, eBioscience). The compensation cocktail was made with a 1:200 dilution of CD3 Biotin (Biotin Conjugated Anti-mouse CD3e Cat# 13-0033-82 eBioscience) in FACS buffer. Cocktails were vortexed for 5 seconds. 50µL of the antibody cocktail was added to each sample well, 50µL of the compensation cocktail was added to the color compensation wells, and 50µL of FACs buffer was added to the negative compensation well. Plates were incubated at room temperature for 20 minutes in the dark. Plates were washed two times, with one wash being: adding 200µL FACS to each well, spinning the plates at 1800rpm for 5 minutes, and flicking off the FACS buffer. Plates were stored in a drawer and streptavidin cocktails were made. One 1.5mL ependorf tube was used for each individual streptavidin (Streptavidin FITC Catolog#11-4317-87 eBioscience, Streptavidin APC REF#17-4317-82 eBioscience, Streptavidin eFluor®450 REF#48-4317-82 eBioscience, Streptavidin PE REF#12-4317-87 eBioscience). 500µL of FACS buffer was added to 1µL of the streptavidin. 50µL of the streptavidin cocktail was added to the respective color compensation well. 50µL of FACS was added to all sample wells and to the negative compensation well. Plates were incubated at room temperature for 15 minutes in the dark. The wash step was performed as done before for a total of one wash. 200µL of FACS buffer was added to each well, and contents were transferred to flow cytometry tubes and run on a Cyan Flow Cytometry Machine.

Bone Homogenization

Femurs harvested from Balb/C and C57BL/6 bones were freeze-fractured and placed into homogenizer tubes containing 500µL of lysis buffer before being placed into a power homogenizer. The homogenized lysate sample was placed in a sonicator for 3-second bursts with 20 seconds between each burst. This was done three times. The lysate sample was transferred to ependorf tubes, placed in a sonicator as done previously, and then spun at 4°C for 5 minutes in a micro-centrifuge. A BCA Protein Assay Kit (Pierce 23225) was used to determine the bone protein concentration for the Balb/C lysate sample and for the C57BL/6 lysate sample.

Western Blot Sample Preparation

Balb/C lysate samples were mixed with SDS 6x buffer and deionized water at: 15µL bone lysate, 11µL SDS 6x buffer, and 40µL water. C57BL/6 lysate was mixed at: 54.2µL bone lysate, 11µL SDS 6x buffer, and 0.8µL water. A final loading concentration of 20mg/mL bone protein was achieved with the above solutions. Solutions were made in ependorf tubes, and boiled for 5 minutes.

Western Blot

20µL of the bone lysate sample were added to their respective gel wells, and 5µL of the protein standard (Precision Plus Protein™ Standards Kaleidoscope™ Bio-Rad #161-0375) was added to the standard wells. The charge of the loading system was set to 180 volts and ran for 41 minutes. A tupperware was filled with 2 blot papers and 4 sponges, and soaked with transfer buffer. Four box containers were filled with: transfer buffer,

transfer buffer, milliQ water, and filtered methanol, respectively. A PVDF transfer membrane (Immun-Blot® PVDF Membrane) was placed in the methanol box for 30 seconds and transferred into the milliQ box for 2 minutes. The SDS gel was carefully removed from its plastic casing and placed into the first box containing transfer buffer. The blot papers were moved into the second box containing transfer buffer, and allowed to sit for 5 minutes, along with the SDS gel. After 5 minutes, the blot papers, gel, and sponges were assembled in the following order and loaded into a blot module (XCell Sure Lock™): sponge, sponge, blot paper, gel, blot paper, sponge, and sponge. The blot module was run at 30 volts and 0.17Amps for 40 minutes.

Pooled serum from five recipients of an allograft bone vaccine was placed into a 50 mL conical tube. The same was done with pooled serum from five recipients of an autograft bone vaccine. Both tubes were filld to the 5mL line with a TBST blocking buffer, resulting in a 1:1 dilution of serum: buffer. A third 50mL conical tube was filled to the 5mL line with the blocking buffer and 2µL of tubulin was added to serve as a loading control. The three tubes were stored at 4°C.

A container was filled with blocking buffer, and the blot paper was placed in the container after being removed from the blot module. The container was placed on a gentle rocker for 1 hour. The liquid was then dumped off, and the gel was cut into three pieces along the middle of the 2 protein standard wells. One gel piece was placed into the 50mL conical tube containing the pooled allograft serum. One gel piece was placed into the 50mL conical tube containing the pooled autograft serum. One gel piece was placed in the loading control 50mL conical tube. Gel pieces were placed so they were stuck to the side of the tube. The tubes were placed in a spinning carousal and stored at 4°C overnight.

The gel pieces were removed and placed into a container filled with 1x TBST and placed on a slow rocker for 5 minutes. The liquid was dumped off and new 1x TBST was added before the container was placed on the slow rocker for 5 minutes. The liquid was changed 2 times for a total of 3 washes. After the last wash, the container was filled with blocking buffer and 10µL of anti-mouse IgG secondary antibody was added for a 1:2000 dilution. The container was placed on a slow rocker for 1 hour, and the wash step was then repeated three times.

A Super Signal West Dura Extended Duration Substrate Kit (Thermo Scientific Product 34075) was used to prepare the blot papers for analysis in a Bio Rad Molecular Imager® ChemiDoc™ XRST with Image Lab™ Software.

K7M2 Co-culture

The pooled serum from recipients of either an allograft vaccine or an autograft vaccine used in the Western Blot was incubated with 50,000 cells of the K7M2 murine osteosarcoma line with a 1:100 final dilution of serum in blocking buffer for 30 minutes. Non-stimulated cells were suspended in FACS. Cells were plated on a 96-well round bottom plate (96 well U-Bottom Plate, Tissue Culture, Treated by Vacuum Gas, Plasma Polystyrene, Non-pyrogenic REF 353077 Falcon). A donkey-anti mouse IgG antibody with fluorescent tag (Fluorescein [FITC]-conjugated Affini Pure $F(ab')_2$ Fragment Donkey anti-mouse IgG (H&L), JacksonImmuno Code # 715-096-150) was added to each serum: cell well at a 1:100 dilution in FACS buffer. Cells were incubated for 20 minutes, resuspended in FACS buffer, and run through a CyAn ADP DakoCytomation flow cytometry machine with Summit V4.3.02 Build 2451 software. The flow data was analyzed using FlowJo vX0.7. A K7M2 cell

gate was established on all samples and the mean intensity of the FITC channel was evaluated to look at the number of staining events as an indirect measure of the amount of antibody bound to the cell. A histogram of FITC expression in the cells only sample was used to create a lower threshold expression level of 1% to account for random binding. FITC histograms of the other cell populations were created to look at the percentage of cells expressing antibody above the threshold level.

RECIPES

Cationic Liposomal DNA Complex (CLDC)

37.5µL DOTAP Liposomal Transfection Reagent
12.5µL polyinosinic-polycytidylic acid (poly I:C) (1mg/mL)

Vaccine Formula

Equal amount of CLDC resuspended in sterile PBS
Antigen at 10µg/mL concentration

Bone Vaccine Antigens

Balb/C bone dust
C57BL/6 bone dust
Bovine alkaline phosphatase (Phosphatase, Alkaline from bovine intestinal mucosa, Sigma-Aldrich P7640-500MG)

FACS Buffer

980mL PBS (1x)
20mL FBS
0.5g Sodium Azide
*Sterile filtered and stored at 4°C

MSC Media

1L low glucose DMEM (Corning Cellgro DMEM 11885)
150mL FBS (Atlas Fetal Bovine Serum Lot F12073011)
20mL MEM Vitamins
10mL Antibiotics/Antimycotics (Gemini Bio-Products Lot 30009111)
10mL MEM with non-essential amino acids

Freeze Media

11mL sterile DMSO
45mL RPMI
45mL FBS

Growth Media

50mL Atlas FBS Serum
5mL Antibiotic/Antimycotics (Gemini Bio-Products Lot 30009111)
500mL MEM (Corning Cellgro MEM, 1x [minimum essential medium eagle] with Earle's Salts and L-glutamate, lot 10010266 REF 10-010-CV)
*Sterile filtered and stored at 4°C

Mouse Block

Resuspended lyophilized mouse serum (Jackson ImmunoResearch) in 5mL deionized water
83µL human IgG
1:100 dilution of mouse anti-FcR III (CD16/32) (eBioscience)

1N HCl Stop Solution

9mL 37% hydrochloric acid
99mL deionized water

Lysis Buffer

10µL Tris-HCl 1M pH 7.5
50µL 3M NaCl
10µL Tritan 100x
0.3mL deionized water

1µL sodium orthovaninate
3.48µL PMSF protease inhibitor 10mg/mL
7µL Proteinase Inhibitor Cocktail 7x
*Kept on ice

TBST Blocking Buffer

100mL 1x TBST
2.5g non-fat powdered milk
1g BSA

APPENDIX II: ELISA DATA

Ready-SET-Go! Mouse IgG ELISA Results

Software Version 2.00.18

Plate Number Plate 1
Date 5/30/13
Time 4:52:26 PM
Reader Type: Synergy
Reader Serial Number: 267524
Reading Type Reader

Procedure Details
Plate Type 96 WELL PLATE
Read Absorbance Endpoint
Full Plate
Wavelengths: 450, 570
Read Speed: Normal

Layout

	1	2	3	4	5	6	7	8	9	10	11	12	
A		STD1	STD1	BLK	SPL5	SPL12	SPL19	SPL26	SPL33	SPL40	SPL47	SPL54	Well ID
		250	250		10000	10000	10000	10000	10000	10000	10000	10000	Conc/Dil
B		STD2	STD2	BLK	SPL6	SPL13	SPL20	SPL27	SPL34	SPL41	SPL48	SPL55	Well ID
		125	125		10000	10000	10000	10000	10000	10000	10000	10000	Conc/Dil
C		STD3	STD3	BLK	SPL7	SPL14	SPL21	SPL28	SPL35	SPL42	SPL49	SPL56	Well ID
		62.5	62.5		10000	10000	10000	10000	10000	10000	10000	10000	Conc/Dil
D		STD4	STD4	SPL1	SPL8	SPL15	SPL22	SPL29	SPL36	SPL43	SPL50	SPL57	Well ID
		31.25	31.25	10000	10000	10000	10000	10000	10000	10000	10000	10000	Conc/Dil
E		STD5	STD5	SPL2	SPL9	SPL16	SPL23	SPL30	SPL37	SPL44	SPL51	SPL58	Well ID
		15.625	15.625	10000	10000	10000	10000	10000	10000	10000	10000	10000	Conc/Dil
F		STD6	STD6	SPL3	SPL10	SPL17	SPL24	SPL31	SPL38	SPL45	SPL52	SPL59	Well ID
		7.8125	7.8125	10000	10000	10000	10000	10000	10000	10000	10000	10000	Conc/Dil
G		STD7	STD7	SPL4	SPL11	SPL18	SPL25	SPL32	SPL39	SPL46	SPL53	SPL60	Well ID
		3.9063	3.9063	10000	10000	10000	10000	10000	10000	10000	10000	10000	Conc/Dil
H													Well ID
													Conc/Dil

Results
Actual Temperature: 27.1
Actual Temperature: 27.1

	1	2	3	4	5	6	7	8	9	10	11	12	
A		0	0	0	0	0	0	0	0	0	0	0	450
		0	0	0	0	0	0	0	0	0	0	0	570
		0	0	0	0	0	0	0	0	0	0	0	Blank 450
		0	0	0	0	0	0	0	0	0	0	0	Blank 570
B		0	0	0	0	0	0	0	0	0	0	0	450
		0	0	0	0	0	0	0	0	0	0	0	570
		0	0	0	0	0	0	0	0	0	0	0	Blank 450
		0	0	0	0	0	0	0	0	0	0	0	Blank 570
C		0	0	0	0	0	0	0	0	0	0	0	450
		0	0	0	0	0	0	0	0	0	0	0	570
		0	0	0	0	0	0	0	0	0	0	0	Blank 450
		0	0	0	0	0	0	0	0	0	0	0	Blank 570
D		0	0	0	0	0	0	0	0	0	0	0	450
		0	0	0	0	0	0	0	0	0	0	0	570
		0	0	0	0	0	0	0	0	0	0	0	Blank 450
		0	0	0	0	0	0	0	0	0	0	0	Blank 570
E		0	0	0	0	0	0	0	0	0	0	0	450
		0	0	0	0	0	0	0	0	0	0	0	570
		0	0	0	0	0	0	0	0	0	0	0	Blank 450
		0	0	0	0	0	0	0	0	0	0	0	Blank 570
F		0	0	0	0	0	0	0	0	0	0	0	450
		0	0	0	0	0	0	0	0	0	0	0	570
		0	0	0	0	0	0	0	0	0	0	0	Blank 450
		0	0	0	0	0	0	0	0	0	0	0	Blank 570
G		0	0	0	0	0	0	0	0	0	0	0	450
		0	0	0	0	0	0	0	0	0	0	0	570
		0	0	0	0	0	0	0	0	0	0	0	Blank 450
		0	0	0	0	0	0	0	0	0	0	0	Blank 570
H													450
													570
													Blank 450
													Blank 570

Software Version 2.00.18

Plate Number Plate 2
Date 5/30/13
Time 7:37:26 PM
Reader Type: Synergy
Reader Serial Number: 267524
Reading Type Reader

Procedure Details

Plate Type 96 WELL PLATE
Read Absorbance Endpoint
Full Plate
Wavelengths: 450, 570
Read Speed: Normal

Layout

	1	2	3	4	5	6	7	8	9	10	11	12	
A		STD1	STD1	BLK	SPL5	SPL12	SPL19	SPL26	SPL33	SPL40	SPL47	SPL54	Well ID
		250	250		10000	10000	10000	10000	10000	10000	10000	10000	Conc/Dil
B		STD2	STD2	BLK	SPL6	SPL13	SPL20	SPL27	SPL34	SPL41	SPL48	SPL55	Well ID
		125	125		10000	10000	10000	10000	10000	10000	10000	10000	Conc/Dil
C		STD3	STD3	BLK	SPL7	SPL14	SPL21	SPL28	SPL35	SPL42	SPL49	SPL56	Well ID
		62.5	62.5		10000	10000	10000	10000	10000	10000	10000	10000	Conc/Dil
D		STD4	STD4	SPL1	SPL8	SPL15	SPL22	SPL29	SPL36	SPL43	SPL50	SPL57	Well ID
		31.25	31.25	10000	10000	10000	10000	10000	10000	10000	10000	10000	Conc/Dil
E		STD5	STD5	SPL2	SPL9	SPL16	SPL23	SPL30	SPL37	SPL44	SPL51	SPL58	Well ID
		15.625	15.625	10000	10000	10000	10000	10000	10000	10000	10000	10000	Conc/Dil
F		STD6	STD6	SPL3	SPL10	SPL17	SPL24	SPL31	SPL38	SPL45	SPL52	SPL59	Well ID
		7.8125	7.8125	10000	10000	10000	10000	10000	10000	10000	10000	10000	Conc/Dil
G		STD7	STD7	SPL4	SPL11	SPL18	SPL25	SPL32	SPL39	SPL46	SPL53	SPL60	Well ID
		3.9063	3.9063	10000	10000	10000	10000	10000	10000	10000	10000	10000	Conc/Dil
H													Well ID
													Conc/Dil

Results

Actual Temperature: 27.5
Actual Temperature: 27.5

	1	2	3	4	5	6	7	8	9	10	11	12	
A		0.876	0.76	0.067	0.146	0.074	0.085	0.17	0.116	0.072	0.107	0.108	450
		0.057	0.051	0.042	0.077	0.044	0.054	0.115	0.04	0.05	0.042	0.048	570
		0.775	0.659	-0.034	0.045	-0.027	-0.016	0.069	0.015	-0.029	0.006	0.007	Blank 450
		-0.012	-0.018	-0.027	0.008	-0.025	-0.015	0.046	-0.029	-0.019	-0.027	-0.021	Blank 570
B		0.754	0.767	0.082	0.098	0.119	0.07	0.114	0.104	0.088	0.097	0.07	450
		0.066	0.05	0.056	0.039	0.039	0.043	0.066	0.04	0.052	0.045	0.04	570
		0.653	0.666	-0.019	-0.003	0.018	-0.031	0.013	0.003	-0.013	-0.004	-0.031	Blank 450
		-0.003	-0.019	-0.013	-0.03	-0.03	-0.026	-0.003	-0.029	-0.017	-0.024	-0.029	Blank 570
C		0.246	0.584	0.153	0.081	0.147	0.104	0.117	0.086	0.102	0.1	0.105	450
		0.051	0.049	0.108	0.039	0.04	0.046	0.049	0.04	0.046	0.048	0.069	570
		0.145	0.483	0.052	-0.02	0.046	0.003	0.016	-0.015	0.001	-0.001	0.004	Blank 450
		-0.018	-0.02	0.039	-0.03	-0.029	-0.023	-0.02	-0.029	-0.023	-0.021	0	Blank 570
D		0.474	0.459	0.09	0.088	0.073	0.076	0.135	0.072	0.081	0.085	0.082	450
		0.073	0.051	0.044	0.055	0.039	0.038	0.084	0.04	0.052	0.049	0.054	570
		0.373	0.358	-0.011	-0.013	-0.028	-0.025	0.034	-0.029	-0.02	-0.016	-0.019	Blank 450
		0.004	-0.018	-0.025	-0.014	-0.03	-0.031	0.015	-0.029	-0.017	-0.02	-0.015	Blank 570
E		0.346	0.4	0.128	0.158	0.106	0.111	0.13	0.097	0.093	0.075	0.069	450
		0.055	0.069	0.072	0.106	0.067	0.074	0.074	0.071	0.06	0.046	0.041	570
		0.245	0.299	0.027	0.057	0.005	0.01	0.029	-0.004	-0.008	-0.026	-0.032	Blank 450
		-0.014	0	0.003	0.037	-0.002	0.005	0.005	0.002	-0.009	-0.023	-0.028	Blank 570
F		0.171	0.224	0.073	0.172	0.069	0.086	0.069	0.08	0.076	0.173	0.095	450
		0.046	0.051	0.041	0.121	0.042	0.052	0.042	0.054	0.05	0.131	0.066	570
		0.07	0.123	-0.028	0.071	-0.032	-0.015	-0.032	-0.021	-0.025	0.072	-0.006	Blank 450
		-0.023	-0.018	-0.028	0.052	-0.027	-0.017	-0.027	-0.015	-0.019	0.062	-0.003	Blank 570
G		0.102	0.118	0.121	0.072	0.074	0.083	0.076	0.073	0.077	0.093	0.07	450
		0.042	0.043	0.085	0.044	0.045	0.049	0.045	0.046	0.051	0.041	0.04	570
		0.001	0.017	0.02	-0.029	-0.027	-0.018	-0.025	-0.028	-0.024	-0.008	-0.031	Blank 450
		-0.027	-0.026	0.016	-0.025	-0.024	-0.02	-0.024	-0.023	-0.018	-0.028	-0.029	Blank 570
H													450
													570
													Blank 450
													Blank 570

Software Version 2.00.18

Plate Number Plate 1
Date 6/19/13
Time 5:42:41 PM
Reader Type: Synergy
Reader Serial Number: 267524
Reading Type Reader

Procedure Details
Plate Type 96 WELL PLATE
Read Absorbance Endpoint
Full Plate
Wavelengths: 450, 570
Read Speed: Normal

Layout

	1	2	3	4	5	6	7	8	9	10	11	12	
A	STD1 250	STD1 250	BLK	SPL1:1 10	SPL1:3 500	SPL1:6 8000	SPL2:2 100	SPL2:5 5000					Well ID Conc/Dil
B	STD2 125	STD2 125	BLK	SPL1:1 10	SPL1:4 1000	SPL1:6 8000	SPL2:3 500	SPL2:5 5000					Well ID Conc/Dil
C	STD3 62.5	STD3 62.5	BLK	SPL1:1 10	SPL1:4 1000		SPL2:3 500	SPL2:6 8000					Well ID Conc/Dil
D	STD4 31.25	STD4 31.25	BLK	SPL1:2 100	SPL1:4 1000	SPL2:1 10	SPL2:3 500	SPL2:6 8000					Well ID Conc/Dil
E	STD5 15.625	STD5 15.625	BLK	SPL1:2 100	SPL1:5 5000	SPL2:1 10	SPL2:4 1000	SPL2:6 8000					Well ID Conc/Dil
F	STD6 7.8125	STD6 7.8125	BLK	SPL1:2 100	SPL1:5 5000	SPL2:1 10	SPL2:4 1000						Well ID Conc/Dil
G	STD7 3.9063	STD7 3.9063	BLK	SPL1:3 500	SPL1:5 5000	SPL2:2 100	SPL2:4 1000						Well ID Conc/Dil
H				SPL1:3 500	SPL1:6 8000	SPL2:2 100	SPL2:5 5000						Well ID Conc/Dil

Results
Actual Temperature: 27.6
Actual Temperature: 27.6

	1	2	3	4	5	6	7	8	9	10	11	12	
A	0.067	0.04	0.051	0.044	0.059	0.044	0.095	0.043					450
	0.06	0.037	0.049	0.04	0.052	0.041	0.086	0.038					570
	-0.004	-0.031	-0.02	-0.027	-0.012	-0.027	0.024	-0.028					Blank 450
	-0.007	-0.03	-0.018	-0.027	-0.015	-0.026	0.019	-0.029					Blank 570
B	0.327	0.061	0.059	0.072	0.051	0.054	0.064	0.047					450
	0.303	0.056	0.056	0.067	0.047	0.048	0.059	0.043					570
	0.256	-0.01	-0.012	0.001	-0.02	-0.017	-0.007	-0.024					Blank 450
	0.236	-0.011	-0.011	0	-0.02	-0.019	-0.008	-0.024					Blank 570
C	0.047	0.082	0.057	0.052	0.044		0.057	0.067					450
	0.042	0.084	0.054	0.048	0.039		0.053	0.062					570
	-0.024	0.011	-0.014	-0.019	-0.027		-0.014	-0.004					Blank 450
	-0.025	0.017	-0.013	-0.019	-0.028		-0.014	-0.005					Blank 570
D	0.063	0.094	0.05	0.05	0.051	0.041	0.043	0.039					450
	0.056	0.091	0.047	0.047	0.046	0.038	0.038	0.037					570
	-0.008	0.023	-0.021	-0.021	-0.02	-0.03	-0.028	-0.032					Blank 450
	-0.011	0.024	-0.02	-0.02	-0.021	-0.029	-0.029	-0.03					Blank 570
E	0.149	0.052	0.071	0.09	0.047	0.043	0.042	0.042					450
	0.139	0.047	0.069	0.084	0.042	0.037	0.038	0.039					570
	0.078	-0.019	0	0.019	-0.024	-0.028	-0.029	-0.029					Blank 450
	0.072	-0.02	0.002	0.017	-0.025	-0.03	-0.029	-0.028					Blank 570
F	0.05	0.047	0.116	0.054	0.045	0.063	0.042						450
	0.046	0.042	0.111	0.048	0.041	0.059	0.039						570
	-0.021	-0.024	0.045	-0.017	-0.026	-0.008	-0.029						Blank 450
	-0.021	-0.025	0.044	-0.019	-0.026	-0.008	-0.028						Blank 570
G	0.043	0.045	0.09	0.049	0.06	0.045	0.045						450
	0.039	0.041	0.083	0.046	0.055	0.042	0.042						570
	-0.028	-0.026	0.019	-0.022	-0.011	-0.026	-0.026						Blank 450
	-0.028	-0.026	0.016	-0.021	-0.012	-0.025	-0.025						Blank 570
H				0.081	0.046	0.047	0.041						450
				0.066	0.041	0.044	0.039						570
				0.01	-0.025	-0.024	-0.03						Blank 450
				-0.001	-0.026	-0.023	-0.028						Blank 570

Software Version 2.00.18

Plate Number Plate 1
Date 7/31/13
Time 4:29:47 PM
Reader Type: Synergy
Reader Serial Number: 267524
Reading Type Reader

Procedure Details
Plate Type 96 WELL PLATE
Read Absorbance Endpoint
Full Plate
Wavelengths: 450
Read Speed: Normal

Results
Actual Temperature: 27.5

	1	2	3	4	5	6	7	8	9	10	11	12	
A	1.121	0.321	0.036	0.038	2.723	2.027	2.941	2.526	0.036	0.037	0.58	0.28	450
B	1.178	0.558	1.075	0.253	0.032	0.037	3.145	2.447	3.126	2.055	0.038	0.033	450
C	0.035	0.037	1.086	0.083	1.151	0.203	0.075	0.041	3.158	1.773	2.265	0.763	450
D	1.74	0.605	0.035	0.033	1.174	0.305	0.327	0.112	0.043	0.038	2.07	0.617	450
E	1.698	0.93	1.883	0.846	0.038	0.037	0.254	0.082	0.433	0.111	0.037	0.041	450
F	0.03	0.039	1.843	0.747	1.308	0.587	0.036	0.034	0.443	0.166	0.05	0.047	450
G	2.26	1.166	0.035	0.041	1.191	0.628	0.972	0.428	0.037	0.034	0.05	0.049	450
H	2.411	1.825	2.685	2.295	0.037	0.038	0.937	0.469	0.882	0.341	0.058	0.048	450

Antibody Detection ELISA Serum Samples

Software Version	2.00.18
Plate Number	Plate 1
Date	10/31/13
Time	3:30:08 PM
Reader Type:	Synergy
Reader Serial Number:	267524
Reading Type	Reader

Procedure Details

Plate Type	96 WELL PLATE
Read	Absorbance Endpoint Full Plate Wavelengths: 450 Read Speed: Normal

Layout

	1	2	3	4	5	6	7	8	9	10	11	12	
A	SPL1:1	SPL1:1	SPL3:1	SPL3:1	SPL5:1	SPL5:1	SPL7:1	SPL7:1	SPL9:1	SPL9:1	SPL11:1	SPL11:1	Well ID
	100	100	100	100	100	100	100	100	100	100	100	100	Conc/Dil
B	SPL1:2	SPL1:2	SPL3:2	SPL3:2	SPL5:2	SPL5:2	SPL7:2	SPL7:2	SPL9:2	SPL9:2	SPL11:2	SPL11:2	Well ID
	1000	1000	1000	1000	1000	1000	1000	1000	1000	1000	1000	1000	Conc/Dil
C	SPL1:3	SPL1:3	SPL3:3	SPL3:3	SPL5:3	SPL5:3	SPL7:3	SPL7:3	SPL9:3	SPL9:3	SPL11:3	SPL11:3	Well ID
	10000	10000	10000	10000	10000	10000	10000	10000	10000	10000	10000	10000	Conc/Dil
D	SPL1:4	SPL1:4	SPL3:4	SPL3:4	SPL5:4	SPL5:4	SPL7:4	SPL7:4	SPL9:4	SPL9:4	SPL11:4	SPL11:4	Well ID
	1.00E+05	1.00E+05	1.00E+05	1.00E+05	1.00E+05	1.00E+05	1.00E+05	1.00E+05	1.00E+05	1.00E+05	1.00E+05	1.00E+05	Conc/Dil
E	SPL2:1	SPL2:1	SPL4:1	SPL4:1	SPL6:1	SPL6:1	SPL8:1	SPL8:1	SPL10:1	SPL10:1	BLK	BLK	Well ID
	100	100	100	100	100	100	100	100	100	100			Conc/Dil
F	SPL2:2	SPL2:2	SPL4:2	SPL4:2	SPL6:2	SPL6:2	SPL8:2	SPL8:2	SPL10:2	SPL10:2	BLK	BLK	Well ID
	1000	1000	1000	1000	1000	1000	1000	1000	1000	1000			Conc/Dil
G	SPL2:3	SPL2:3	SPL4:3	SPL4:3	SPL6:3	SPL6:3	SPL8:3	SPL8:3	SPL10:3	SPL10:3	BLK	BLK	Well ID
	10000	10000	10000	10000	10000	10000	10000	10000	10000	10000			Conc/Dil
H	SPL2:4	SPL2:4	SPL4:4	SPL4:4	SPL6:4	SPL6:4	SPL8:4	SPL8:4	SPL10:4	SPL10:4	BLK	BLK	Well ID
	1.00E+05	1.00E+05	1.00E+05	1.00E+05	1.00E+05	1.00E+05	1.00E+05	1.00E+05	1.00E+05	1.00E+05			Conc/Dil

Results

Actual Temperature: 25

	1	2	3	4	5	6	7	8	9	10	11	12	
A	0.065	0.074	0.109	0.07	0.079	0.067	0.066	0.062	0.084	0.077	0.187	0.086	450
	0.011	0.02	0.055	0.016	0.025	0.013	0.012	0.008	0.03	0.023	0.133	0.032	Blank 450
B	0.061	0.052	0.044	0.046	0.051	0.052	0.056	0.05	0.054	0.051	0.052	0.058	450
	0.007	-0.002	-0.01	-0.008	-0.003	-0.002	0.002	-0.004	0	-0.003	-0.002	0.004	Blank 450
C	0.063	0.042	0.046	0.05	0.05	0.049	0.052	0.052	0.05	0.054	0.048	0.054	450
	0.009	-0.012	-0.008	-0.004	-0.004	-0.005	-0.002	-0.002	-0.004	0	-0.006	0	Blank 450
D	0.051	0.044	0.045	0.04	0.051	0.108	0.061	0.132	0.051	0.051	0.049	0.099	450
	-0.003	-0.01	-0.009	-0.014	-0.003	0.054	0.007	0.078	-0.003	-0.003	-0.005	0.045	Blank 450
E	0.06	0.079	0.07	0.063	0.061	0.064	0.089	0.083	0.075	0.072	0.051	0.05	450
	0.006	0.025	0.016	0.009	0.007	0.01	0.035	0.029	0.021	0.018	-0.003	-0.004	Blank 450
F	0.053	0.056	0.055	0.053	0.054	0.05	0.09	0.062	0.089	0.053	0.051	0.05	450
	-0.001	0.002	0.001	-0.001	0	-0.004	0.036	0.008	0.035	-0.001	-0.003	-0.004	Blank 450
G	0.058	0.053	0.051	0.045	0.049	0.051	0.051	0.051	0.051	0.073	0.07	0.05	450
	0.004	-0.001	-0.003	-0.009	-0.005	-0.003	-0.003	-0.003	-0.003	0.019	0.016	-0.004	Blank 450
H	0.07	0.05	0.05	0.051	0.05	0.046	0.055	0.064	0.054	0.062	0.053	0.057	450
	0.016	-0.004	-0.004	-0.003	-0.004	-0.008	0.001	0.01	0	0.008	-0.001	0.003	Blank 450

Software Version 2.00.18

Plate Number Plate 2
Date 10/31/13
Time 3:34:01 PM
Reader Type: Synergy
Reader Serial Number: 267524
Reading Type Reader

Procedure Details

Plate Type 96 WELL PLATE
Read Absorbance Endpoint
Full Plate
Wavelengths: 450
Read Speed: Normal

Layout

	1	2	3	4	5	6	7	8	9	10	11	12	
A	SPL1:1	SPL1:1	SPL3:1	SPL3:1	SPL5:1	SPL5:1	SPL7:1	SPL7:1	SPL9:1	SPL9:1	SPL11:1	SPL11:1	Well ID
	100	100	100	100	100	100	100	100	100	100	100	100	Conc/Dil
B	SPL1:2	SPL1:2	SPL3:2	SPL3:2	SPL5:2	SPL5:2	SPL7:2	SPL7:2	SPL9:2	SPL9:2	SPL11:2	SPL11:2	Well ID
	1000	1000	1000	1000	1000	1000	1000	1000	1000	1000	1000	1000	Conc/Dil
C	SPL1:3	SPL1:3	SPL3:3	SPL3:3	SPL5:3	SPL5:3	SPL7:3	SPL7:3	SPL9:3	SPL9:3	SPL11:3	SPL11:3	Well ID
	10000	10000	10000	10000	10000	10000	10000	10000	10000	10000	10000	10000	Conc/Dil
D	SPL1:4	SPL1:4	SPL3:4	SPL3:4	SPL5:4	SPL5:4	SPL7:4	SPL7:4	SPL9:4	SPL9:4	SPL11:4	SPL11:4	Well ID
	1.00E+05	1.00E+05	1.00E+05	1.00E+05	1.00E+05	1.00E+05	1.00E+05	1.00E+05	1.00E+05	1.00E+05	1.00E+05	1.00E+05	Conc/Dil
E	SPL2:1	SPL2:1	SPL4:1	SPL4:1	SPL6:1	SPL6:1	SPL8:1	SPL8:1	SPL10:1	SPL10:1	BLK	BLK	Well ID
	100	100	100	100	100	100	100	100	100	100			Conc/Dil
F	SPL2:2	SPL2:2	SPL4:2	SPL4:2	SPL6:2	SPL6:2	SPL8:2	SPL8:2	SPL10:2	SPL10:2	BLK	BLK	Well ID
	1000	1000	1000	1000	1000	1000	1000	1000	1000	1000			Conc/Dil
G	SPL2:3	SPL2:3	SPL4:3	SPL4:3	SPL6:3	SPL6:3	SPL8:3	SPL8:3	SPL10:3	SPL10:3	BLK	BLK	Well ID
	10000	10000	10000	10000	10000	10000	10000	10000	10000	10000			Conc/Dil
H	SPL2:4	SPL2:4	SPL4:4	SPL4:4	SPL6:4	SPL6:4	SPL8:4	SPL8:4	SPL10:4	SPL10:4	BLK	BLK	Well ID
	1.00E+05	1.00E+05	1.00E+05	1.00E+05	1.00E+05	1.00E+05	1.00E+05	1.00E+05	1.00E+05	1.00E+05			Conc/Dil

Results

Actual Temperature: 24.9

	1	2	3	4	5	6	7	8	9	10	11	12	
A	0.094	0.09	0.065	0.074	0.064	0.058	0.145	0.058	0.127	0.059	0.06	0.062	450
	0.034	0.03	0.005	0.014	0.004	-0.002	0.085	-0.002	0.067	-0.001	0	0.002	Blank 450
B	0.059	0.077	0.064	0.063	0.058	0.073	0.053	0.052	0.054	0.053	0.053	0.06	450
	-0.001	0.017	0.004	0.003	-0.002	0.013	-0.007	-0.008	-0.006	-0.007	-0.007	0	Blank 450
C	0.064	0.059	0.072	0.059	0.055	0.053	0.054	0.053	0.057	0.054	0.068	0.068	450
	0.004	-0.001	0.012	-0.001	-0.005	-0.007	-0.006	-0.007	-0.003	-0.006	0.008	0.008	Blank 450
D	0.067	0.063	0.057	0.056	0.065	0.052	0.054	0.059	0.058	0.06	0.063	0.065	450
	0.007	0.003	-0.003	-0.004	0.005	-0.008	-0.006	-0.001	-0.002	0	0.003	0.005	Blank 450
E	0.062	0.061	0.076	0.055	0.166	0.063	0.057	0.069	0.063	0.067	0.056	0.059	450
	0.002	0.001	0.016	-0.005	0.106	0.003	-0.003	0.009	0.003	0.007	-0.004	-0.001	Blank 450
F	0.054	0.056	0.061	0.058	0.071	0.05	0.065	0.059	0.064	0.063	0.055	0.059	450
	-0.006	-0.004	0.001	-0.002	0.011	-0.01	0.005	-0.001	0.004	0.003	-0.005	-0.001	Blank 450
G	0.052	0.058	0.053	0.053	0.06	0.055	0.055	0.058	0.06	0.057	0.059	0.063	450
	-0.008	-0.002	-0.007	-0.007	0	-0.005	-0.005	-0.002	0	-0.003	-0.001	0.003	Blank 450
H	0.058	0.059	0.058	0.057	0.057	0.058	0.08	0.06	0.061	0.067	0.064	0.065	450
	-0.002	-0.001	-0.002	-0.003	-0.003	-0.002	0.02	0	0.001	0.007	0.004	0.005	Blank 450

Software Version 2.00.18

Plate Number Plate 1
Date 11/15/13
Time 6:39:06 PM
Reader Type: Synergy
Reader Serial Number: 267524
Reading Type Reader

Procedure Details

Plate Type 96 WELL PLATE
Read Absorbance Endpoint
Full Plate
Wavelengths: 450
Read Speed: Normal

Layout

	1	2	3	4	5	6	7	8	9	10	11	12	
A	SPL1:1	SPL1:1	SPL3:1	SPL3:1	SPL5:1	SPL5:1	SPL7:1	SPL7:1	SPL9:1	SPL9:1	SPL11:1	SPL11:1	Well ID
	100	100	100	100	100	100	100	100	100	100	100	100	Conc/Dil
B	SPL1:2	SPL1:2	SPL3:2	SPL3:2	SPL5:2	SPL5:2	SPL7:2	SPL7:2	SPL9:2	SPL9:2	SPL11:2	SPL11:2	Well ID
	1000	1000	1000	1000	1000	1000	1000	1000	1000	1000	1000	1000	Conc/Dil
C	SPL1:3	SPL1:3	SPL3:3	SPL3:3	SPL5:3	SPL5:3	SPL7:3	SPL7:3	SPL9:3	SPL9:3	SPL11:3	SPL11:3	Well ID
	10000	10000	10000	10000	10000	10000	10000	10000	10000	10000	10000	10000	Conc/Dil
D	SPL1:4	SPL1:4	SPL3:4	SPL3:4	SPL5:4	SPL5:4	SPL7:4	SPL7:4	SPL9:4	SPL9:4	SPL11:4	SPL11:4	Well ID
	1.00E+05	1.00E+05	1.00E+05	1.00E+05	1.00E+05	1.00E+05	1.00E+05	1.00E+05	1.00E+05	1.00E+05	1.00E+05	1.00E+05	Conc/Dil
E	SPL2:1	SPL2:1	SPL4:1	SPL4:1	SPL6:1	SPL6:1	SPL8:1	SPL8:1	SPL10:1	SPL10:1	BLK	BLK	Well ID
	100	100	100	100	100	100	100	100	100	100			Conc/Dil
F	SPL2:2	SPL2:2	SPL4:2	SPL4:2	SPL6:2	SPL6:2	SPL8:2	SPL8:2	SPL10:2	SPL10:2	BLK	BLK	Well ID
	1000	1000	1000	1000	1000	1000	1000	1000	1000	1000			Conc/Dil
G	SPL2:3	SPL2:3	SPL4:3	SPL4:3	SPL6:3	SPL6:3	SPL8:3	SPL8:3	SPL10:3	SPL10:3	BLK	BLK	Well ID
	10000	10000	10000	10000	10000	10000	10000	10000	10000	10000			Conc/Dil
H	SPL2:4	SPL2:4	SPL4:4	SPL4:4	SPL6:4	SPL6:4	SPL8:4	SPL8:4	SPL10:4	SPL10:4	BLK	BLK	Well ID
	1.00E+05	1.00E+05	1.00E+05	1.00E+05	1.00E+05	1.00E+05	1.00E+05	1.00E+05	1.00E+05	1.00E+05			Conc/Dil

Results

Actual Temperature: 25.8

	1	2	3	4	5	6	7	8	9	10	11	12	
A	0.165	0.175	0.182	0.142	0.129	0.114	0.104	0.089	0.119	0.096	0.123	0.144	450
	0.1	0.11	0.117	0.077	0.064	0.049	0.039	0.024	0.054	0.031	0.058	0.079	Blank 450
B	0.081	0.078	0.084	0.082	0.099	0.081	0.088	0.071	0.076	0.079	0.077	0.064	450
	0.016	0.013	0.019	0.017	0.034	0.016	0.023	0.006	0.011	0.014	0.012	-0.001	Blank 450
C	0.063	0.069	0.066	0.064	0.073	0.066	0.064	0.069	0.062	0.062	0.071	0.062	450
	-0.002	0.004	0.001	-0.001	0.008	0.001	-0.001	0.004	-0.003	-0.003	0.006	-0.003	Blank 450
D	0.061	0.056	0.057	0.059	0.059	0.057	0.059	0.061	0.059	0.057	0.062	0.057	450
	-0.004	-0.009	-0.008	-0.006	-0.006	-0.008	-0.006	-0.004	-0.006	-0.008	-0.003	-0.008	Blank 450
E	0.21	0.26	0.159	0.135	0.105	0.113	0.121	0.122	0.155	0.328	0.056	0.055	450
	0.145	0.195	0.094	0.07	0.04	0.048	0.056	0.057	0.09	0.263	-0.009	-0.01	Blank 450
F	0.074	0.068	0.064	0.063	0.063	0.073	0.077	0.069	0.068	0.069	0.07	0.058	450
	0.009	0.003	-0.001	-0.002	-0.002	0.008	0.012	0.004	0.003	0.004	0.005	-0.007	Blank 450
G	0.054	0.063	0.062	0.056	0.06	0.06	0.059	0.058	0.058	0.058	0.063	0.088	450
	-0.011	-0.002	-0.003	-0.009	-0.005	-0.005	-0.006	-0.007	-0.007	-0.007	-0.002	0.023	Blank 450
H	0.056	0.065	0.056	0.06	0.06	0.06	0.068	0.056	0.062	0.078	0.076	0.057	450
	-0.009	0	-0.009	-0.005	-0.005	-0.005	0.003	-0.009	-0.003	0.013	0.011	-0.008	Blank 450

Software Version 2.00.18

Plate Number Plate 1
Date 11/15/13
Time 6:43:04 PM
Reader Type: Synergy
Reader Serial Number: 267524
Reading Type Reader

Procedure Details
Plate Type 96 WELL PLATE
Read Absorbance Endpoint
Full Plate
Wavelengths: 450
Read Speed: Normal

Layout

	1	2	3	4	5	6	7	8	9	10	11	12	
A	SPL1:1	SPL1:1	SPL3:1	SPL3:1	SPL5:1	SPL5:1	SPL7:1	SPL7:1	SPL9:1	SPL9:1	SPL11:1	SPL11:1	Well ID
	100	100	100	100	100	100	100	100	100	100	100	100	Conc/Dil
B	SPL1:2	SPL1:2	SPL3:2	SPL3:2	SPL5:2	SPL5:2	SPL7:2	SPL7:2	SPL9:2	SPL9:2	SPL11:2	SPL11:2	Well ID
	1000	1000	1000	1000	1000	1000	1000	1000	1000	1000	1000	1000	Conc/Dil
C	SPL1:3	SPL1:3	SPL3:3	SPL3:3	SPL5:3	SPL5:3	SPL7:3	SPL7:3	SPL9:3	SPL9:3	SPL11:3	SPL11:3	Well ID
	10000	10000	10000	10000	10000	10000	10000	10000	10000	10000	10000	10000	Conc/Dil
D	SPL1:4	SPL1:4	SPL3:4	SPL3:4	SPL5:4	SPL5:4	SPL7:4	SPL7:4	SPL9:4	SPL9:4	SPL11:4	SPL11:4	Well ID
	1.00E+05	1.00E+05	1.00E+05	1.00E+05	1.00E+05	1.00E+05	1.00E+05	1.00E+05	1.00E+05	1.00E+05	1.00E+05	1.00E+05	Conc/Dil
E	SPL2:1	SPL2:1	SPL4:1	SPL4:1	SPL6:1	SPL6:1	SPL8:1	SPL8:1	SPL10:1	SPL10:1	BLK	BLK	Well ID
	100	100	100	100	100	100	100	100	100	100			Conc/Dil
F	SPL2:2	SPL2:2	SPL4:2	SPL4:2	SPL6:2	SPL6:2	SPL8:2	SPL8:2	SPL10:2	SPL10:2	BLK	BLK	Well ID
	1000	1000	1000	1000	1000	1000	1000	1000	1000	1000			Conc/Dil
G	SPL2:3	SPL2:3	SPL4:3	SPL4:3	SPL6:3	SPL6:3	SPL8:3	SPL8:3	SPL10:3	SPL10:3	BLK	BLK	Well ID
	10000	10000	10000	10000	10000	10000	10000	10000	10000	10000			Conc/Dil
H	SPL2:4	SPL2:4	SPL4:4	SPL4:4	SPL6:4	SPL6:4	SPL8:4	SPL8:4	SPL10:4	SPL10:4	BLK	BLK	Well ID
	1.00E+05	1.00E+05	1.00E+05	1.00E+05	1.00E+05	1.00E+05	1.00E+05	1.00E+05	1.00E+05	1.00E+05			Conc/Dil

Results
Actual Temperature: 25.7

	1	2	3	4	5	6	7	8	9	10	11	12	
A	0.182	0.169	0.166	0.147	0.103	0.077	0.148	0.142	0.225	0.231	0.128	0.101	450
	0.055	0.043	0.04	0.02	-0.023	-0.05	0.021	0.016	0.099	0.105	0.002	-0.025	Blank 450
B	0.121	0.1	0.125	0.088	0.065	0.063	0.102	0.074	0.175	0.144	0.08	0.087	450
	-0.006	-0.026	-0.002	-0.039	-0.061	-0.064	-0.024	-0.053	0.049	0.018	-0.047	-0.039	Blank 450
C	0.074	0.065	0.071	0.067	0.062	0.064	0.072	0.069	0.07	0.078	0.064	0.057	450
	-0.053	-0.061	-0.055	-0.059	-0.065	-0.063	-0.054	-0.057	-0.056	-0.049	-0.063	-0.07	Blank 450
D	0.089	0.06	0.059	0.059	0.063	0.056	0.063	0.059	0.071	0.057	0.065	0.059	450
	-0.038	-0.067	-0.068	-0.068	-0.064	-0.071	-0.064	-0.068	-0.055	-0.07	-0.061	-0.068	Blank 450
E	0.176	0.16	0.146	0.122	0.16	0.13	0.191	0.204	0.136	0.145	0.207	0.058	450
	0.049	0.034	0.019	-0.005	0.034	0.004	0.065	0.078	0.01	0.018	0.081	-0.069	Blank 450
F	0.091	0.085	0.078	0.074	0.082	0.066	0.097	0.096	0.074	0.072	0.219	0.26	450
	-0.036	-0.041	-0.049	-0.053	-0.044	-0.06	-0.029	-0.03	-0.053	-0.054	0.092	0.134	Blank 450
G	0.067	0.092	0.072	0.067	0.063	0.067	0.07	0.068	0.075	0.139	0.092	0.056	450
	-0.059	-0.035	-0.054	-0.059	-0.064	-0.059	-0.056	-0.058	-0.052	0.013	-0.035	-0.071	Blank 450
H	0.075	0.074	0.079	0.067	0.067	0.116	0.064	0.067	0.066	0.059	0.055	0.065	450
	-0.052	-0.053	-0.048	-0.059	-0.059	-0.01	-0.063	-0.059	-0.06	-0.068	-0.072	-0.061	Blank 450

Software Version 2.00.18

Plate Number Plate 1
Date 11/15/13
Time 6:47:06 PM
Reader Type: Synergy
Reader Serial Number: 267524
Reading Type Reader

Procedure Details

Plate Type 96 WELL PLATE
Read Absorbance Endpoint
Full Plate
Wavelengths: 450
Read Speed: Normal

Layout

	1	2	3	4	5	6	7	8	9	10	11	12	
A	SPL1:1	SPL1:1	SPL3:1	SPL3:1	SPL5:1	SPL5:1	SPL7:1	SPL7:1	SPL9:1	SPL9:1	SPL11:1	SPL11:1	Well ID
	100	100	100	100	100	100	100	100	100	100	100	100	Conc/Dil
B	SPL1:2	SPL1:2	SPL3:2	SPL3:2	SPL5:2	SPL5:2	SPL7:2	SPL7:2	SPL9:2	SPL9:2	SPL11:2	SPL11:2	Well ID
	1000	1000	1000	1000	1000	1000	1000	1000	1000	1000	1000	1000	Conc/Dil
C	SPL1:3	SPL1:3	SPL3:3	SPL3:3	SPL5:3	SPL5:3	SPL7:3	SPL7:3	SPL9:3	SPL9:3	SPL11:3	SPL11:3	Well ID
	10000	10000	10000	10000	10000	10000	10000	10000	10000	10000	10000	10000	Conc/Dil
D	SPL1:4	SPL1:4	SPL3:4	SPL3:4	SPL5:4	SPL5:4	SPL7:4	SPL7:4	SPL9:4	SPL9:4	SPL11:4	SPL11:4	Well ID
	1.00E+05	1.00E+05	1.00E+05	1.00E+05	1.00E+05	1.00E+05	1.00E+05	1.00E+05	1.00E+05	1.00E+05	1.00E+05	1.00E+05	Conc/Dil
E	SPL2:1	SPL2:1	SPL4:1	SPL4:1	SPL6:1	SPL6:1	SPL8:1	SPL8:1	SPL10:1	SPL10:1	BLK	BLK	Well ID
	100	100	100	100	100	100	100	100	100	100			Conc/Dil
F	SPL2:2	SPL2:2	SPL4:2	SPL4:2	SPL6:2	SPL6:2	SPL8:2	SPL8:2	SPL10:2	SPL10:2	BLK	BLK	Well ID
	1000	1000	1000	1000	1000	1000	1000	1000	1000	1000			Conc/Dil
G	SPL2:3	SPL2:3	SPL4:3	SPL4:3	SPL6:3	SPL6:3	SPL8:3	SPL8:3	SPL10:3	SPL10:3	BLK	BLK	Well ID
	10000	10000	10000	10000	10000	10000	10000	10000	10000	10000			Conc/Dil
H	SPL2:4	SPL2:4	SPL4:4	SPL4:4	SPL6:4	SPL6:4	SPL8:4	SPL8:4	SPL10:4	SPL10:4	BLK	BLK	Well ID
	1.00E+05	1.00E+05	1.00E+05	1.00E+05	1.00E+05	1.00E+05	1.00E+05	1.00E+05	1.00E+05	1.00E+05			Conc/Dil

Results

Actual Temperature: 25.7

	1	2	3	4	5	6	7	8	9	10	11	12	
A	0.178	0.184	0.138	0.147	0.223	0.207	0.332	0.298	0.129	0.113	0.085	0.088	450
	0.111	0.117	0.071	0.08	0.156	0.14	0.265	0.231	0.062	0.046	0.018	0.021	Blank 450
B	0.113	0.107	0.079	0.077	0.068	0.065	0.094	0.064	0.075	0.072	0.055	0.062	450
	0.046	0.04	0.012	0.01	0.001	-0.002	0.027	-0.003	0.008	0.005	-0.012	-0.005	Blank 450
C	0.065	0.069	0.065	0.288	0.078	0.069	0.101	0.067	0.065	0.771	0.057	0.065	450
	-0.002	0.002	-0.002	0.221	0.011	0.002	0.034	0	-0.002	0.704	-0.01	-0.002	Blank 450
D	0.072	0.081	0.059	0.066	0.061	0.06	0.063	0.061	0.078	0.065	0.762	0.059	450
	0.005	0.014	-0.008	-0.001	-0.006	-0.007	-0.004	-0.006	0.011	-0.002	0.695	-0.008	Blank 450
E	0.131	0.135	0.273	1.031	0.348	0.457	0.069	0.071	0.162	0.154	0.069	0.074	450
	0.064	0.068	0.206	0.964	0.281	0.39	0.002	0.004	0.095	0.087	0.002	0.007	Blank 450
F	0.081	0.075	0.108	0.106	0.156	0.124	0.062	0.077	0.099	0.723	0.06	0.067	450
	0.014	0.008	0.041	0.039	0.089	0.057	-0.005	0.01	0.032	0.656	-0.007	0	Blank 450
G	0.073	0.166	0.094	0.075	0.079	0.122	0.111	0.069	0.067	0.066	0.064	0.066	450
	0.006	0.099	0.027	0.008	0.012	0.055	0.044	0.002	0	-0.001	-0.003	-0.001	Blank 450
H	0.119	0.071	0.117	0.064	0.066	0.068	0.073	0.124	0.065	0.066	0.07	0.067	450
	0.052	0.004	0.05	-0.003	-0.001	0.001	0.006	0.057	-0.002	-0.001	0.003	0	Blank 450

Software Version 2.00.18

Plate Number Plate 1
Date 11/15/13
Time 6:39:06 PM
Reader Type: Synergy
Reader Serial Number: 267524
Reading Type Reader

Procedure Details

Plate Type 96 WELL PLATE
Read Absorbance Endpoint
Full Plate
Wavelengths: 450
Read Speed: Normal

Layout

	1	2	3	4	5	6	7	8	9	10	11	12	
A	SPL1:1	SPL1:1	SPL3:1	SPL3:1	SPL5:1	SPL5:1	SPL7:1	SPL7:1	SPL9:1	SPL9:1	SPL11:1	SPL11:1	Well ID
	100	100	100	100	100	100	100	100	100	100	100	100	Conc/Dil
B	SPL1:2	SPL1:2	SPL3:2	SPL3:2	SPL5:2	SPL5:2	SPL7:2	SPL7:2	SPL9:2	SPL9:2	SPL11:2	SPL11:2	Well ID
	1000	1000	1000	1000	1000	1000	1000	1000	1000	1000	1000	1000	Conc/Dil
C	SPL1:3	SPL1:3	SPL3:3	SPL3:3	SPL5:3	SPL5:3	SPL7:3	SPL7:3	SPL9:3	SPL9:3	SPL11:3	SPL11:3	Well ID
	10000	10000	10000	10000	10000	10000	10000	10000	10000	10000	10000	10000	Conc/Dil
D	SPL1:4	SPL1:4	SPL3:4	SPL3:4	SPL5:4	SPL5:4	SPL7:4	SPL7:4	SPL9:4	SPL9:4	SPL11:4	SPL11:4	Well ID
	1.00E+05	1.00E+05	1.00E+05	1.00E+05	1.00E+05	1.00E+05	1.00E+05	1.00E+05	1.00E+05	1.00E+05	1.00E+05	1.00E+05	Conc/Dil
E	SPL2:1	SPL2:1	SPL4:1	SPL4:1	SPL6:1	SPL6:1	SPL8:1	SPL8:1	SPL10:1	SPL10:1	BLK	BLK	Well ID
	100	100	100	100	100	100	100	100	100	100			Conc/Dil
F	SPL2:2	SPL2:2	SPL4:2	SPL4:2	SPL6:2	SPL6:2	SPL8:2	SPL8:2	SPL10:2	SPL10:2	BLK	BLK	Well ID
	1000	1000	1000	1000	1000	1000	1000	1000	1000	1000			Conc/Dil
G	SPL2:3	SPL2:3	SPL4:3	SPL4:3	SPL6:3	SPL6:3	SPL8:3	SPL8:3	SPL10:3	SPL10:3	BLK	BLK	Well ID
	10000	10000	10000	10000	10000	10000	10000	10000	10000	10000			Conc/Dil
H	SPL2:4	SPL2:4	SPL4:4	SPL4:4	SPL6:4	SPL6:4	SPL8:4	SPL8:4	SPL10:4	SPL10:4	BLK	BLK	Well ID
	1.00E+05	1.00E+05	1.00E+05	1.00E+05	1.00E+05	1.00E+05	1.00E+05	1.00E+05	1.00E+05	1.00E+05			Conc/Dil

Results

Actual Temperature: 25.8

	1	2	3	4	5	6	7	8	9	10	11	12	
A	0.165	0.175	0.182	0.142	0.129	0.114	0.104	0.089	0.119	0.096	0.123	0.144	450
	0.1	0.11	0.117	0.077	0.064	0.049	0.039	0.024	0.054	0.031	0.058	0.079	Blank 450
B	0.081	0.078	0.084	0.082	0.099	0.081	0.088	0.071	0.076	0.079	0.077	0.064	450
	0.016	0.013	0.019	0.017	0.034	0.016	0.023	0.006	0.011	0.014	0.012	-0.001	Blank 450
C	0.063	0.069	0.066	0.064	0.073	0.066	0.064	0.069	0.062	0.062	0.071	0.062	450
	-0.002	0.004	0.001	-0.001	0.008	0.001	-0.001	0.004	-0.003	-0.003	0.006	-0.003	Blank 450
D	0.061	0.056	0.057	0.059	0.059	0.057	0.059	0.061	0.059	0.057	0.062	0.057	450
	-0.004	-0.009	-0.008	-0.006	-0.006	-0.008	-0.006	-0.004	-0.006	-0.008	-0.003	-0.008	Blank 450
E	0.21	0.26	0.159	0.135	0.105	0.113	0.121	0.122	0.155	0.328	0.056	0.055	450
	0.145	0.195	0.094	0.07	0.04	0.048	0.056	0.057	0.09	0.263	-0.009	-0.01	Blank 450
F	0.074	0.068	0.064	0.063	0.063	0.073	0.077	0.069	0.068	0.069	0.07	0.058	450
	0.009	0.003	-0.001	-0.002	-0.002	0.008	0.012	0.004	0.003	0.004	0.005	-0.007	Blank 450
G	0.054	0.063	0.062	0.056	0.06	0.06	0.059	0.058	0.058	0.058	0.063	0.088	450
	-0.011	-0.002	-0.003	-0.009	-0.005	-0.005	-0.006	-0.007	-0.007	-0.007	-0.002	0.023	Blank 450
H	0.056	0.065	0.056	0.06	0.06	0.06	0.068	0.056	0.062	0.078	0.076	0.057	450
	-0.009	0	-0.009	-0.005	-0.005	-0.005	0.003	-0.009	-0.003	0.013	0.011	-0.008	Blank 450

Software Version 2.00.18

Plate Number Plate 2
Date 11/15/13
Time 7:26:15 PM
Reader Type: Synergy
Reader Serial Number: 267524
Reading Type Reader

Procedure Details
Plate Type 96 WELL PLATE
Read Absorbance Endpoint
Full Plate
Wavelengths: 450
Read Speed: Normal

Layout

	1	2	3	4	5	6	7	8	9	10	11	12	
A	SPL1:1 100	SPL1:1 100	SPL3:1 100	SPL3:1 100	SPL5:1 100	SPL5:1 100	SPL7:1 100	SPL7:1 100	SPL9:1 100	SPL9:1 100	SPL11:1 100	SPL11:1 100	Well ID Conc/Dil
B	SPL1:2 1000	SPL1:2 1000	SPL3:2 1000	SPL3:2 1000	SPL5:2 1000	SPL5:2 1000	SPL7:2 1000	SPL7:2 1000	SPL9:2 1000	SPL9:2 1000	SPL11:2 1000	SPL11:2 1000	Well ID Conc/Dil
C	SPL1:3 10000	SPL1:3 10000	SPL3:3 10000	SPL3:3 10000	SPL5:3 10000	SPL5:3 10000	SPL7:3 10000	SPL7:3 10000	SPL9:3 10000	SPL9:3 10000	SPL11:3 10000	SPL11:3 10000	Well ID Conc/Dil
D	SPL1:4 1.00E+05	SPL1:4 1.00E+05	SPL3:4 1.00E+05	SPL3:4 1.00E+05	SPL5:4 1.00E+05	SPL5:4 1.00E+05	SPL7:4 1.00E+05	SPL7:4 1.00E+05	SPL9:4 1.00E+05	SPL9:4 1.00E+05	SPL11:4 1.00E+05	SPL11:4 1.00E+05	Well ID Conc/Dil
E	SPL2:1 100	SPL2:1 100	SPL4:1 100	SPL4:1 100	SPL6:1 100	SPL6:1 100	SPL8:1 100	SPL8:1 100	SPL10:1 100	SPL10:1 100	BLK	BLK	Well ID Conc/Dil
F	SPL2:2 1000	SPL2:2 1000	SPL4:2 1000	SPL4:2 1000	SPL6:2 1000	SPL6:2 1000	SPL8:2 1000	SPL8:2 1000	SPL10:2 1000	SPL10:2 1000	BLK	BLK	Well ID Conc/Dil
G	SPL2:3 10000	SPL2:3 10000	SPL4:3 10000	SPL4:3 10000	SPL6:3 10000	SPL6:3 10000	SPL8:3 10000	SPL8:3 10000	SPL10:3 10000	SPL10:3 10000	BLK	BLK	Well ID Conc/Dil
H	SPL2:4 1.00E+05	SPL2:4 1.00E+05	SPL4:4 1.00E+05	SPL4:4 1.00E+05	SPL6:4 1.00E+05	SPL6:4 1.00E+05	SPL8:4 1.00E+05	SPL8:4 1.00E+05	SPL10:4 1.00E+05	SPL10:4 1.00E+05	BLK	BLK	Well ID Conc/Dil

Results
Actual Temperature: 25.6

	1	2	3	4	5	6	7	8	9	10	11	12	
A	0.208 0.134	0.233 0.159	0.157 0.083	0.129 0.055	0.314 0.24	0.249 0.175	0.071 -0.003	0.068 -0.006	0.068 -0.006	0.069 -0.005	0.067 -0.007	0.072 -0.002	450 Blank 450
B	0.099 0.025	0.087 0.013	0.078 0.004	0.076 0.002	0.145 0.071	0.121 0.047	0.071 -0.003	0.066 -0.008	0.069 -0.005	0.07 -0.004	0.119 0.045	0.073 -0.001	450 Blank 450
C	0.075 0.001	0.073 -0.001	0.068 -0.006	0.07 -0.004	0.073 -0.001	0.077 0.003	0.069 -0.005	0.073 -0.001	0.078 0.004	0.067 -0.007	0.071 -0.003	0.075 0.001	450 Blank 450
D	0.073 -0.001	0.067 -0.007	0.073 -0.001	0.068 -0.006	0.07 -0.004	0.072 -0.002	0.133 0.059	0.068 -0.006	0.074 0	0.072 -0.002	0.071 -0.003	0.08 0.006	450 Blank 450
E	0.304 0.23	0.26 0.186	0.223 0.149	0.2 0.126	0.067 -0.007	0.067 -0.007	0.068 -0.006	0.069 -0.005	0.07 -0.004	0.07 -0.004	0.07 -0.004	0.076 0.002	450 Blank 450
F	0.151 0.077	0.166 0.092	0.132 0.058	0.106 0.032	0.067 -0.007	0.122 0.048	0.072 -0.002	0.072 -0.002	0.069 -0.005	0.088 0.014	0.07 -0.004	0.074 0	450 Blank 450
G	0.081 0.007	0.078 0.004	0.075 0.001	0.075 0.001	0.077 0.003	0.07 -0.004	0.071 -0.003	0.075 0.001	0.07 -0.004	0.071 -0.003	0.072 -0.002	0.079 0.005	450 Blank 450
H	0.075 0.001	0.079 0.005	0.071 -0.003	0.072 -0.002	0.071 -0.003	0.077 0.003	0.072 -0.002	0.073 -0.001	0.071 -0.003	0.074 0	0.07 -0.004	0.079 0.005	450 Blank 450

Software Version 2.00.18

Plate Number Plate 1
Date 11/17/13
Time 6:17:48 PM
Reader Type: Synergy
Reader Serial Number: 267524
Reading Type Reader

Procedure Details
Plate Type 96 WELL PLATE
Read Absorbance Endpoint
Full Plate
Wavelengths: 450
Read Speed: Normal

Layout

	1	2	3	4	5	6	7	8	9	10	11	12	
A	SPL1:1	SPL1:1	SPL3:1	SPL3:1	SPL5:1	SPL5:1	SPL7:1	SPL7:1	SPL9:1	SPL9:1	SPL11:1	SPL11:1	Well ID
	100	100	100	100	100	100	100	100	100	100	100	100	Conc/Dil
B	SPL1:2	SPL1:2	SPL3:2	SPL3:2	SPL5:2	SPL5:2	SPL7:2	SPL7:2	SPL9:2	SPL9:2	SPL11:2	SPL11:2	Well ID
	1000	1000	1000	1000	1000	1000	1000	1000	1000	1000	1000	1000	Conc/Dil
C	SPL1:3	SPL1:3	SPL3:3	SPL3:3	SPL5:3	SPL5:3	SPL7:3	SPL7:3	SPL9:3	SPL9:3	SPL11:3	SPL11:3	Well ID
	10000	10000	10000	10000	10000	10000	10000	10000	10000	10000	10000	10000	Conc/Dil
D	SPL1:4	SPL1:4	SPL3:4	SPL3:4	SPL5:4	SPL5:4	SPL7:4	SPL7:4	SPL9:4	SPL9:4	SPL11:4	SPL11:4	Well ID
	1.00E+05	1.00E+05	1.00E+05	1.00E+05	1.00E+05	1.00E+05	1.00E+05	1.00E+05	1.00E+05	1.00E+05	1.00E+05	1.00E+05	Conc/Dil
E	SPL2:1	SPL2:1	SPL4:1	SPL4:1	SPL6:1	SPL6:1	SPL8:1	SPL8:1	SPL10:1	SPL10:1	BLK	BLK	Well ID
	100	100	100	100	100	100	100	100	100	100			Conc/Dil
F	SPL2:2	SPL2:2	SPL4:2	SPL4:2	SPL6:2	SPL6:2	SPL8:2	SPL8:2	SPL10:2	SPL10:2	BLK	BLK	Well ID
	1000	1000	1000	1000	1000	1000	1000	1000	1000	1000			Conc/Dil
G	SPL2:3	SPL2:3	SPL4:3	SPL4:3	SPL6:3	SPL6:3	SPL8:3	SPL8:3	SPL10:3	SPL10:3	BLK	BLK	Well ID
	10000	10000	10000	10000	10000	10000	10000	10000	10000	10000			Conc/Dil
H	SPL2:4	SPL2:4	SPL4:4	SPL4:4	SPL6:4	SPL6:4	SPL8:4	SPL8:4	SPL10:4	SPL10:4	BLK	BLK	Well ID
	1.00E+05	1.00E+05	1.00E+05	1.00E+05	1.00E+05	1.00E+05	1.00E+05	1.00E+05	1.00E+05	1.00E+05			Conc/Dil

Results
Actual Temperature: 25.7

	1	2	3	4	5	6	7	8	9	10	11	12	
A	0.282	0.36	0.415	0.463	0.252	0.324	0.275	0.249	0.326	0.493	0.232	0.237	450
	-0.011	0.067	0.122	0.17	-0.041	0.031	-0.018	-0.044	0.033	0.2	-0.061	-0.056	Blank 450
B	0.378	0.25	0.231	0.239	0.268	0.28	0.284	0.217	0.226	0.217	0.16	0.148	450
	0.085	-0.043	-0.062	-0.054	-0.025	-0.013	-0.009	-0.076	-0.067	-0.076	-0.133	-0.145	Blank 450
C	0.272	0.282	0.25	0.236	0.241	0.227	0.246	0.183	0.21	0.223	0.178	0.185	450
	-0.021	-0.011	-0.043	-0.057	-0.052	-0.066	-0.047	-0.11	-0.083	-0.07	-0.115	-0.108	Blank 450
D	0.259	0.225	0.213	0.219	0.139	0.197	0.289	0.179	0.199	0.216	0.188	0.196	450
	-0.034	-0.068	-0.08	-0.074	-0.154	-0.096	-0.004	-0.114	-0.094	-0.077	-0.105	-0.097	Blank 450
E	0.44	0.502	0.459	0.375	0.295	0.321	0.354	0.275	0.237	0.196	0.202	0.231	450
	0.147	0.209	0.166	0.082	0.002	0.028	0.061	-0.018	-0.056	-0.097	-0.091	-0.062	Blank 450
F	0.433	0.261	0.322	0.344	0.302	0.281	0.217	0.256	0.28	0.281	0.344	0.101	450
	0.14	-0.032	0.029	0.051	0.009	-0.012	-0.076	-0.037	-0.013	-0.012	0.051	-0.192	Blank 450
G	0.336	0.49	0.529	0.435	0.276	0.352	0.438	0.485	0.317	0.307	0.395	0.407	450
	0.043	0.197	0.236	0.142	-0.017	0.059	0.145	0.192	0.024	0.014	0.102	0.114	Blank 450
H	0.33	0.431	0.487	0.33	0.625	0.278	0.273	0.344	0.229	0.36	0.34	0.324	450
	0.037	0.138	0.194	0.037	0.332	-0.015	-0.02	0.051	-0.064	0.067	0.047	0.031	Blank 450

Software Version 2.00.18

Plate Number Plate 1
Date 1/10/14
Time 6:21:20 PM
Reader Type: Synergy
Reader Serial Number: 267524
Reading Type Reader

Procedure Details
Plate Type 96 WELL PLATE
Read Absorbance Endpoint
Full Plate
Wavelengths: 450
Read Speed: Normal

Results
Actual Temperature: 25.7

	1	2	3	4	5	6	7	8	9	10	11	12	
A	0.174	0.142	0.191	0.16	0.166	0.162	0.179	0.183	0.169	0.177	0.118	0.121	450
B	0.121	0.133	0.117	0.139	0.127	0.133	0.133	0.134	0.143	0.141	0.165	0.133	450
C	0.158	0.136	0.135	0.152	0.133	0.142	0.122	0.161	0.128	0.129	0.129	0.127	450
D	0.154	0.138	0.131	0.133	0.127	0.125	0.139	0.121	0.125	0.133	0.132	0.133	450
E	0.206	0.194	0.21	0.202	0.18	0.187	0.173	0.18	0.23	0.201	0.145	0.127	450
F	0.152	0.134	0.131	0.116	0.115	0.137	0.16	0.127	0.172	0.162	0.163	0.137	450
G	0.134	0.143	0.125	0.15	0.123	0.131	0.139	0.128	0.239	0.129	0.14	0.132	450
H	0.184	0.135	0.121	0.128	0.135	0.149	0.131	0.137	0.142	0.175	0.133	0.175	450

Software Version 2.00.18

Plate Number Plate 2
Date 1/10/14
Time 6:23:23 PM
Reader Type: Synergy
Reader Serial Number: 267524
Reading Type Reader

Procedure Details
Plate Type 96 WELL PLATE
Read Absorbance Endpoint
Full Plate
Wavelengths: 450
Read Speed: Normal

Results
Actual Temperature: 25.7

	1	2	3	4	5	6	7	8	9	10	11	12	
A	0.177	0.221	0.177	0.16	0.175	0.163	0.12	0.109	0.067	0.062	0.045	0.046	450
B	0.066	0.08	0.061	0.078	0.064	0.067	0.069	0.086	0.063	0.062	0.047	0.047	450
C	0.073	0.07	0.064	0.065	0.066	0.069	0.07	0.066	0.064	0.064	0.046	0.046	450
D	0.067	0.074	0.071	0.106	0.063	0.073	0.08	0.072	0.066	0.136	0.058	0.048	450
E	0.684	0.641	0.609	0.607	0.251	0.277	0.357	0.382	0.065	0.075	0.066	0.048	450
F	0.065	0.071	0.069	0.063	0.067	0.073	0.066	0.069	0.062	0.061	0.046	0.046	450
G	0.072	0.138	0.149	0.072	0.068	0.071	0.061	0.069	0.063	0.062	0.064	0.047	450
H	0.089	0.064	0.083	0.068	0.065	0.072	0.064	0.068	0.064	0.079	0.058	0.048	450

Software Version 2.00.18

Plate Number Plate 1
Date 2/12/14
Time 1:45:03 PM
Reader Type: Synergy
Reader Serial Number: 267524
Reading Type Reader

Procedure Details
Plate Type 96 WELL PLATE
Read Absorbance Endpoint
Full Plate
Wavelengths: 450
Read Speed: Normal

Results
Actual Temperature: 22

	1	2	3	4	5	6	7	8	9	10	11	12	
A	0.141	0.053	0.17	0.048	0.141	0.048	0.146	0.052	0.13	0.054	0.083	0.051	450
B	0.096	0.045	0.103	0.068	0.138	0.049	0.124	0.059	0.097	0.051	0.105	0.118	450
C	0.127	0.047	0.102	0.048	0.141	0.049	0.115	0.061	0.102	0.043	0.07	0.054	450
D	0.127	0.047	0.099	0.047	0.135	0.054	0.145	0.052	0.041	0.045	0.05	0.056	450
E	0.101	0.048	0.117	0.047	0.089	0.049	0.143	0.05	0.042	0.052	0.049	0.047	450
F	0.087	0.046	0.109	0.047	0.085	0.048	0.159	0.048	0.046	0.056	0.053	0.059	450
G	0.128	0.045	0.172	0.048	0.156	0.051	0.141	0.048	0.047	0.049	0.048	0.047	450
H	0.146	0.045	0.205	0.047	0.098	0.046	0.098	0.064	0.089	0.049	0.094	0.049	450

Software Version 2.00.18

Plate Number Plate 1
Date 2/19/14
Time 12:31:38 PM
Reader Type: Synergy
Reader Serial Number: 267524
Reading Type Reader

Procedure Details
Plate Type 96 WELL PLATE
Read Absorbance Endpoint
Full Plate
Wavelengths: 450
Read Speed: Normal

Results
Actual Temperature: 23.6

	1	2	3	4	5	6	7	8	9	10	11	12	
A	0.244	0.394	0.734	0.265	0.33	0.157	0.179	0.112	0.161	0.182	0.156	0.171	450
B	0.477	0.207	0.223	0.153	0.16	0.155	0.145	0.165	0.162	0.125	0.128	0.082	450
C	0.16	0.167	0.278	0.168	0.192	0.133	0.111	0.158	0.105	0.087	0.095	0.111	450
D	0.115	0.297	0.452	0.183	0.144	0.269	0.157	0.147	0.139	0.138	0.122	0.089	450
E	0.177	0.202	0.264	0.417	0.304	0.215	0.187	0.135	0.14	0.118	0.144	0.116	450
F	0.299	0.095	0.136	0.137	0.146	0.163	0.156	0.121	0.148	0.123	0.125	0.147	450
G	0.301	0.197	0.229	0.162	0.231	0.133	0.115	0.192	0.159	0.132	0.099	0.155	450
H	0.425	0.178	0.216	0.161	0.159	0.116	0.224	0.13	0.114	0.138	0.121	0.085	450

Software Version 2.00.18

Plate Number Plate 2
Date 2/19/14
Time 12:33:06 PM
Reader Type: Synergy
Reader Serial Number: 267524
Reading Type Reader

Procedure Details
Plate Type 96 WELL PLATE
Read Absorbance Endpoint
Full Plate
Wavelengths: 450
Read Speed: Normal

Results
Actual Temperature: 23.6

	1	2	3	4	5	6	7	8	9	10	11	12	
A	0.118	0.149	0.267	0.14	0.143	0.149	0.185	0.14	0.212	0.142	0.216	0.365	450
B	0.162	0.124	0.142	0.121	0.133	0.134	0.155	0.153	0.149	0.156	0.212	0.08	450
C	0.092	0.154	0.185	0.156	0.16	0.146	0.136	0.155	0.147	0.166	0.147	0.294	450
D	0.1	0.084	0.109	0.091	0.109	0.148	0.162	0.161	0.183	0.186	0.15	0.221	450
E	0.176	0.121	0.233	0.152	0.166	0.156	0.187	0.132	0.205	0.147	0.134	0.112	450
F	0.166	0.118	0.131	0.137	0.134	0.129	0.143	0.131	0.166	0.178	0.147	0.067	450
G	0.119	0.097	0.123	0.117	0.109	0.12	0.12	0.121	0.181	0.161	0.115	0.117	450
H	0.116	0.167	0.158	0.158	0.146	0.282	0.111	0.14	0.134	0.152	0.112	0.079	450

Software Version 2.00.18

Plate Number Plate 3
Date 2/19/14
Time 12:34:16 PM
Reader Type: Synergy
Reader Serial Number: 267524
Reading Type Reader

Procedure Details
Plate Type 96 WELL PLATE
Read Absorbance Endpoint
Full Plate
Wavelengths: 450
Read Speed: Normal

Results
Actual Temperature: 23.6

	1	2	3	4	5	6	7	8	9	10	11	12	
A	0.129	0.146	0.161	0.121	0.158	0.127	0.172	0.13	0.221	0.175	0.213	0.129	450
B	0.132	0.088	0.139	0.108	0.13	0.126	0.138	0.144	0.149	0.139	0.178	0.077	450
C	0.134	0.884	0.321	0.205	0.141	0.129	0.131	0.137	0.124	0.104	0.108	0.153	450
D	0.4	0.121	0.113	0.12	0.11	0.123	0.139	0.155	0.175	0.101	0.126	0.067	450
E	0.176	0.238	0.195	0.149	0.179	0.175	0.212	0.176	0.201	0.145	0.149	0.178	450
F	0.213	0.104	0.146	0.153	0.167	0.136	0.148	0.155	0.201	0.157	0.136	0.099	450
G	0.109	0.105	0.11	0.12	0.131	0.143	0.135	0.117	0.15	0.127	0.124	0.12	450
H	0.067	0.087	0.099	0.186	0.146	0.124	0.165	0.15	0.133	0.157	0.149	0.101	450

Software Version 2.00.18

Plate Number Plate 4
Date 2/19/14
Time 12:35:23 PM
Reader Type: Synergy
Reader Serial Number: 267524
Reading Type Reader

Procedure Details
Plate Type 96 WELL PLATE
Read Absorbance Endpoint
Full Plate
Wavelengths: 450
Read Speed: Normal

Results
Actual Temperature: 23.6

	1	2	3	4	5	6	7	8	9	10	11	12	
A	0.157	0.115	0.171	0.127	0.202	0.12	0.148	0.154	0.209	0.177	0.257	0.112	450
B	0.124	0.166	0.189	0.193	0.179	0.165	0.199	0.21	0.238	0.173	0.24	0.137	450
C	0.183	0.553	0.146	0.156	0.144	0.139	0.152	0.162	0.196	0.237	0.173	0.249	450
D	0.407	0.111	0.137	0.142	0.136	0.174	0.152	0.134	0.25	0.213	0.19	0.118	450
E	0.243	0.15	0.198	0.152	0.274	0.281	0.237	0.207	0.244	0.13	0.199	0.327	450
F	0.108	0.101	0.139	0.143	0.258	0.14	0.227	0.141	0.196	0.125	0.147	0.096	450
G	0.103	0.09	0.097	0.219	0.155	0.132	0.257	0.205	0.155	0.142	0.145	0.112	450
H	0.227	0.121	0.124	0.13	0.137	0.136	0.109	0.151	0.126	0.151	0.135	0.08	450

Software Version 2.00.18

Plate Number Plate 5
Date 2/19/14
Time 12:36:27 PM
Reader Type: Synergy
Reader Serial Number: 267524
Reading Type Reader

Procedure Details
Plate Type 96 WELL PLATE
Read Absorbance Endpoint
Full Plate
Wavelengths: 450
Read Speed: Normal

Results
Actual Temperature: 23.6

	1	2	3	4	5	6	7	8	9	10	11	12	
A	0.969	0.138	1.862	0.193	1.746	0.158	0.603	0.125	0.616	0.14	0.119	0.102	450
B	0.387	0.129	1.181	0.145	0.831	0.135	0.273	0.159	0.28	0.15	0.241	0.094	450
C	0.152	0.221	0.355	0.156	0.267	0.151	0.157	0.159	0.18	0.149	0.159	0.114	450
D	0.085	0.125	0.161	0.141	0.139	0.176	0.142	0.191	0.159	0.138	0.125	0.085	450
E	0.867	0.143	0.819	0.146	1.506	0.162	0.404	0.158	1.692	0.151	0.117	0.116	450
F	0.32	0.115	0.264	0.122	0.563	0.162	0.193	0.137	1.052	0.135	0.123	0.115	450
G	0.106	0.111	0.149	0.183	0.209	0.157	0.142	0.19	0.373	0.104	0.086	0.196	450
H	0.192	0.106	0.108	0.087	0.13	0.12	0.093	0.093	0.112	0.108	0.087	0.059	450

Software Version 2.00.18

Plate Number Plate 1
Date 2/27/14
Time 12:25:59 PM
Reader Type: Synergy
Reader Serial Number: 267524
Reading Type Reader

Procedure Details
Plate Type 96 WELL PLATE
Read Absorbance Endpoint
Full Plate
Wavelengths: 450
Read Speed: Normal

Results
Actual Temperature: 23.2

	1	2	3	4	5	6	7	8	9	10	11	12	
A	0.673	0.067	0.93	0.055	1.223	0.057	0.551	0.058	0.053	0.063	0.058	0.051	450
B	0.161	0.053	0.232	0.061	0.557	0.055	0.236	0.056	0.061	0.056	0.061	0.055	450
C	0.065	0.056	0.08	0.052	0.141	0.06	0.089	0.064	0.058	0.062	0.126	0.055	450
D	0.052	0.06	0.055	0.057	0.064	0.057	0.06	0.057	0.058	0.061	0.065	0.059	450
E	0.053	0.066	0.071	0.058	0.062	0.067	0.059	0.067	0.058	0.055	0.056	0.063	450
F	0.05	0.057	0.059	0.055	0.091	0.068	0.057	0.055	0.067	0.059	0.054	0.054	450
G	0.056	0.062	0.053	0.059	0.057	0.068	0.062	0.065	0.053	0.052	0.055	0.053	450
H	0.061	0.052	0.05	0.05	0.052	0.05	0.05	0.051	0.057	0.05	0.049	0.587	450

Software Version 2.00.18

Plate Number Plate 1
Date 4/11/14
Time 12:30:52 PM
Reader Type: Synergy
Reader Serial Number: 267524
Reading Type Reader

Procedure Details
Plate Type 96 WELL PLATE
Read Absorbance Endpoint
Full Plate
Wavelengths: 450
Read Speed: Normal

Results
Actual Temperature: 26

	1	2	3	4	5	6	7	8	9	10	11	12	
A	0.077	0.084	0.09	0.151	0.173	0.125	0.33	0.186	0.065	0.043	0.038	0.036	450
B	0.058	0.07	0.123	0.121	0.133	0.085	0.092	0.1	0.05	0.037	0.034	0.036	450
C	0.054	0.048	0.064	0.089	0.139	0.094	0.062	0.076	0.048	0.036	0.039	0.062	450
D	0.058	0.047	0.047	0.055	0.053	0.124	0.08	0.054	0.05	0.037	0.123	0.035	450
E	0.182	0.082	0.107	0.085	0.067	0.117	0.077	0.081	0.099	0.034	0.039	0.179	450
F	0.117	0.079	0.085	0.086	0.161	0.152	0.064	0.067	0.122	0.035	0.036	0.065	450
G	0.075	0.051	0.06	0.05	0.09	0.064	0.051	0.107	0.096	0.037	0.037	0.036	450
H	0.066	0.047	0.094	0.049	0.047	0.05	0.047	0.048	0.103	0.036	0.117	0.15	450

Software Version 2.00.18

Plate Number Plate 1
Date 4/16/14
Time 3:21:52 PM
Reader Type: Synergy
Reader Serial Number: 267524
Reading Type Reader

Procedure Details
Plate Type 96 WELL PLATE
Read Absorbance Endpoint
Full Plate
Wavelengths: 450
Read Speed: Normal

Results
Actual Temperature: 25.8

	1	2	3	4	5	6	7	8	9	10	11	12	
A	0.204	0.086	0.103	0.075	0.226	0.079	0.072	0.077	0.071	0.07	0.082	0.091	450
B	0.163	0.119	0.06	0.066	0.076	0.07	0.062	0.056	0.056	0.057	0.056	0.08	450
C	0.073	0.081	0.068	0.092	0.056	0.112	0.077	0.069	0.059	0.074	0.054	0.057	450
D	0.066	0.068	0.063	0.109	0.07	0.128	0.139	0.059	0.055	0.085	0.062	0.065	450
E	0.083	0.105	0.083	0.153	0.133	0.221	0.183	0.167	0.159	0.135	0.084	0.087	450
F	0.072	0.061	0.25	0.088	0.066	0.063	0.064	0.054	0.073	0.059	0.061	0.066	450
G	0.105	0.061	0.078	0.095	0.093	0.072	0.056	0.08	0.149	0.142	0.114	0.156	450
H	0.058	0.08	0.17	0.102	0.056	0.055	0.053	0.063	0.047	0.071	0.062	0.054	450

Software Version 2.00.18

Plate Number Plate 2
Date 4/16/14
Time 3:23:55 PM
Reader Type: Synergy
Reader Serial Number: 267524
Reading Type Reader

Procedure Details
Plate Type 96 WELL PLATE
Read Absorbance Endpoint
Full Plate
Wavelengths: 450
Read Speed: Normal

Results
Actual Temperature: 25.8

	1	2	3	4	5	6	7	8	9	10	11	12	
A	0.147	0.091	0.135	0.073	0.219	0.092	0.2	0.078	0.073	0.072	0.091	0.085	450
B	0.08	0.093	0.071	0.088	0.073	0.207	0.049	0.124	0.066	0.111	0.055	0.061	450
C	0.117	0.144	0.085	0.222	0.168	0.125	0.076	0.118	0.177	0.128	0.054	0.067	450
D	0.097	0.101	0.066	0.074	0.079	0.099	0.137	0.095	0.078	0.101	0.08	0.07	450
E	0.088	0.18	0.2	0.104	0.076	0.087	0.095	0.189	0.069	0.066	0.068	0.081	450
F	0.088	0.147	0.278	0.071	0.065	0.073	0.075	0.073	0.057	0.079	0.093	0.201	450
G	0.063	0.102	0.063	0.062	0.059	0.073	0.08	0.067	0.059	0.056	0.054	0.051	450
H	0.057	0.111	0.223	0.072	0.121	0.076	0.176	0.055	0.055	0.051	0.084	0.126	450

Software Version 2.00.18

Plate Number Plate 3
Date 4/16/14
Time 3:25:14 PM
Reader Type: Synergy
Reader Serial Number: 267524
Reading Type Reader

Procedure Details
Plate Type 96 WELL PLATE
Read Absorbance Endpoint
Full Plate
Wavelengths: 450
Read Speed: Normal

Results
Actual Temperature: 25.8

	1	2	3	4	5	6	7	8	9	10	11	12	
A	0.126	0.089	0.093	0.069	0.143	0.081	0.046	0.088	0.113	0.113	0.118	0.082	450
B	0.089	0.056	0.066	0.072	0.053	0.056	0.049	0.065	0.058	0.094	0.056	0.12	450
C	0.094	0.106	0.094	0.164	0.062	0.071	0.128	0.072	0.095	0.083	0.07	0.138	450
D	0.065	0.126	0.059	0.117	0.083	0.126	0.115	0.074	0.08	0.074	0.072	0.09	450
E	0.152	0.089	0.22	0.148	0.103	0.16	0.111	0.123	0.064	0.085	0.07	0.074	450
F	0.324	0.066	0.07	0.064	0.11	0.063	0.061	0.068	0.06	0.057	0.075	0.099	450
G	0.056	0.061	0.079	0.062	0.115	0.053	0.056	0.062	0.072	0.053	0.065	0.072	450
H	0.051	0.127	0.245	0.375	0.049	0.104	0.047	0.091	0.046	0.065	0.125	0.055	450

Software Version 2.00.18

Plate Number Plate 4
Date 4/16/14
Time 3:26:50 PM
Reader Type: Synergy
Reader Serial Number: 267524
Reading Type Reader

Procedure Details
Plate Type 96 WELL PLATE
Read Absorbance Endpoint
Full Plate
Wavelengths: 450
Read Speed: Normal

Results
Actual Temperature: 25.7

	1	2	3	4	5	6	7	8	9	10	11	12	
A	0.083	0.083	0.338	0.083	0.115	0.121	0.09	0.056	0.18	0.066	0.06	0.07	450
B	0.224	0.063	0.11	0.062	0.073	0.136	0.063	0.06	0.116	0.067	0.079	0.065	450
C	0.098	0.126	0.058	0.094	0.092	0.073	0.099	0.096	0.061	0.074	0.12	0.179	450
D	0.075	0.083	0.099	0.097	0.181	0.11	0.108	0.106	0.183	0.178	0.295	0.183	450
E	0.086	0.058	0.117	0.172	0.107	0.103	0.091	0.09	0.057	0.087	0.069	0.079	450
F	0.145	0.054	0.127	0.061	0.148	0.061	0.071	0.068	0.086	0.135	0.065	0.067	450
G	0.053	0.049	0.071	0.056	0.111	0.081	0.049	0.058	0.083	0.06	0.062	0.071	450
H	0.051	0.085	0.049	0.136	0.049	0.072	0.051	0.064	0.093	0.066	0.082	0.064	450

Software Version 2.00.18

Plate Number Plate 5
Date 4/16/14
Time 3:28:04 PM
Reader Type: Synergy
Reader Serial Number: 267524
Reading Type Reader

Procedure Details
Plate Type 96 WELL PLATE
Read Absorbance Endpoint
Full Plate
Wavelengths: 450
Read Speed: Normal

Results
Actual Temperature: 25.7

	1	2	3	4	5	6	7	8	9	10	11	12	
A	0.144	0.067	0.729	0.069	0.074	0.065	0.134	0.052	0.064	0.121	0.071	0.103	450
B	0.09	0.157	0.087	0.067	0.064	0.107	0.052	0.055	0.087	0.079	0.059	0.065	450
C	0.07	0.197	0.1	0.11	0.116	0.088	0.053	0.113	0.096	0.061	0.123	0.095	450
D	0.072	0.089	0.213	0.07	0.158	0.095	0.072	0.105	0.068	0.092	0.075	0.071	450
E	0.244	0.135	0.073	0.085	0.099	0.128	0.144	0.083	0.074	0.102	0.079	0.133	450
F	0.165	0.073	0.097	0.073	0.08	0.065	0.131	0.103	0.063	0.145	0.074	0.068	450
G	0.087	0.065	0.116	0.055	0.075	0.07	0.111	0.104	0.085	0.133	0.075	0.086	450
H	0.06	0.103	0.053	0.103	0.059	0.087	0.07	0.08	0.049	0.055	0.117	0.166	450

Software Version 2.00.18

Plate Number Plate 6
Date 4/16/14
Time 3:29:20 PM
Reader Type: Synergy
Reader Serial Number: 267524
Reading Type Reader

Procedure Details
Plate Type 96 WELL PLATE
Read Absorbance Endpoint
Full Plate
Wavelengths: 450
Read Speed: Normal

Results
Actual Temperature: 25.7

	1	2	3	4	5	6	7	8	9	10	11	12	
A	0.07	0.125	0.078	0.061	0.169	0.089	0.08	0.24	0.079	0.083	0.13	0.076	450
B	0.086	0.167	0.099	0.101	0.069	0.165	0.07	0.15	0.164	0.071	0.066	0.072	450
C	0.075	0.084	0.072	0.088	0.133	0.148	0.189	0.184	0.092	0.073	0.059	0.104	450
D	0.075	0.233	0.07	0.12	0.197	0.098	0.112	0.318	0.089	0.073	0.076	0.104	450
E	0.092	0.075	0.089	0.164	0.086	0.077	0.12	0.142	0.062	0.079	0.138	0.156	450
F	0.187	0.125	0.067	0.151	0.134	0.069	0.115	0.163	0.06	0.076	0.132	0.18	450
G	0.068	0.069	0.103	0.118	0.082	0.056	0.085	0.115	0.166	0.07	0.079	0.145	450
H	0.344	0.071	0.062	0.071	0.05	0.085	0.056	0.057	0.049	0.11	0.052	0.084	450

Software Version 2.00.18

Plate Number Plate 7
Date 4/16/14
Time 3:30:34 PM
Reader Type: Synergy
Reader Serial Number: 267524
Reading Type Reader

Procedure Details
Plate Type 96 WELL PLATE
Read Absorbance Endpoint
Full Plate
Wavelengths: 450
Read Speed: Normal

Results
Actual Temperature: 25.6

	1	2	3	4	5	6	7	8	9	10	11	12	
A	0.362	0.127	0.1	0.069	0.141	0.085	0.141	0.058	0.096	0.13	0.149	0.07	450
B	0.268	0.11	0.074	0.074	0.075	0.108	0.114	0.124	0.098	0.21	0.093	0.125	450
C	0.121	0.083	0.081	0.107	0.085	0.099	0.115	0.201	0.137	0.161	0.097	0.345	450
D	0.066	0.063	0.081	0.268	0.077	0.136	0.167	0.111	0.114	0.116	0.145	0.075	450
E	0.157	0.084	0.089	0.114	0.19	0.176	0.084	0.145	0.131	0.127	0.133	0.084	450
F	0.075	0.066	0.115	0.097	0.097	0.068	0.128	0.09	0.133	0.078	0.123	0.06	450
G	0.244	0.086	0.116	0.074	0.087	0.095	0.088	0.109	0.099	0.119	0.078	0.07	450
H	0.083	0.099	0.066	0.305	0.059	0.116	0.05	0.073	0.059	0.091	0.066	0.081	450

Software Version 2.00.18

Plate Number Plate 8
Date 4/16/14
Time 3:31:45 PM
Reader Type: Synergy
Reader Serial Number: 267524
Reading Type Reader

Procedure Details
Plate Type 96 WELL PLATE
Read Absorbance Endpoint
Full Plate
Wavelengths: 450
Read Speed: Normal

Results
Actual Temperature: 25.6

	1	2	3	4	5	6	7	8	9	10	11	12	
A	0.13	0.121	0.241	0.081	0.144	0.103	0.089	0.081	0.13	0.107	0.138	0.08	450
B	0.104	0.138	0.117	0.103	0.175	0.121	0.164	0.067	0.093	0.114	0.181	0.112	450
C	0.14	0.127	0.129	0.197	0.1	0.163	0.159	0.103	0.089	0.089	0.304	0.104	450
D	0.136	0.093	0.154	0.267	0.141	0.154	0.128	0.132	0.063	0.193	0.166	0.108	450
E	0.124	0.117	0.145	0.153	0.233	0.146	0.137	0.103	0.064	0.062	0.159	0.111	450
F	0.096	0.13	0.192	0.274	0.12	0.173	0.088	0.073	0.081	0.084	0.107	0.089	450
G	0.125	0.143	0.12	0.088	0.088	0.122	0.122	0.064	0.102	0.089	0.07	0.053	450
H	0.053	0.081	0.059	0.103	0.057	0.069	0.059	0.136	0.05	0.09	0.058	0.049	450

Software Version 2.00.18

Plate Number Plate 9
Date 4/16/14
Time 3:32:56 PM
Reader Type: Synergy
Reader Serial Number: 267524
Reading Type Reader

Procedure Details
Plate Type 96 WELL PLATE
Read Absorbance Endpoint
Full Plate
Wavelengths: 450
Read Speed: Normal

Results
Actual Temperature: 25.6

	1	2	3	4	5	6	7	8	9	10	11	12	
A	0.758	0.942	1.519	0.44	0.841	1.445	0.441	0.678	1.57	0.584	1.139	1.677	450
B	0.397	0.425	0.849	0.226	0.3	0.794	0.211	0.216	0.904	0.37	0.347	1.22	450
C	0.146	0.42	0.38	0.143	0.19	0.205	0.141	0.144	0.376	0.322	0.22	0.33	450
D	0.145	0.245	0.153	0.298	0.19	0.107	0.118	0.271	0.27	0.24	0.186	0.173	450
E	0.39	0.84	1.553	0.426	0.585	1.362	0.575	0.742	1.374	0.613	0.683	0.162	450
F	0.28	0.49	1.279	0.399	0.415	0.747	0.297	0.462	0.728	0.335	0.322	0.167	450
G	0.078	0.207	0.247	0.232	0.213	0.154	0.187	0.201	0.229	0.138	0.174	0.105	450
H	0.057	0.26	0.105	0.09	0.183	0.14	0.081	0.148	0.12	0.061	0.089	0.105	450

Software Version 2.00.18

Plate Number Plate 1
Date 5/2/14
Time 12:05:09 PM
Reader Type: Synergy
Reader Serial Number: 267524
Reading Type Reader

Procedure Details
Plate Type 96 WELL PLATE
Read Absorbance Endpoint
Full Plate
Wavelengths: 450
Read Speed: Normal

Results
Actual Temperature: 25.3

	1	2	3	4	5	6	7	8	9	10	11	12	
A	1.51	1.341	1.041	1.473	0.601	1.028	1.751	0.714	0.819	1.501	0.57	0.987	450
B	0.932	0.167	0.319	1.162	0.118	0.299	1.023	0.307	0.219	0.906	0.143	0.321	450
C	0.137	0.082	0.086	0.376	0.054	0.107	0.056	0.05	0.072	0.206	0.072	0.084	450
D	0.069	0.073	0.053	0.105	0.054	0.072	0.053	0.058	0.135	0.087	0.065	0.055	450
E	1.571	0.58	0.698	1.021	0.929	0.728	0.764	0.599	1.026	1.637	0.069	0.099	450
F	1.208	0.161	0.139	0.187	0.277	0.243	0.21	0.201	0.262	1.259	0.045	0.42	450
G	0.174	0.458	0.054	0.124	0.076	0.067	0.061	0.097	0.073	0.35	0.044	0.06	450
H	0.067	0.048	0.74	0.045	0.089	0.056	0.076	0.057	0.049	0.076	0.054	0.045	450

Antibody Detection ELISA Spleen Samples

Software Version 2.00.18

Plate Number Plate 1
Date 7/25/14
Time 2:07:09 PM
Reader Type: Synergy
Reader Serial Number: 267524
Reading Type Reader

Procedure Details
Plate Type 96 WELL PLATE
Read Absorbance Endpoint
Full Plate
Wavelengths: 450
Read Speed: Normal

Results
Actual Temperature: 28.4

	1	2	3	4	5	6	7	8	9	10	11	12	
A	0.097	0.235	0.188	0.134	0.128	0.144	0.13	0.154	0.123	0.134	0.158	0.108	450
B	0.124	0.155	0.154	1.006	0.154	0.168	0.146	0.143	0.138	0.146	0.218	0.12	450
C	0.145	0.145	0.148	0.305	0.156	0.189	0.153	0.138	0.15	0.192	0.526	0.107	450
D	0.149	0.147	0.144	0.156	0.17	0.152	0.154	0.158	0.173	0.202	0.127	0.139	450
E	0.117	0.149	0.173	0.159	0.167	0.177	0.192	0.167	0.162	0.152	0.133	0.046	450
F	0.128	0.162	0.179	0.168	0.154	0.157	0.14	0.142	0.154	0.179	0.209	0.057	450
G	0.111	0.147	0.165	0.18	0.159	0.169	0.181	0.242	0.23	0.255	0.15	0.04	450
H	0.147	0.133	0.136	0.139	0.133	0.15	0.155	0.125	0.179	0.141	0.162	0.079	450

Software Version 2.00.18

Plate Number Plate 2
Date 7/25/14
Time 2:08:49 PM
Reader Type: Synergy
Reader Serial Number: 267524
Reading Type Reader

Procedure Details
Plate Type 96 WELL PLATE
Read Absorbance Endpoint
Full Plate
Wavelengths: 450
Read Speed: Normal

Results
Actual Temperature: 28.3

	1	2	3	4	5	6	7	8	9	10	11	12	
A	0.096	0.115	0.1	0.137	0.12	0.13	0.096	0.107	0.112	0.104	0.165	0.256	450
B	0.089	0.161	0.111	0.132	0.119	0.11	0.105	0.114	0.097	0.101	0.117	0.161	450
C	0.098	0.122	0.132	0.124	0.138	0.145	0.102	0.138	0.114	0.116	0.158	0.105	450
D	0.103	0.105	0.141	0.111	0.128	0.139	0.123	0.163	0.155	0.17	0.169	0.226	450
E	0.099	0.096	0.147	0.118	0.127	0.114	0.245	0.158	0.144	0.105	0.198	0.105	450
F	0.1	0.098	0.118	0.123	0.173	0.119	0.118	0.133	0.152	0.123	0.122	0.129	450
G	0.09	0.105	0.115	0.109	0.119	0.154	0.115	0.119	0.123	0.108	0.16	0.104	450
H	0.109	0.097	0.109	0.107	0.137	0.134	0.116	0.108	0.131	0.126	0.279	0.051	450

Software Version 2.00.18

Plate Number Plate 3
Date 7/25/14
Time 2:10:07 PM
Reader Type: Synergy
Reader Serial Number: 267524
Reading Type Reader

Procedure Details
Plate Type 96 WELL PLATE
Read Absorbance Endpoint
Full Plate
Wavelengths: 450
Read Speed: Normal

Results
Actual Temperature: 28.3

	1	2	3	4	5	6	7	8	9	10	11	12	
A	0.154	0.209	0.206	0.167	0.17	0.363	0.172	0.17	0.169	0.229	0.191	0.156	450
B	0.16	0.185	0.166	0.152	0.157	0.174	0.181	0.185	0.184	0.176	0.221	0.154	450
C	0.188	0.185	0.208	0.192	0.342	0.267	0.218	0.196	0.187	0.194	0.205	0.135	450
D	0.168	0.168	0.185	0.185	0.267	0.379	0.2	0.213	0.185	0.197	0.193	0.177	450
E	0.161	0.168	0.591	0.224	0.279	0.373	0.186	0.22	0.193	0.208	0.169	0.047	450
F	0.166	0.163	0.201	0.184	0.196	0.241	0.175	0.172	0.186	0.191	0.177	0.053	450
G	0.204	0.224	0.295	0.22	0.251	0.305	0.247	0.213	0.193	0.22	0.286	0.046	450
H	0.162	0.199	0.239	0.203	0.232	0.309	0.179	0.222	0.194	0.179	0.241	0.045	450

Software Version 2.00.18

Plate Number Plate 4
Date 7/25/14
Time 2:11:20 PM
Reader Type: Synergy
Reader Serial Number: 267524
Reading Type Reader

Procedure Details
Plate Type 96 WELL PLATE
Read Absorbance Endpoint
Full Plate
Wavelengths: 450
Read Speed: Normal

Results
Actual Temperature: 28.2

	1	2	3	4	5	6	7	8	9	10	11	12	
A	0.118	0.407	0.203	0.226	0.16	0.184	0.157	0.164	0.175	0.168	0.152	0.181	450
B	0.142	0.183	0.219	0.181	0.207	0.197	0.193	0.305	0.184	0.389	0.161	0.163	450
C	0.366	0.17	0.171	0.205	0.192	0.205	0.196	0.217	0.22	0.204	0.158	0.236	450
D	0.145	0.175	0.199	0.296	0.171	0.163	0.236	0.245	0.164	0.22	0.28	0.158	450
E	0.162	0.173	0.178	0.199	0.254	0.212	0.235	0.2	0.222	0.192	0.267	0.054	450
F	0.123	0.143	0.168	0.169	0.169	0.179	0.206	0.21	0.201	0.17	0.382	0.048	450
G	0.145	0.156	0.2	0.23	0.222	0.215	0.217	0.215	0.24	0.24	0.173	0.044	450
H	0.152	0.16	0.172	0.174	0.189	0.17	0.22	0.171	0.17	0.265	0.207	0.051	450

Software Version 2.00.18

Plate Number Plate 5
Date 7/25/14
Time 2:12:30 PM
Reader Type: Synergy
Reader Serial Number: 267524
Reading Type Reader

Procedure Details
Plate Type 96 WELL PLATE
Read Absorbance Endpoint
Full Plate
Wavelengths: 450
Read Speed: Normal

Results
Actual Temperature: 28.2

	1	2	3	4	5	6	7	8	9	10	11	12	
A	0.076	0.106	0.102	0.088	0.096	0.105	0.116	0.101	0.108	0.054	0.043	0.04	450
B	0.15	0.092	0.11	0.109	0.124	0.115	0.183	0.126	0.135	0.04	0.041	0.039	450
C	0.107	0.092	0.107	0.103	0.1	0.109	0.107	0.104	0.135	0.039	0.042	0.042	450
D	0.094	0.097	0.106	0.103	0.115	0.128	0.126	0.127	0.115	0.041	0.042	0.043	450
E	0.1	0.128	0.101	0.12	0.144	0.153	0.232	0.149	0.199	0.043	0.04	0.042	450
F	0.132	0.1	0.102	0.151	0.15	0.153	0.187	0.15	0.156	0.042	0.043	0.049	450
G	0.122	0.097	0.13	0.159	0.174	0.177	0.165	0.151	0.171	0.042	0.041	0.033	450
H	0.124	0.114	0.103	0.109	0.128	0.138	0.133	0.152	0.146	0.044	0.042	0.043	450

Software Version 2.00.18

Plate Number Plate 6
Date 7/25/14
Time 2:13:38 PM
Reader Type: Synergy
Reader Serial Number: 267524
Reading Type Reader

Procedure Details
Plate Type 96 WELL PLATE
Read Absorbance Endpoint
Full Plate
Wavelengths: 450
Read Speed: Normal

Results
Actual Temperature: 28.1

	1	2	3	4	5	6	7	8	9	10	11	12	
A	0.07	0.094	0.102	0.094	0.13	0.108	0.094	0.096	0.104	0.043	0.043	0.036	450
B	0.093	0.11	0.13	0.098	0.117	0.119	0.113	0.13	0.116	0.047	0.043	0.047	450
C	0.114	0.146	0.11	0.133	0.116	0.131	0.129	0.127	0.112	0.153	0.043	0.049	450
D	0.081	0.101	0.089	0.115	0.122	0.115	0.112	0.12	0.126	0.041	0.041	0.039	450
E	0.081	0.099	0.104	0.119	0.118	0.117	0.138	0.119	0.113	0.042	0.043	0.045	450
F	0.121	0.168	0.121	0.11	0.135	0.115	0.125	0.132	0.115	0.042	0.047	0.046	450
G	0.195	0.127	0.112	0.106	0.14	0.191	0.171	0.136	0.159	0.042	0.039	0.042	450
H	0.267	0.118	0.114	0.111	0.134	0.137	0.128	0.102	0.112	0.033	0.042	0.045	450

APPENDIX III: BCA DATA

BCA Data

Software Version 2.00.18

Plate Number Plate 1
Date 10/15/13
Time 3:50:46 PM
Reader Type: Synergy
Reader Serial Number: 267524
Reading Type Reader

Procedure Details
Plate Type 96 WELL PLATE
Read Absorbance Endpoint
Full Plate
Wavelengths: 562
Read Speed: Normal

Layout

	1	2	3	4	5	6	7	8	9	10	11	12	
A	SPL1	SPL2	SPL3		SPL25	SPL26	SPL27						Well ID
B	SPL4	SPL5	SPL6		SPL28	SPL29	SPL30						Well ID
C	SPL7	SPL8	SPL9		SPL31	SPL32	SPL33						Well ID
D	SPL10	SPL11	SPL12		SPL34	SPL35	SPL36						Well ID
E	SPL13	SPL14	SPL15										Well ID
F	SPL16	SPL17	SPL18										Well ID
G	SPL19	SPL20	SPL21										Well ID
H	SPL22	SPL23	SPL24										Well ID

Results
Actual Temperature: 25.4

	1	2	3	4	5	6	7	8	9	10	11	12	
A	0.083	0.081	0.08		0.283	0.291	0.328						562
B	0.151	0.155	0.154		0.321	0.351	0.385						562
C	0.236	0.229	0.221		0.152	0.157	0.189						562
D	0.376	0.372	0.371		0.123	0.117	0.166						562
E	0.488	0.5	0.495										562
F	0.645	0.603	0.591										562
G	0.858	0.856	0.849										562
H	1.084	1.099	1.055										562

Software Version 2.00.18

Plate Number Plate 1
Date 2/6/14
Time 11:54:35 AM
Reader Type: Synergy
Reader Serial Number: 267524
Reading Type Reader

Procedure Details
Plate Type 96 WELL PLATE
Read Absorbance Endpoint
Full Plate
Wavelengths: 562
Read Speed: Normal

Results
Actual Temperature: 16.5

	1	2	3	4	5	6	7	8	9	10	11	12	
A	0.09	0.088	0.042	0.043	0.412	0.412	0.044	0.043	0.043	0.043	0.044	0.043	562
B	0.279	0.203	0.043	0.043	0.043	0.044	0.044	0.046	0.044	0.047	0.044	0.043	562
C	0.409	0.343	0.043	0.043	0.044	0.043	0.044	0.043	0.044	0.044	0.044	0.043	562
D	0.708	0.553	0.043	0.044	0.043	0.043	0.043	0.044	0.044	0.044	0.044	0.044	562
E	0.994	0.873	0.043	0.043	0.043	0.043	0.043	0.045	0.044	0.044	0.044	0.043	562
F	0.805	1.146	0.043	0.043	0.042	0.043	0.043	0.043	0.043	0.044	0.044	0.043	562
G	1.791	1.461	0.042	0.044	0.043	0.043	0.043	0.043	0.044	0.043	0.043	0.043	562
H	2.388	1.892	0.042	0.043	0.043	0.043	0.043	0.043	0.043	0.043	0.043	0.043	562

Software Version 2.00.18

Plate Number Plate 1
Date 5/20/14
Time 2:31:31 PM
Reader Type: Synergy
Reader Serial Number: 267524
Reading Type Reader

Procedure Details

Plate Type 96 WELL PLATE
Read Absorbance Endpoint
Full Plate
Wavelengths: 562
Read Speed: Normal

Results

Actual Temperature: 27

	1	2	3	4	5	6	7	8	9	10	11	12	
A	0.087	0.081	0.081	0.083	0.36	0.365	0.387	0.043	0.043	0.042	0.041	0.043	562
B	0.201	0.17	0.153	0.08	0.083	0.084	0.087	0.043	0.042	0.045	0.044	0.043	562
C	0.342	0.233	0.206	0.08	0.099	0.104	0.108	0.044	0.043	0.043	0.043	0.043	562
D	0.563	0.503	0.298	0.081	0.081	0.081	0.081	0.044	0.044	0.044	0.044	0.044	562
E	0.685	0.59	0.508	0.082	0.084	0.09	0.084	0.043	0.045	0.043	0.044	0.043	562
F	0.941	0.723	0.61	0.043	0.044	0.045	0.044	0.048	0.044	0.044	0.044	0.044	562
G	1.244	0.919	0.897	0.041	0.043	0.045	0.045	0.043	0.044	0.043	0.043	0.043	562
H	1.363	1.327	1.178	0.043	0.043	0.043	0.043	0.044	0.043	0.042	0.043	0.043	562

STD	Abs Avg	Sub Blank
2	1.289333	1.206333
1.5	1.02	0.937
1	0.758	0.675
0.75	0.594333	0.511333
0.5	0.454667	0.371667
0.25	0.260333	0.177333
0.125	0.174667	0.091667
0	0.083	0

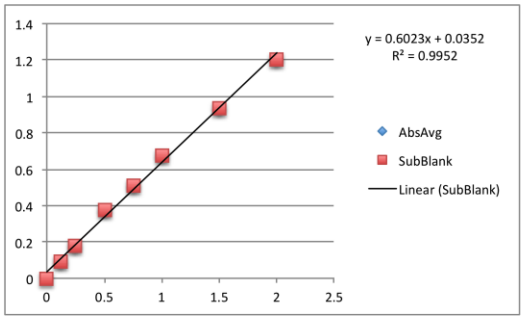

Sample Name	Abs Avg	Sub Blank	Conc	Sample	Buffer
1 to 5	0.370667	0.287667	2.679413	20.52688	5479.473

Protein	Bicarb
20.5	5479

	1	2	3	4	5	6	7	8	9	10	11	12	
A	0.097	0.094	0.085	0.042	0.043	0.043	0.251	0.252	0.254	0.041	0.041	0.046	560
B	0.174	0.195	0.171	0.041	0.038	0.04	0.041	0.039	0.042	0.042	0.043	0.043	560
C	0.269	0.33	0.278	0.039	0.039	0.042	0.11	0.112	0.115	0.043	0.044	0.044	560
D	0.447	0.52	0.47	0.044	0.038	0.037	0.043	0.044	0.044	0.04	0.044	0.042	560
E	0.608	0.864	0.671	0.044	0.043	0.038	0.492	0.486	0.493	0.043	0.04	0.04	560
F	0.769	0.856	0.794	0.043	0.043	0.042	0.04	0.043	0.039	0.043	0.043	0.042	560
G	0.946	1.388	1.002	0.042	0.043	0.042	0.152	0.151	0.156	0.041	0.043	0.038	560
H	1.239	1.552	1.254	0.042	0.043	0.043	0.044	0.046	0.043	0.042	0.043	0.042	560

STd	Abs Avg	Sub Blank
2	1.348333	1.256333
1.5	1.112	1.02
1	0.806333	0.714333
0.75	0.714333	0.622333
0.5	0.479	0.387
0.25	0.292333	0.200333
0.125	0.18	0.088
0	0.092	0

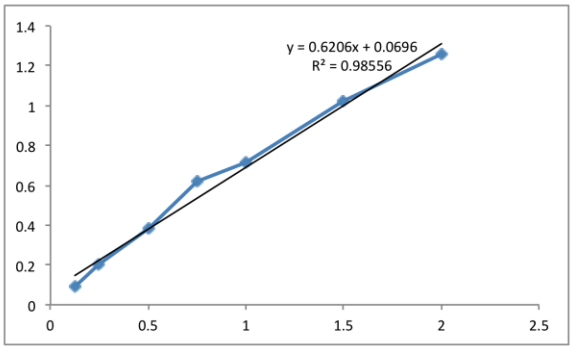

Name	Avg	Sub Blank	Conc	Sample	SDS	Water
Auto	0.252333	0.160333	1.462026	54.2	11	0.8
Allo	0.490333	0.398333	5.297024	15.0	11	40.0

APPENDIX IV: FLOW DATA

Samples	# Lymphocytes	CD3+	CD3 Proliferation
292.1	4.13	55.4	37.1
292.2	1.66	15.9	57.1
292.3	1.35	34	33.3
	2.38	**35.1**	**42.5**
292.4	3.96	55.7	14.1
292.5	45.7	97.5	5.8
	24.83	**76.6**	**9.95**
292.7	12.7	86	20.3
292.8	28.6	89.6	20.4
292.9	1.44	13.3	16.7
	14.24666667	**62.96666667**	**19.13333333**
293.1	**1.53**	**16.5**	**32.3**
293.4	**28.7**	**21.2**	**28**
293.7	**2.5**	**3**	**20**
296.1	**2.25**	**31.2**	**58.8**
296.4	**29.7**	**36.9**	**28**
296.7	**0.77**	**38.3**	**44.4**
721.1	1.36	57.8	59.7
721.2	14.8	57.1	42.5
721.3	19.6	60.5	32
	11.92	**58.46666667**	**44.73333333**
721.4	25	58.4	20.1
721.5	31.9	61.3	20
721.6	33.8	60.8	20.3
	30.23333333	**60.16666667**	**20.13333333**
721.7	8.49	47	43.2
721.8	1.79	31.1	52.7
721.9	0.76	21.6	50
	3.68	**33.23333333**	**48.63333333**
722.1	7.47	60.2	31.1
722.2	2.51	30.1	31.8
722.3	5.8	50.5	34.6
	5.26	**46.93333333**	**32.5**
722.4	5.86	41.3	29.8
722.5	5.89	48.9	23.4

722.6	2.02	17.5	21.4
	4.59	**35.9**	**24.86666667**
722.7	1.67	11.8	50
722.8	1.53	20.7	41.2
722.9	1.91	13.6	37.5
	1.703333333	**15.36666667**	**42.9**
756.1	0.82	73.6	65.4
756.2	1.06	67.9	66.3
	0.94	**70.75**	**65.85**
756.4	**0.38**	**62.5**	**63.3**
756.7	**1.16**	**81.4**	**68.6**
765.1	0.61	74.4	22.4
765.2	4.86	76	22.6
765.3	2.44	56.7	29
	2.636666667	**69.03333333**	**24.66666667**
765.4	7.4	60.5	13.7
765.5	4.52	67.2	15
	5.96	**63.85**	**14.35**
765.7	0.61	47.7	28.6
765.8	1.34	49.6	19
765.9	1.78	55.4	31.1
	1.243333333	**50.9**	**26.23333333**
775.1	**10.1**	**85.8**	**4.33**
775.7	**1.08**	**42.4**	**36**

Samples	**# Lymphocytes**	**CD3+**	**CD3 Proliferation**
297.1	**0.8**	**36.6**	**46.7**
297.4	**2.02**	**46**	**4.35**
297.7	**0.57**	**31.7**	**15.4**
298.1	**1**	**35.8**	**31.6**
298.4	**3.2**	**67.5**	**24.1**
298.7	**0.97**	**43.2**	**28.1**
723.1	**0.16**	**20**	**0**

723.4	**2.32**	**85**	**7.81**
723.7	**3.23**	**83.8**	**14.4**
758.1	**1.14**	**11.5**	**33.3**
758.7	**0.67**	**5**	**0**
761.1	1.23	47.5	32.1
761.2	0.73	17.9	40
			36.05
761.4	**6.36**	**79**	**18.9**
761.7	1.45	1.69	100
761.8	0.81	26.3	50
			75
770.1	0.12	13.3	50
770.2	0.24	17.2	20
770.3	0.12	26.7	50
			40
770.4	17.7	90.4	19.1
770.5	42.5	92.6	19.9
770.6	33.5	89.6	33.4
			24.13333333
770.7	0.88	60.2	43.1
770.8	0.1	27.8	30
770.9	0.32	6.45	50
			41.03333333
772.1	**21.1**	**95.6**	**13.6**
772.4	**13.5**	**93.3**	**25.5**
772.7	1.1	50.9	26.7
772.8	0.91	16.7	0
772.9	0.84	0	0
			8.9
781.2	36.4	88.3	43.5
782.1	33.3	89.7	40.6
782.3	40.1	90.4	55.5
			46.53333333
782.4	35.4	87.7	41.6
782.5	38.1	92.2	41.3

782.6	34.9	88.1	24.8
			35.9
782.7	29.6	88.9	47.4
782.8	33	85.8	42.6
782.9	10.6	79	48.3
			46.1

Samples	**# Lymphocytes**	**CD3+**	**CD3 Proliferation**
751.1	0.2	25	14.3
751.2	0.64	35.9	3.57
751.3	0.28	13.5	14.3
			10.72333333
751.4	0.45	80.4	8.89
751.5	0.78	85.1	11.2
			10.045
752.1	0.68	87.8	4.17
752.2	0.66	92.5	2.7
			3.435
752.4	0.58	31.6	28
752.5	1.44	78.9	9.3
			18.65
753.1	0.23	73.3	13.6
753.2	0.24	83.9	15.4
753.3	0.21	61.5	12.5
			13.83333333
753.4	0.28	88.6	0
753.5	0.19	87.5	9.52
753.6	0.22	81.5	4.55
			4.69
754.1	0.84	85.4	2.27
754.2	0.72	88.8	5.06
754.3	0.67	87.7	2.82
			3.383333333
754.4	0.86	93.3	5.15
754.5	0.81	88	2.27
			3.71
756.2	17.2	96.7	6.08
756.3	21.3	97.1	6.88
			6.48
756.4	21.7	97.9	4.64
756.5	28.7	97.4	7.01
756.6	32	97	5.61

			5.753333333
757.1	9.18	83.9	5.55
757.2	11.8	82.1	7.1
757.3	11.5	80.9	8.15
			6.933333333
757.4	21.1	84.6	7.43
757.5	16.6	81.7	7.16
757.6	22.4	83.1	8.59
			7.726666667
760.1	50.4	96	13.7
760.2	45.3	95.7	12.3
760.3	45.6	95.8	12.6
			12.86666667
760.4	66.9	97.2	10.7
760.5	66.8	96.9	12.4
760.6	59.1	96.5	11.9
			11.66666667
761.1	41.6	92.2	14.9
761.2	43.5	93	14.9
761.3	38.3	92.9	14.8
			14.86666667
761.4	50.9	96.4	12.4
761.5	50.5	95.5	12.4
761.6	57.2	95.8	13.3
			12.7
764.1	14.3	98.5	1.18
764.2	6.09	97.3	1.32
764.3	15.7	98.7	0.52
			1.006666667
764.4	34.7	98.7	0.65
764.5	39.6	98.7	0.63
764.6	30.7	98.5	0.8
			0.693333333
951.1	8.73	96.1	7.37
951.2	8.91	96	6.22
			6.795
951.4	4.96	94.7	4.17
951.5	3.9	87.1	3.41
			3.79
959.1	56	98.9	4.02
959.2	52.4	98.9	2.13
959.3	46.9	99.3	2.66
			2.936666667

959.4	70	98.8	2.72
959.5	65.7	98.7	2.41
959.6	66.1	98.7	2.54
			2.556666667
972.1	3.38	70	15
972.2	2.66	64.2	19.4
972.3	3.14	68.9	15.3
			16.56666667
972.4	4.07	74.4	16.1
972.5	3.12	68.9	15.4
			15.75
981.1	41.3	98.1	6.93
981.2	39.9	97.9	6.13
981.3	37.4	98.1	6.65
			6.57
981.5	37.3	99	5.08
981.6	62.4	99.1	4.88
			4.98
982.1	6.08	34.4	7
982.2	6.44	30	8.97
982.3	7.49	33.3	7.59
			7.853333333
982.4	7.2	31.6	4.73
982.5	10.5	30.2	3.93
982.6	10.6	29.4	12.2
			6.953333333
985.1	36.1	93.7	16.8
985.2	42.1	94.2	17.3
985.3	45.7	93.8	17.5
			17.2
985.4	61	95.9	13.1
985.5	54.3	94.9	15.7
985.6	61.9	96.3	13
			13.93333333

Samples	**# Lymphocytes**	**CD3+**	**CD3 Proliferation**
726.1	1.48	49.2	46.7
726.2	1.65	54.9	38.5
762.3	1.49	56.3	58.6
			47.93333333
726.4	2.2	73	32.3

726.5	1.7	63.3	52.6
			42.45
726.7	1.18	60.6	50
726.8	0.56	21.7	46.7
			48.35
728.1	38.4	98.3	15
728.2	41.8	98.8	16.8
728.3	39.1	98.6	13.1
			14.96666667
728.4	47.7	98.7	17.1
728.5	46.5	99.1	14.6
728.6	48.3	98.7	15.6
			15.76666667
728.7	42.5	99	16.9
728.8	41.9	98.9	17.8
728.9	46.6	99	18.9
			17.86666667
886.1	77.1	99.9	11.8
886.2	56.8	99.7	11.2
886.3	63.9	99.9	12
			11.66666667
886.4	64.7	100	11.9
886.5	64.1	99.9	14.1
886.6	63.1	99.8	12.7
			12.9
886.7	66.8	99.9	13.9
886.8	68	99.9	11.9
886.9	59.3	99.8	7.03
			10.94333333
887.1	64	99.8	3.7
887.2	66.8	99.9	5.24
887.3	65.3	99.8	5.26
			4.733333333
887.4	60	99.7	5.83
887.55	53.4	99.5	2.62
887.66	66.5	99.9	2.31
			3.586666667
887.7	65.4	99.9	1.97
887.8	49.6	99.5	3.07
887.9	44.8	99.4	3.22
			2.753333333
926.1	3.05	93.5	33.1
926.2	3.6	90.4	32.7

962.3	4.19	89.2	30.8
			32.2
926.4	4.3	94.7	42.4
926.5	0.65	89.9	50.7
926.6	3.65	87.2	45.9
			46.33333333
926.7	5.48	92.4	39.8
926.8	3.44	92.1	43.9
926.9	0.71	45.2	59.6
			47.76666667
927.1	28.6	98.2	30.5
927.2	33.5	99.1	31.4
927.3	36	98.8	33.5
			31.8
927.4	24.6	98.5	31
927.5	21.8	97.9	30.7
927.6	39.7	98.9	29
			30.23333333
927.7	28.2	99.2	26.6
927.8	5.35	95.7	42.1
928.9	33.8	98.9	31.1
			33.26666667
948.1	3.61	94.5	22.7
948.2	3.92	89.2	25.4
			24.05
948.4	4.06	91.2	27.2
948.5	4.62	92.5	30.1
			28.65
948.7	1.51	68.3	33.1
948.8	4.54	91.8	23.8
			28.45
954.1	39.1	99.3	22.2
954.2	39.2	99.2	20.7
954.3	37.5	99	20.9
			21.26666667
954.4	46.2	99	21
954.5	44.7	99.3	19.4
954.6	46	99.3	21.1
			20.5
954.7	0.38	55.7	47.6
954.8	34.8	99.5	4.07
954.9	42.5	99	10.9
			20.85666667

976.1	48.9	99.8	5.12
976.2	54.9	99.9	5.88
976.3	49.9	99.9	6.01
			5.67
976.4	53.9	100	6.46
976.5	44	99.6	7.42
976.6	52.1	99.9	6.61
			6.83
976.7	50.7	99.8	6.22
976.8	49.6	99.8	12.1
976.9	46.5	99.4	12.7
			10.34
977.1	41.5	99	15.6
977.2	47.9	99.4	14.2
977.3	51.3	99.8	13
			14.26666667
977.4	61.1	99.9	12.2
977.5	50.4	100	12
977.6	51	99.5	13.2
			12.46666667
977.7	57.9	99.9	11.2
977.8	54.1	99.8	12.8
977.9	49.5	99.3	10.5
			11.5

Samples	**# Lymphocytes**	**CD3+**	**CD3 Proliferation**
692.1	33.5	98.6	12.6
692.2	36.4	98.7	12.5
692.3	33.3	98.9	11.4
			12.16666667
692.4	13.8	96.7	11.5
692.5	41.9	98.9	11.3
692.6	41.9	98.4	12.1
			11.63333333
692.7	33.2	98.6	11.3
692.8	34.4	98.7	14
692.9	38.6	98.6	12.8
			12.7
693.1	47.4	97.4	15.3
693.2	41.9	97	14.9
693.3	40.4	97.2	15

			15.06666667
693.4	46.3	97	14.8
693.5	48.7	97	15.8
693.6	49.1	97.4	13.7
			14.76666667
693.7	41.4	96.9	15.1
693.8	41.2	97.2	16.4
693.9	49.2	96.5	15.9
			15.8
694.1	48.6	97.8	15.5
694.2	47.1	97.1	15.6
694.3	46.4	98.1	15.1
			15.4
694.4	52.2	98.2	14.9
694.5	48.1	97.2	17.2
694.6	49.4	97.5	16.3
			16.13333333
694.7	46.6	98	12.7
694.8	45.5	97.5	16
694.9	45.5	97.4	15.2
			14.63333333
729.1	5.92	83.9	19.1
729.2	5.18	81.3	22.3
			20.7
729.4	4.59	84	22.7
729.5	0.31	0	0
			11.35
729.7	4.41	82.2	26.7
729.9	5.03	84.7	23.9
			25.3
738.1	24.2	98.4	16.5
738.2	27.6	98.1	19.4
738.3	28.7	98.1	18
			17.96666667
738.4	25.2	98.1	17.9
738.5	25.5	97.9	15.4
738.6	28.6	98.2	18.2
			17.16666667
738.7	30.8	98.3	18.8
738.8	28	98.5	20.2
738.9	31.3	98.2	20.7
			19.9
758.1	56.5	97	18

758.2	59.3	97.3	18
758.3	59.2	97.2	18.2
			18.06666667
758.4	52.7	98.2	17.3
758.5	55.2	98.1	15.6
758.6	59.6	98	18.7
			17.2
762.1	42.2	94.3	27.4
762.2	43.5	91.9	30.3
762.3	43	92.9	29.1
			28.93333333
762.4	53.9	94.8	25.1
762.5	54.6	94	27.3
762.6	55.5	94.1	28.3
			26.9
881.1	55.8	92.2	33.1
881.2	55.4	89.9	37.1
881.3	51.4	88.9	40
			36.73333333
881.4	50.5	90.3	37.7
881.5	53.6	91.5	36.8
881.6	48.4	90.9	37.9
			37.46666667
881.7	45.9	89.9	40.2
881.8	46.1	90.4	38.3
881.9	47.5	91.1	36.7
			38.4
883.1	40.5	95.8	23.4
883.2	43.3	96.2	22.7
883.3	43.9	95.2	24.3
			23.46666667
883.4	42.2	95.7	25
883.5	43.6	96.3	26
883.6	46.7	95.2	27.7
			26.23333333
883.7	45.8	95.8	25.5
883.8	43.5	95.8	24.3
883.9	46.1	94.5	26.1
			25.3
888.1	58.6	94.8	23.5
888.2	57.3	94.7	24.1
888.3	56.2	94.6	24.1
			23.9

888.4	63.6	94.3	25.2
888.5	66	94.1	25.1
888.6	63.1	94.2	25.1
			25.13333333
888.7	21.7	94.8	23.1
888.8	53.9	95.3	22.7
888.9	66.9	94.6	21.2
			22.33333333
931.1	51	94.5	31.5
931.2	42.7	94.6	31.5
			31.5
931.4	49.3	94.3	31.2
931.5	51.7	93.6	34.1
			32.65
931.7	42.9	95	33.1
931.8	45.4	94.7	31.2
			32.15
933.1	39.1	97.7	24.3
933.2	39.6	97.8	23.6
933.3	35.5	97.6	21.9
			23.26666667
933.4	46.6	97.7	21.3
933.5	37.3	97.7	22.7
933.6	42.6	97.9	23.1
			22.36666667
933.7	36.9	97.6	24.8
933.8	42.1	97.9	22.2
933.9	40.4	97.9	22.4
			23.13333333
949.1	2.17	78.9	26.3
949.2	2.32	75.5	26.8
949.3	2.28	74.5	21.7
			24.93333333
949.4	1.63	75.1	25
949.5	2.8	74.6	23.8
			24.4
952.1	31.4	72.6	49
952.2	26.9	72.3	47.4
952.3	33.9	72.3	49.5
			48.63333333
952.4	24.3	69	49.2
952.5	24.2	70.4	48.9
952.6	36.2	70.4	48.2

			48.76666667
952.7	0.45	58.5	39.5
952.8	29	79.4	47.2
952.9	25.2	79	48.7
			45.13333333
953.1	30.7	97	21.3
953.2	35.8	94.8	21.6
953.3	35.7	96.3	23.9
			22.26666667
953.4	3.59	95.4	24.2
953.5	42.6	95.9	25.2
953.6	33.2	96.1	23.2
			24.2
953.7	33.2	97	22.1
953.8	36	96.5	23.5
953.9	36.5	91.8	25.3
			23.63333333
956.1	30.3	92.9	35.6
956.2	5.69	13.8	42.4
956.3	26.1	91.3	37.8
			38.6
956.4	29.6	91	37.9
956.5	30.9	91.9	36.2
956.6	30.7	90.2	37.8
			37.3
956.7	22.8	92.3	38.2
956.8	28.3	91	36.9
956.9	35.5	92.9	33.1
			36.06666667
957.1	2.76	68.9	18.3
957.2	3.16	54.7	23.4
957.3	2.93	73.4	25.5
			22.4
957.4	2.71	79.3	26.1
957.5	2.63	74.4	26.4
			26.25
957.7	0.33	8.79	66.7
957.8	3.41	75	32.1
957.9	1.81	73.2	29.8
			42.86666667
969.1	50.4	94.7	21
969.2	38	93.9	23.4
969.3	45.5	93.9	24.3

			22.9
969.4	47.2	94.4	20.8
969.5	33.3	94.4	21.2
969.6	47	94.2	22.2
			21.4
969.7	39.2	94	21.8
969.8	26.4	92.9	23.7
969.9	36.6	93.6	22.5
			22.66666667
978.1	6.2	85.8	34.6
978.2	3.9	83.7	32
978.3	3.73	82.5	39
			35.2
978.4	3.61	82.3	34.5
978.5	5.21	85.3	32
			33.25
978.7	3.87	82.9	29.8
978.8	5.22	84.4	38
978.9	5.17	84.5	30.1
			32.63333333
980.1	38.1	79.9	45.9
980.2	38.5	80.5	46.2
980.3	33.9	80.1	44.6
			45.56666667
980.4	36	80.1	44.5
980.5	34.7	81.2	44.8
980.6	39.6	80.4	46.4
			45.23333333
980.7	32.4	78.5	47.9
980.8	38.6	80.6	47
980.9	34.6	79.2	45.3
			46.73333333

Samples	**# Lymphocytes**	**CD3+**	**CD3 Proliferation**
700.1	41.4	98.8	22
700.2	46.1	99.4	25.6
700.3	45.5	99.5	21.8
			23.13333333
700.4	45.8	99	22.6
700.5	45.2	98.8	27.8

700.6	51.3	99.1	24
			24.8
700.7	44.4	99.3	26
700.8	42.5	99.2	23.2
700.9	45.2	99.4	21.3
			23.5
730.1	3.27	83.3	24.5
730.2	3.89	77	31.8
			28.15
730.4	2.7	75.3	24.8
730.5	3.95	90.6	19.5
			22.15
730.7	3.37	79.3	27.8
730.8	2.68	64.2	27.4
			27.6
732.1	3.58	82.4	18.3
732.2	2.47	79.2	16.5
			17.4
732.4	**3.73**	**76.8**	**17.6**
732.7	4.03	76.5	17
732.8	3.04	66.2	20.7
			18.85
737.1	3.67	62.5	29.2
737.2	2.15	40.4	42.9
			36.05
737.4	2.9	25.4	40
737.5	3.9	61.2	15.9
			27.95
737.7	1.66	16.9	28.6
737.8	1.79	18	55.6
			42.1
739.1	52.1	99.6	10
739.2	52.4	99.5	11.8
739.3	48	99.5	11.3
			11.03333333
739.4	34.9	97.3	15.8
739.5	54.7	99.4	11.5
739.6	52.5	99.6	11
			12.76666667
739.7	53.9	99.4	11.7
739.8	55.6	99.4	12.1
739.9	53.1	99.6	11.8

			11.86666667
740.1	19.3	99.2	8.77
740.2	24.5	99.1	13.1
740.3	23.5	98.9	14.7
			12.19
740.4	28.7	99.4	16.6
740.5	28.8	99.3	16.2
740.6	26.2	99.1	14.9
			15.9
740.7	24.4	98.8	14.9
740.8	19.8	99	15
740.9	25.2	98.9	17.3
			15.73333333
882.1	50.7	99.8	13.1
882.2	53.1	99.6	11.6
882.3	53	99.7	12.6
			12.43333333
882.4	53.1	99.7	14.5
882.5	50.1	99.7	14.1
882.6	55.3	99.7	14.2
			14.26666667
882.7	45.1	99.6	15.9
882.8	50.3	99.8	12.1
882.9	46.3	98.5	20.5
			16.16666667
884.1	43.9	96.4	23.4
884.2	44.2	99.1	14.7
884.3	47	99.7	17.9
			18.66666667
884.4	47.7	99.8	16.6
884.5	42.7	99.1	17.3
884.6	49.6	99.6	16.9
			16.93333333
884.7	39.8	98.6	16.9
884.8	45.2	99.7	14.9
884.9	36.6	98.4	16.9
			16.23333333
885.1	34.9	98.8	22
885.2	31.5	99.4	20.6
885.3	40.3	98.8	20.1
			20.9
885.4	23.8	95.5	26.1
885.5	32.4	99	21.8

885.6	33.8	99	23.1
			23.66666667
885.7	25.9	97.3	21.7
885.8	29.7	99	22.7
885.9	33.7	98.6	20.8
			21.73333333
971.1	0.84	22.7	0
971.2	1.15	8.7	50
			25
971.4	1.11	15.2	14.3
971.5	0.66	16.7	16.7
			15.5
971.7	1.17	9.26	0
971.8	1.3	11.6	0
			0

Samples	**# Lymphocytes**	**CD3+**	**CD3 Proliferation**
380.1	27.3	95.9	13.8
380.2	27.8	94.9	15.9
380.3	32	95.6	15.6
			15.1
380.4	23.4	93.3	14.3
380.5	34.9	95.8	16.6
380.6	34.7	95.5	15.2
			15.36666667
380.7	25.6	95.3	17.5
380.8	33.6	96.5	14.7
380.9	28.7	96	15.8
			16
387.1	5.35	91.4	19.8
387.2	6.64	95.2	15.2
387.3	3.5	95.6	13.9
			16.3
387.4	3.09	23.5	17
387.5	2.25	74.4	2.99
387.6	2.46	81.9	19.5
			13.16333333
387.7	2.24	94.8	19.1
387.8	2.64	93.8	12.1
387.9	3.69	90.9	16.7
			15.96666667
411.1	46.1	98.7	12.1

411.2	39.4	97.9	13.4
411.3	41.5	98.5	13.8
			13.1
411.4	39.1	96.7	17.3
411.5	42	98	15.4
411.6	28.7	89	18.3
			17
411.7	39.3	97.2	16
411.8	36.1	96.6	12.7
411.9	32.3	94.7	20
			16.23333333
417.1	13.5	91.9	25.2
417.2	13.8	90.8	23.4
417.3	15.7	93.8	22.9
			23.83333333
417.4	22.2	92.3	25.1
417.5	18.7	88.7	28.4
417.6	21.4	87.1	32.3
			28.6
417.7	27.1	88.9	28
417.8	18.3	89.5	24.9
417.9	27	91.7	23.1
			25.33333333
641.1	45.8	94.5	20.9
641.2	36.8	94.2	19.7
641.3	43	94.5	19.2
			19.93333333
641.4	43.7	94.8	18.9
641.5	44.3	94.9	17.3
641.6	43.2	95.3	18.4
			18.2
641.7	40.3	96.2	18.3
641.8	42.6	95.5	18.3
641.9	43.3	94.5	19.6
			18.73333333
642.1	50.1	93.7	21.8
642.2	44.5	93.4	22.4
642.3	44.5	95.4	19.6
			21.26666667
642.4	42.3	94.8	21.8
642.5	45	93.7	21.9
642.6	45.8	93.5	23.6
			22.43333333

642.7	43.3	92	23.3
642.8	46	91.7	22.8
642.9	43.5	92	22.2
			22.76666667
643.1	45.2	82	30.8
643.2	51.3	84.1	30.4
643.3	50.3	82.3	28.5
			29.9
643.4	45.2	81	35
643.5	43.2	80.1	33.5
643.6	46.5	81.3	32
			33.5
643.7	49.3	84.8	31.1
643.8	42.4	83.7	31.1
643.9	45.9	84.4	31
			31.06666667
644.1	31	91.4	29
644.2	32.7	90	28.6
644.3	37.1	91.7	28.3
			28.63333333
644.4	44.3	91.5	24.3
644.5	32.8	92.2	24.6
644.6	25.1	91.4	24.8
			24.56666667
644.7	30.2	91.1	29.2
644.8	28.9	88.8	29.4
644.9	25.1	92.5	23.9
			27.5
780.1	7.34	89.7	14.8
780.2	9.24	90.5	21
780.3	8.59	92.8	26.5
			20.76666667
780.4	3.77	80.6	5.17
780.5	4.55	73.8	17.7
			11.435
932.1	25.7	96.7	14.7
932.2	27.9	96.2	17.6
932.3	26	96.3	16.6
			16.3
932.4	28.3	96.7	17.1
932.5	8.69	72.6	18.6
932.6	20.3	95.9	15.1
			16.93333333

932.7	19	96.4	16.4
932.8	20.4	95	16.4
932.9	23.7	97	15
			15.93333333

Samples	# Lymphocytes	CD3+	CD3 Proliferation
384.1	4.16	46.8	36.1
384.2	1.66	31.6	50
384.3	0.68	9.8	40
			42.03333333
384.4	2.16	53.7	45.5
384.5	1.94	41.9	44.4
384.6	3.1	66.7	48.4
			46.1
384.7	2.23	46.3	36.8
384.8	2.16	39.4	30.8
384.9	2.1	51.5	35.3
			34.3
394.1	2.37	40.5	33.3
394.2	2.38	48.2	11.1
394.3	3.35	51.6	34.4
			26.26666667
394.4	1.88	40.5	35.3
394.5	3.83	35.1	25
394.6	2.01	62.1	25
			28.43333333
394.7	4.31	72.5	20.7
394.8	5.27	60.8	27.1
394.9	1.64	37.1	15.4
			21.06666667
395.1	37.1	96.3	22.1
395.2	32.7	97.5	22.2
395.3	32.5	97.7	21.7
			22
395.4	33.9	97.4	19.4
395.5	33.7	96.4	20.7
395.6	31.2	96.5	22.5
			20.86666667
395.7	27.3	97.1	23.7
395.8	30.1	96.8	22.1

395.9	32.4	96.8	23.1
			22.96666667
396.1	5.89	74.2	25.5
396.2	6.35	76.4	21
396.3	7.22	76.7	25.9
			24.13333333
396.4	6.67	67.9	17.9
396.5	6.96	80.8	23.7
396.6	3.54	70.3	29.5
			23.7
396.7	5.19	58.2	34.8
396.8	3.53	47.7	32.3
396.9	2.82	44.8	23.1
			30.06666667
397.1	27.8	96.2	17
397.2	25	95.5	22.1
397.3	17.6	94.3	18.6
			19.23333333
397.4	18.6	92.8	22.1
397.5	20.6	95.8	21
397.6	14.6	94.6	20.1
			21.06666667
397.7	17.1	89.6	23.8
397.8	18.1	95.8	19.2
397.9	17.6	94.7	21.7
			21.56666667
402.1	14.6	76.2	48.4
402.2	8.71	84.7	49
402.3	11.8	82.2	43.6
			47
402.4	12.9	63.4	49.1
402.5	8.35	51.9	45.6
402.6	8.06	92.3	37.9
			44.2
402.7	5.91	60.4	42.4
402.8	7.7	68.9	41.7
402.9	5.96	80.7	49
			44.36666667
407.1	14.6	88.7	21.5
407.2	18.4	92.2	26.6
407.3	11.5	89.5	29.3
			25.8
407.4	15.9	94	18.5

407.5	10.5	91.5	18.7
407.6	16.4	91.3	24.4
			20.53333333
407.7	16	89.1	18
407.8	18.2	92.8	23.4
407.9	27	93.3	24
			21.8
408.1	22.2	95.2	13.7
408.2	28.8	96.6	17.1
408.3	31.9	95.3	17.5
			16.1
408.4	27	94.9	15.6
408.5	19	95.3	12.1
408.6	26	97.1	11.3
			13
408.7	33.3	97	16.7
408.8	30.2	96.8	19.4
408.9	29.9	96.7	19.5
			18.53333333
412.1	26.3	96.1	15
412.2	29.6	97.7	18.3
412.3	27	97.9	16.3
			16.53333333
412.4	24.8	98.1	18.2
412.5	27	97.3	19.7
412.6	24.7	94.6	16.7
			18.2
412.7	21.2	97.4	20.7
412.8	26.8	88.9	27
412.9	20.4	95.3	16.7
			21.46666667
418.1	7.03	86.2	19.6
418.2	8.98	90.9	16.1
418.3	10.8	81	16.7
			17.46666667
418.4	8.22	88.3	19
418.5	9.23	84.8	18.9
418.6	7.09	86	18.3
			18.73333333
418.7	7.82	83.2	16.9
418.8	10.4	86.5	18.1
418.9	14.6	92.6	23.8
			19.6

Samples	# Lymphocytes	CD3+	CD3 Proliferation
381.1	32.2	95.3	32.5
381.2	32.9	95.8	29.1
381.3	34.5	96.8	28.9
			30.16666667
381.4	34.1	96.4	27.7
381.5	30	96.6	27.1
381.6	26.8	94.2	32.3
			29.03333333
381.7	25.2	96.7	24.6
381.8	30	94	26.9
381.9	31.4	94.9	30.1
			27.2
382.1	6.2	81.8	49.6
382.2	8.64	88	46.7
382.33	47.7	98.9	15.9
			37.4
382.4	9.97	90.6	39
382.5	9.65	85.8	53.1
382.6	8.89	89.4	38.2
			43.43333333
382.7	9.04	89.1	40
382.8	7.99	85	34
382.9	6.26	86.8	35.7
			36.56666667
383.1	45.6	99.1	17.9
383.2	55	99.2	17.4
			17.65
383.4	57.5	99.2	14.5
383.5	48.6	99	21.6
383.6	58	99.4	21.6
			19.23333333
383.7	40.6	95.8	19.8
383.8	51.7	99.2	15.4
383.9	50.2	98.8	22.9
			19.36666667
385.1	28.7	97.5	24.4
385.2	24.9	97	26.5
385.3	24.8	66.5	62.2
			37.7
385.4	22.5	92.4	27.6
385.5	19.7	92.8	25.1

385.6	**29.7**	**96.7**	**24.2**
			25.63333333
385.7	**19.7**	**89.9**	**19.4**
385.8	**13.1**	**27.2**	**25.9**
385.9	**15**	**67**	**17.3**
			20.86666667
386.1	**38.5**	**94.9**	**37.7**
386.2	**36.1**	**95.4**	**38.6**
386.3	**36**	**94.2**	**39.3**
			38.53333333
386.4	**36.9**	**86**	**37.5**
386.5	**39.8**	**95.3**	**35.9**
386.6	**22.5**	**78.2**	**35.3**
			36.23333333
386.7	**30.9**	**94.5**	**32.7**
386.8	**25.6**	**89.6**	**38.3**
386.9	**25.6**	**79.6**	**35.1**
			35.36666667
391.1	**5.68**	**34.4**	**21**
391.2	**3.63**	**35.8**	**16**
391.3	**3.54**	**74.7**	**18.3**
			18.43333333
391.4	**3.43**	**66.7**	**34.2**
391.5	**3.45**	**49.1**	**30.8**
391.6	**1.43**	**76.9**	**20**
			28.33333333
391.7	**4.88**	**52.1**	**20**
391.8	**9.22**	**76.8**	**37.1**
391.9	**7.1**	**62.9**	**30.7**
			29.26666667
392.1	**3.06**	**60.7**	**16.2**
392.2	**2.8**	**50**	**12**
392.3	**4.75**	**24.3**	**16.2**
			14.8
392.4	**2.38**	**39.4**	**38.5**
392.5	**2.75**	**4.63**	**23.5**
392.6	**1.87**	**41.3**	**23.1**
			28.36666667
392.7	**5.56**	**50**	**23.5**
392.8	**1.91**	**59.5**	**31.8**
392.9	**1.83**	**49.1**	**21.4**
			25.56666667
403.1	**16.5**	**88.2**	**32.1**

403.2	**22.7**	**91.4**	**31.6**
403.3	**11.7**	**51.2**	**64.1**
			42.6
403.4	**18.5**	**88.5**	**29.4**
403.5	**11.2**	**85.9**	**26.4**
403.6	**9.85**	**85.9**	**29**
			28.26666667
403.7	**24.6**	**91.4**	**28.3**
403.8	**21.7**	**92.7**	**26.9**
403.9	**14.4**	**87**	**32.3**
			29.16666667
405.1	**20.3**	**95.5**	**20.3**
405.2	**11.4**	**97.2**	**17.4**
405.3	**6.02**	**3.46**	**75**
			37.56666667
405.4	**23.4**	**85**	**21.7**
405.5	**19.4**	**89.1**	**22.3**
405.6	**14.6**	**74.6**	**10**
			18
405.7	**15.5**	**84.8**	**19.5**
405.8	**14.3**	**88.4**	**23.6**
405.9	**13.1**	**88.3**	**23.8**
			22.3
406.1	**10.3**	**89.6**	**15.2**
406.2	**1.78**	**66.7**	**17.5**
406.3	**10.4**	**33.1**	**42.2**
			24.96666667
406.4	**3.23**	**57.3**	**21.3**
406.5	**2.85**	**47.8**	**21.9**
406.6	**2.27**	**25**	**28.6**
			23.93333333
406.7	**2.96**	**66.7**	**15.9**
406.8	**5.14**	**63.7**	**16.9**
406.9	**6.54**	**80.2**	**20.8**
			17.86666667

Samples	**# Lymphocytes**	**CD3+**	**CD3 Proliferation**
390.1	3.14	28.2	27.3
390.2	5.15	4.12	0
			13.65

390.4	5.86	10.2	22.2
			22.2
390.7	2.56	46.2	11
390.8	1.94	29.6	21.9
			16.45
393.1	8.05	59.3	16.9
393.2	9.03	59.5	21.2
393.3	7.55	62	16
			18.03333333
393.4	7.22	68.3	12.8
393.5	10.5	54.5	18.4
393.6	9.06	56.1	11.8
			14.33333333
393.7	12.5	49.6	18.8
393.8	10.9	54.4	32.6
393.9	11.3	55.1	21.8
			24.4
413.1	8.8	44	18.4
413.2	9.76	68.9	13.4
413.3	7.81	57.1	12.8
			14.86666667
413.4	3.99	37.8	23.2
413.5	11.1	63.6	25.7
413.6	11.7	38.5	27.7
			25.53333333
413.7	12.3	67.9	19.4
413.8	15.1	70.3	15.8
413.9	11.1	62.7	21.5
			18.9
419.1	21.3	81.7	14
419.2	23.6	86.2	13.5
419.3	25	86.1	9.92
			12.47333333
419.4	33.7	88	14.4
419.5	17.9	69.2	11.3
419.6	32.3	87.4	16.2
			13.96666667
419.7	18.3	55	15.2
419.8	27	72.5	18.8
419.9	21.8	76	11.1
			15.03333333
926.1	12.5	1.02	50
926.2	6.66	5.63	12.5

926.3	4.38	3.42	50
			37.5
926.4	5.57	2.5	0
926.5	4.95	17.6	17.4
926.6	6.42	8.78	38.5
			18.63333333
926.7	5.12	9.6	50
926.8	5.25	19.7	22.2
926.9	7.45	4.24	28.6
			33.6

Samples	**# Lymphocytes**	**CD3+**	**CD3 Proliferation**
345.1	27.7	92.7	4.46
345.2	11.7	84.6	4.76
345.3	30	91.9	3.7
			4.306666667
345.4	26.2	92.1	4.92
345.5	21.1	90.7	5.53
345.6	28.3	93.1	3.91
			4.786666667
345.7	26.4	91.6	4.41
345.8	29.4	91.7	4.49
345.9	29.7	90.1	6.16
			5.02
347.1	41.4	96.8	1.76
347.2	37.9	96.1	2.57
347.3	32.7	95	3.24
			2.523333333
347.4	37.9	96.6	2.09
347.5	43.6	97	1.89
347.6	37.7	97	1.28
			1.753333333
347.7	31.7	84.8	8.07
347.8	45.4	96.3	2.17
347.9	36.9	95.5	2.24
			4.16
363.1	40.6	94.3	1.42
363.2	47.1	96.6	0.48
363.3	46.2	96.7	0.75
			0.883333333
363.4	47.6	96.5	0.34

363.5	39.2	96.8	0.7
363.6	45.5	96.4	0.28
			0.44
363.7	46.5	96.7	0.3
363.8	49.8	96.6	0.27
363.9	48.1	96.8	0.22
			0.263333333
364.1	32.6	95.6	0.71
364.2	25.9	95.3	0.4
364.3	32	95.2	0.71
			0.606666667
364.4	26.4	93	0.087
364.5	14.5	92.1	0.35
364.6	25.6	94.2	0.063
			0.166666667
364.7	20.5	93.8	0.2
364.8	26	93.2	0.12
364.9	25.7	93.8	0.032
			0.117333333
365.1	2.63	89.3	0.34
365.2	3.21	91	0.24
365.3	3.22	89.7	0.27
			0.283333333
365.4	2.82	91.4	0.3
365.5	3.23	91.3	0.27
365.6	1.91	92.2	0.88
			0.483333333
365.7	3.82	94	0
365.8	2.97	90.6	0.6
365.9	2.2	91.3	0
			0.2
366.1	4.04	86.5	0
366.2	6.23	92.5	0.4
366.3	0.14	60.7	3.36
			1.253333333
366.4	5.21	92.5	1.3
366.5	5.63	94	0.38
366.6	8.24	93.1	0.75
			0.81
366.7	7.92	91.4	0.67
366.8	9.56	90.4	0.63
366.9	6.3	90.9	0.86
			0.72

374.1	30.5	97	0.98
374.2	22.6	97.6	1.07
374.3	35.8	97.5	1.18
			1.076666667
374.4	37.5	98.2	0.51
374.5	31.9	98.2	0.47
374.6	30.7	97.8	0.81
			0.596666667
374.7	28.1	95.6	3.29
374.8	28.7	94.1	3.98
374.9	33.1	96.5	2.99
			3.42
375.1	37.2	96.3	2.36
375.2	33.6	95.3	2.74
375.3	34	94.1	4.19
			3.096666667
375.4	36	96.8	1.18
375.5	33.1	95.8	2.77
375.6	36.6	95.8	2.83
			2.26
375.7	37.1	96.9	1.34
375.8	35.5	96.2	2.12
375.9	38.1	95.9	2.05
			1.836666667

Samples	**# Lymphocytes**	**CD3+**	**CD3 Proliferation**
331.1	32.4	89.2	25.7
331.2	34.7	90.8	24.1
			24.9
331.4	37.4	89.6	23.9
331.5	31.3	88.9	23
			23.45
331.7	30.8	89.1	23.7
331.8	32.7	90.7	24.4
			24.05
336.1	32.2	92.6	22.4
336.2	38.9	89.6	26.8
336.3	31.8	90.8	26.3
			25.16666667
336.4	44.7	94.3	21.4
336.5	39.1	92.6	24.4
336.6	40.4	92.2	25.6

			23.8
336.7	38.8	91.7	25.5
336.8	26.7	89.5	27.5
336.9	38	85.5	32.9
			28.63333333
337.1	1.61	4.44	43.3
337.2	28.1	92.7	18.3
337.3	29.9	84	27
			29.53333333
337.4	32.2	89	23.8
337.5	32.7	87	24
337.6	31.7	86.5	25.1
			24.3
337.7	24.1	62.7	24
337.8	29	89.7	19.6
337.9	23.2	89.2	19.2
			20.93333333
340.1	18.5	57.4	26.8
340.2	17.6	60.8	24.1
340.3	16.4	60.9	24.3
			25.06666667
340.4	17	60.2	24.3
340.5	17.7	60.9	26.5
340.6	12.7	51.3	25.6
			25.46666667
340.7	15.2	54	27.5
340.8	18.6	57.8	25.6
340.9	17.3	52.7	27.8
			26.96666667
344.1	22.5	82.2	20.7
344.2	22.1	81	22.4
344.3	18.6	81.5	22.3
			21.8
344.4	23.8	83.3	23.6
344.5	16.8	74.4	26.2
344.6	22.3	81.7	21.2
			23.66666667
344.7	19.6	82	22.4
344.8	20	77.8	28.3
344.9	20.9	81.5	18.9
			23.2
346.1	5.86	59	25.3
346.2	32.5	84	19

346.3	29.9	83.3	22.8
			22.36666667
346.4	31.9	84.7	21.1
346.5	33	86.1	22.2
346.6	33.7	83.7	23.6
			22.3
346.7	34.7	84.1	24.1
346.8	34.6	83.8	27.1
346.9	30	84.6	24.1
			25.1
367.1	42.2	89.9	22.3
367.2	40.3	87.6	23.5
367.3	42	88.8	24.6
			23.46666667
367.4	36.2	87.3	25.3
367.5	45.7	88	25.1
367.6	37.8	87.6	22.5
			24.3
367.7	42.4	87	24.8
367.8	44.4	88.9	24.1
367.9	36.6	86.7	26.2
			25.03333333
414.1	31.8	80	34.5
414.2	25	81.1	35.4
414.3	24.7	78.9	35.1
			35
414.4	20.8	91.5	13.5
414.5	31.2	82.8	34
414.6	28.7	78.6	39.3
			28.93333333
414.7	25.1	78.1	37.2
414.8	28.1	80.3	35.9
414.9	26.2	80.5	34.4
			35.83333333

Samples	**# Lymphocytes**	**CD3+**	**CD3 Proliferation**
330.1	12.4	71.3	17.6
330.2	13	67.4	25.7
330.3	13.7	75.5	13.7
			19

330.4	9.91	68.8	24.3
330.5	7.04	51.4	20.8
330.6	12.3	76.3	11.6
			18.9
330.7	11.6	89.5	6.78
330.8	8.15	86.2	5.79
330.9	11.3	86.7	5.4
			5.99
332.1	32.2	97.9	6.09
332.2	31.6	97.6	5.86
332.3	35.2	97.3	4.33
			5.426666667
332.4	38.7	97.4	6.91
332.5	31	97.8	5.04
332.6	36.1	97.7	5.47
			5.806666667
332.7	29.7	95.6	6.74
332.8	27.4	96.9	7.17
332.9	28.7	99.2	0.34
			4.75
333.1	22.8	92.6	7.39
333.2	14.9	85.1	18.1
333.3	16.7	92.5	5.38
			10.29
333.4	15.8	91.9	2.43
333.5	19.2	90.9	8.31
333.6	23.6	93.3	6.97
			5.903333333
333.7	16.9	92.1	8.14
333.8	15	90.8	9.96
333.9	21.1	91.6	7.66
			8.586666667
334.1	29.4	95.2	7.14
334.2	28.2	90.2	14.4
334.3	29	90.6	13.3
			11.61333333
334.4	30.2	88.4	13.5
334.5	32.9	91	14.1
334.6	34.4	86.9	16.6
			14.73333333
334.7	33.9	88.4	14.2
334.8	30.4	75.7	29.7
334.9	27.2	79.6	27.6

			23.83333333
335.1	24	46.3	28.1
335.2	22.6	53.5	23.7
335.3	21.3	45.4	23.7
			25.16666667
335.4	27.7	54.4	29.8
335.5	24.3	52	31.7
335.6	29.8	59.2	37.6
			33.03333333
335.7	23.8	52.8	22.2
335.8	26.6	51.9	24.9
335.9	25.6	45.2	29.6
			25.56666667
338.1	26.8	75.3	17.5
338.2	36.5	70.1	27.2
338.3	33.7	72.9	33.7
			26.13333333
338.4	38.7	67.7	32.9
338.5	20	79.6	5.71
338.6	35.3	89.6	12.4
			17.00333333
338.7	32.1	86.9	13.5
338.8	30	91.3	7.21
338.9	31.5	89.7	10.6
			10.43666667
339.1	23.7	72.4	20.9
339.2	20.1	73.9	17.7
339.3	20.7	67.6	18.4
			19
339.4	23.8	58.5	19.7
339.5	26.1	63.6	17.2
339.6	24.7	58.5	21.4
			19.43333333
339.7	25.6	48.9	25.7
339.8	22.9	56.3	21
339.9	25.3	58.2	20.8
			22.5
343.1	25.2	76.2	22.4
343.2	26.8	75.6	25.4
343.3	24.9	75.8	24.3
			24.03333333
343.4	27.4	78.4	28.7
343.5	31.1	75.8	28.3

343.6	31.7	80.1	23.9
			26.96666667
343.7	26.1	73.3	21.3
343.8	30.8	73.5	24.5
343.9	27.6	80.7	29.9
			25.23333333
350.1	17	42.1	29.5
350.2	18.7	44.9	26.5
350.3	15.8	55.1	23.3
			26.43333333
350.4	21	52.4	26.3
350.5	19.7	50.9	24.6
350.6	23.1	49.6	23.2
			24.7
350.7	19.9	50.2	22.7
350.8	20.7	62.1	15
350.9	20.3	51.5	20.6
			19.43333333
357.1	36.9	45.5	27.9
357.2	25.4	81	11.9
357.3	41	40.9	32.3
			24.03333333
357.4	37.5	57.9	31.8
357.5	33.9	54	31.1
357.6	41.7	49.6	31.4
			31.43333333
357.7	46	47.6	34.4
357.8	40.7	46.5	36.2
357.9	41.7	54.6	30.6
			33.73333333
358.1	33.8	89.4	14.8
358.2	4.66	75.7	14
358.3	34.9	78.7	17.8
			15.53333333
358.4	36.9	91.9	12.6
358.5	44.2	93	11.2
358.6	41.6	95.3	9.22
			11.00666667
358.7	45	94.7	10.2
358.8	36.4	98.6	1.7
358.9	35.2	90.9	3.56
			5.153333333
359.1	48.8	82.1	22.5

359.2	48.3	79.4	19.4
359.3	43.5	82.4	19.7
			20.53333333
359.4	48.5	80	18.8
359.5	51.3	86	20.2
359.6	48.7	84.3	21.6
			20.2
359.7	48.3	80.8	20.5
359.8	47.4	80.4	22.3
359.9	41.8	82.6	18.9
			20.56666667
361.1	45.2	90.7	5.8
361.2	39.2	88.6	6.35
361.3	37.2	89.2	5.62
			5.923333333
361.4	40.6	90.7	4.56
361.5	40.5	88.9	4.95
361.6	48.2	91.6	13
			7.503333333
361.7	46.8	91.8	13
361.8	37.5	90.1	15.7
361.9	39.3	89.3	15.8
			14.83333333
368.1	29.7	76.3	27.7
368.2	27.9	72.6	24.5
368.3	29.1	76.5	25.7
			25.96666667
368.4	32.2	77.9	19.9
368.5	31	81.4	15.7
368.6	26.6	74.4	22.5
			19.36666667
368.7	25.2	69.9	21.6
368.8	27.3	75.1	27.7
368.9	28.6	73.8	20.7
			23.33333333
369.1	40.4	90.7	13
369.2	36.9	88.7	13.8
369.3	34.8	90.3	14.5
			13.76666667
369.4	41.9	80.4	20.9
369.5	40.1	87.9	15.2
369.6	41	84.9	16.1
			17.4

369.7	40.4	81	19.9
369.8	37.4	79.3	20.4
369.9	37.1	84.3	13.9
			18.06666667
370.1	28.9	86	4.48
370.2	25.6	83.8	5.39
370.3	25.9	82.2	5.84
			5.236666667
370.4	30.9	86.5	4.34
370.5	30.4	73.9	14
370.6	30.8	84.6	5.44
			7.926666667
370.7	27.7	82.1	5.12
370.8	34.1	83.1	5.11
370.9	31.5	86	5.05
			5.093333333
420.1	16.6	50.7	26.6
420.2	31.7	71.7	31.1
420.3	27.5	60.2	27.7
			28.46666667
420.4	30.5	79.1	19.7
420.5	27	87.5	16.9
420.6	23.6	88.4	19.6
			18.73333333
420.7	31.6	35.1	29.4
420.8	30.2	58.9	23.4
420.9	28.1	61.2	21.7
			24.83333333
421.1	33	68.8	35.1
421.2	31.5	53.4	26.2
421.3	28.1	51.8	24.9
			28.73333333
421.4	24.4	49.6	29.9
421.5	36.1	63.8	36.9
421.6	39.2	39.5	35.4
			34.06666667
421.7	34.3	59.2	26.8
421.8	30.1	63.2	23.6
			25.2

Samples	**Freq. of CD4+**	**CD4 Proliferation**
292.1	9.68	4.84

292.2	14.3	14.3
292.3	55.6	27.8
	26.52666667	**15.64666667**
292.4	35.9	12.8
292.5	34	3.39
	34.95	**8.095**
292.7	4.75	0.68
292.8	7.69	3.17
292.9	66.7	33.3
	26.38	**12.38333333**
293.1	**90.3**	**45.2**
293.4	**86.3**	**34.8**
293.7	**80**	**30**
296.1	**97.1**	**64.7**
296.4	**69.5**	**28.5**
296.7	**77.8**	**44.4**
721.1	82.9	63.6
721.2	86.8	50.1
721.3	72.9	35.2
	80.86666667	**49.63333333**
721.4	72.5	23.6
721.5	69.2	22.6
721.6	68.2	23.6
	69.96666667	**23.26666667**
721.7	64.6	40.2
721.8	81.1	56.8
721.9	77.3	54.5
	74.33333333	**50.5**
722.1	18.2	12.8
722.2	27.3	13.6
722.3	11.5	11.5
	19	**12.63333333**
722.4	56.1	26.3
722.5	45.3	18.8
722.6	71.4	14.3
	57.6	**19.8**
722.7	50	33.3

722.8	94.1	58.8
722.9	75	37.5
	73.03333333	**43.2**
756.1	83.3	70.5
756.2	88.8	70.8
	86.05	**70.65**
756.4	**93.3**	**73.3**
756.7	**93.2**	**78.8**
765.1	81	25.9
765.2	15.7	6.27
765.3	37.6	20.4
	44.76666667	**17.52333333**
765.4	40.7	11.4
765.5	42.5	11
	41.6	**11.2**
765.7	83.3	45.2
765.8	33.3	15.9
765.9	50.5	25.2
	55.7	**28.76666667**
775.1	**4.69**	**0.36**
775.7	**20**	**8**

Samples	**Freq. of CD4+**	**CD4 Proliferation**
297.1	**6.67**	**n/a**
297.4	**17.4**	**n/a**
297.7	**23.1**	**n/a**
298.1	**0**	**n/a**
298.4	**16.7**	**n/a**
298.7	**12.5**	**n/a**
723.1	**0**	**n/a**
723.4	**23.4**	**n/a**

723.7	**3.67**	**n/a**
758.1	**0**	**n/a**
758.7	**0**	**n/a**
761.1	0	n/a
761.2	0	n/a
	0	
761.4	**26.6**	**n/a**
761.7	0	n/a
761.8	0	n/a
	0	
770.1	50	n/a
770.2	40	n/a
770.3	0	n/a
	30	
770.4	21.8	n/a
770.5	20.8	n/a
770.6	20.4	n/a
	21	
770.7	3.08	n/a
770.8	40	n/a
770.9	0	n/a
	14.36	
772.1	**20**	**n/a**
772.4	**15.7**	**n/a**
772.7	16.3	n/a
772.8	0	n/a
772.9	0	n/a
	5.433333333	
781.2	16.1	n/a
782.1	16.3	n/a
782.3	16.4	n/a
	16.26666667	
782.4	15.9	n/a
782.5	16	n/a
782.6	9.23	n/a
	13.71	
782.7	16.9	n/a

782.8	16.2	n/a
782.9	14.3	n/a
	15.8	

Samples	**Freq. of CD4+**	**CD4 Proliferation**
751.1	14.3	33.3
751.2	0	0
751.3	0	0
	4.766666667	
751.4	15.6	17.9
751.5	11.2	18
	13.4	
752.1	5.56	9.09
752.2	2.7	5.88
	4.13	
752.4	40	40
752.5	8.14	15.9
	24.07	
753.1	9.09	13.3
753.2	15.4	17.4
753.3	18.8	30
	14.43	
753.4	3.23	3.85
753.5	9.52	12.5
753.6	4.55	4.76
	5.766666667	
754.1	3.41	7.14
754.2	5.06	9.52
754.3	5.63	12.1
	4.7	
754.4	5.15	8.06
754.5	6.82	11.8
	5.985	
756.2	8.01	12.4
756.3	8.06	12.9
	8.035	
756.4	6.58	8.52
756.5	9.03	11.8
756.6	7.67	10.1
	7.76	
757.1	4.4	12
757.2	6.34	14.3

757.3	7.98	17.8
	6.24	
757.4	8.16	14.8
757.5	10	16.4
757.6	10.2	16.6
	9.453333333	
760.1	5	18.8
760.2	4.89	17.2
760.3	5.48	17.1
	5.123333333	
760.4	9.24	15.9
760.5	8.96	17.4
760.6	8.65	17
	8.95	
761.1	6.91	20.6
761.2	6.32	20.2
761.3	6.92	19.9
	6.716666667	
761.4	7.26	16.8
761.5	7.43	16.1
761.6	7.64	17.7
	7.443333333	
764.1	0.84	1.43
764.2	1.06	1.86
764.3	0.73	1.28
	0.876666667	
764.4	0.56	0.81
764.5	0.61	0.87
764.6	0.9	1.31
	0.69	
951.1	2.55	20
951.2	2.52	20.3
	2.535	
951.4	5.56	27.6
951.5	5.68	26.3
	5.62	
959.1	1.49	5.96
959.2	0.93	3.55
959.3	0.99	4.2
	1.136666667	
959.4	1.91	5.09
959.5	1.42	4.04
959.6	1.97	4.22

	1.766666667	
972.1	15.3	25.1
972.2	16	26.8
972.3	13.4	22.6
	14.9	
972.4	18.3	25.4
972.5	16.6	23
	17.45	
981.1	3.48	13
981.2	3.12	11.8
981.3	3.7	13.4
	3.433333333	
981.5	5.54	10.7
981.6	5.72	11.1
	5.63	
982.1	6.23	14
982.2	7.26	16.5
982.3	6.6	14
	6.696666667	
982.4	4	7.33
982.5	4.97	9.05
982.6	8.51	16.8
	5.826666667	
985.1	7.73	23.1
985.2	8.77	25.8
985.3	7.87	24.2
	8.123333333	
985.4	13.9	20.3
985.5	14.5	22.4
985.6	11.5	20
	13.3	

Samples	**Freq. of CD4+**	**CD4 Proliferation**
726.1	0	0
726.2	25.6	12.8
762.3	31	31
	18.86666667	
726.4	18.5	9.23
726.5	21.1	13.2
	19.8	
726.7	22.5	17.5

726.8	6.67	6.67
	14.585	
728.1	16.9	3.08
728.2	17.9	3.32
728.3	16.9	2.82
	17.23333333	
728.4	18.6	3.43
728.5	19.2	2.9
728.6	18.6	2.95
	18.8	
728.7	17	3.35
728.8	17.7	3.27
728.9	19.4	3.97
	18.03333333	
886.1	18.3	2.69
886.2	19.6	2.57
886.3	18.6	2.31
	18.83333333	
886.4	19.1	2.59
886.5	19.4	2.78
886.6	20.4	3.1
	19.63333333	
886.7	19.7	3.17
886.8	19.3	2.67
886.9	20.2	1.45
	19.73333333	
887.1	19.2	0.77
887.2	19.4	1.28
887.3	18.8	1.38
	19.13333333	
887.4	18.8	1.13
887.55	21.2	0.39
887.66	20.6	0.62
	20.2	
887.7	19	0.46
887.8	19.4	0.67
887.9	18.9	0.57
	19.1	
926.1	16.9	5.81
926.2	13.8	2.3
962.3	8.59	2.02
	13.09666667	
926.4	17.2	6.06

926.5	32.4	23.9
926.6	13.8	5.5
	21.13333333	
926.7	14.3	3.8
926.8	11	4.27
926.9	44.7	38.3
	23.33333333	
927.1	18.6	5.38
927.2	16.8	5.23
927.3	16.9	5.3
	17.43333333	
927.4	16.4	4.71
927.5	17.6	4.88
927.6	17.3	5.34
	17.1	
927.7	15.8	4.34
927.8	19.7	8.02
928.9	14.8	4.33
	16.76666667	
948.1	16.6	6.27
948.2	10.8	5.88
	13.7	
948.4	9.38	4.69
948.5	12.7	8.29
	11.04	
948.7	22.8	15.7
948.8	9.7	4.16
	16.25	
954.1	16.4	4.32
954.2	16.7	3.75
954.3	15.9	3.49
	16.33333333	
954.4	16	3.38
954.5	17.5	3.42
954.6	17	3.87
	16.83333333	
954.7	52.4	34.6
954.8	17.2	0.95
954.9	16.2	2.25
	28.6	
976.1	17.6	0.91
976.2	17.8	0.94
976.3	17.2	0.98

	17.53333333	
976.4	17.7	1.22
976.5	17.8	1.05
976.6	17.6	1.22
	17.7	
976.7	17	1.15
976.8	17.4	2.85
976.9	16.7	2.47
	17.03333333	
977.1	22.4	4.11
977.2	18.4	3.54
977.3	17.6	3.01
	19.46666667	
977.4	17.1	2.54
977.5	18.4	2.74
977.6	18.8	2.85
	18.1	
977.7	17.3	2.47
977.8	18.2	3.15
977.9	18	1.97
	17.83333333	

Samples	**Freq. of CD4+**	**CD4 Proliferation**
692.1	4.99	16.7
692.2	5.25	17.2
692.3	4.49	14.7
	4.91	
692.4	5.52	16.9
692.5	5.21	15.7
692.6	4.81	15.3
	5.18	
692.7	4.15	14.5
692.8	5.53	17.4
692.9	5.49	18
	5.056666667	
693.1	4.38	17.7
693.2	4.83	20
693.3	4.84	20
	4.683333333	
693.4	4.34	17.8
693.5	4.87	19.1

693.6	3.95	16.1
	4.386666667	
693.7	4.56	19.8
693.8	4.88	19.8
693.9	5.07	19.5
	4.836666667	
694.1	3.87	18.7
694.2	3.72	17.5
694.3	3.84	18.5
	3.81	
694.4	4.07	18.3
694.5	4.26	19.1
694.6	4.13	19
	4.153333333	
694.7	3.73	17.5
694.8	3.99	21
694.9	4.28	20.1
	4	
729.1	5.64	23.6
729.2	6.45	22.8
	6.045	
729.4	8.14	31.9
729.5	0	0
	4.07	
729.7	9.11	31
729.9	6.42	29.5
	7.765	
738.1	5.74	18.9
738.2	7.32	21.6
738.3	6.19	19.4
	6.416666667	
738.4	6.45	21.6
738.5	5.93	20.2
738.6	7.38	24.7
	6.586666667	
738.7	7.38	20.8
738.8	6.84	21.6
738.9	6.4	22.4
	6.873333333	
758.1	5.1	19
758.2	5.46	18.7
758.3	5.18	19.5
	5.246666667	

758.4	5.54	17.6
758.5	5.53	16.9
758.6	5.61	18.5
	5.56	
762.1	9.62	26.7
762.2	10.6	32.3
762.3	9.96	31.5
	10.06	
762.4	11.1	25.1
762.5	10.5	25.6
762.6	11	27.3
	10.86666667	
881.1	15	41.6
881.2	16.6	42.8
881.3	18.8	47.3
	16.8	
881.4	15.4	41.6
881.5	15.9	42.8
881.6	15.8	42.9
	15.7	
881.7	17.6	44.9
881.8	16.3	43.6
881.9	15.9	40.4
	16.6	
883.1	8.86	27.2
883.2	8.38	25
883.3	9.28	26.2
	8.84	
883.4	8.78	25.7
883.5	9.48	27.9
883.6	10.3	31.3
	9.52	
883.7	9.63	27.4
883.8	8.95	26.1
883.9	10.1	28.6
	9.56	
888.1	7.33	25.1
888.2	7.33	25.5
888.3	7.61	25.9
	7.423333333	
888.4	7.78	25.9
888.5	7.74	25.8
888.6	7.21	24.2

	7.576666667	
888.7	7.34	21
888.8	7.08	24.2
888.9	6.34	21.4
	6.92	
931.1	15.8	32.9
931.2	14.8	34
	15.3	
931.4	14.3	33
931.5	15.9	36.6
	15.1	
931.7	17.2	36.8
931.8	14.5	33.2
	15.85	
933.1	7.95	27.2
933.2	8.32	27.2
933.3	7.62	24.8
	7.963333333	
933.4	8.36	26
933.5	8.64	26.4
933.6	8.19	26
	8.396666667	
933.7	8.03	27
933.8	7.61	23.6
933.9	8.22	26.5
	7.953333333	
949.1	7.18	42.9
949.2	10.3	56.4
949.3	8.7	48.6
	8.726666667	
949.4	8.11	42.9
949.5	9.52	42.1
	8.815	
952.1	30.4	58.8
952.2	31.7	58.6
952.3	29.2	59.9
	30.43333333	
952.4	26.5	59
952.5	29.4	58.8
952.6	27.2	59.7
	27.7	
952.7	18.4	36.8
952.8	29	58.5

952.9	32.6	59.8
	26.66666667	
953.1	2.16	19.5
953.2	6.42	24.3
953.3	6.67	23.7
	5.083333333	
953.4	6.54	27.8
953.5	6.82	26.1
953.6	6.69	25.8
	6.683333333	
953.7	6.66	25.3
953.8	6.36	25.7
953.9	7.48	27.8
	6.833333333	
956.1	10.4	36.8
956.2	21.2	48.1
956.3	12	40.5
	14.53333333	
956.4	13.5	43.8
956.5	13.6	38.2
956.6	12.1	40.2
	13.06666667	
956.7	14.8	40.3
956.8	15.3	42.4
956.9	13	36.3
	14.36666667	
957.1	3.66	16.7
957.2	0	0
957.3	10.8	45.8
	4.82	
957.4	2.27	15.4
957.5	11.5	40
	6.885	
957.7	62.5	78.9
957.8	13.5	56.8
957.9	7.69	36.4
	27.89666667	
969.1	6	20.5
969.2	6.61	22.6
969.3	6.7	24.5
	6.436666667	
969.4	6.98	21
969.5	7.07	22

969.6	6.38	21.8
	6.81	
969.7	6.23	22.1
969.8	6.75	22.9
969.9	6.68	20.1
	6.553333333	
978.1	10.8	37
978.2	10.7	35.7
978.3	14	44.1
	11.83333333	
978.4	12.3	40.4
978.5	12.4	37.4
	12.35	
978.7	8.81	31
978.8	14.5	41.2
978.9	10.4	32.5
	11.23666667	
980.1	14.5	49.2
980.2	16.8	51.7
980.3	17.7	54.2
	16.33333333	
980.4	16.6	51.9
980.5	16.4	49.9
980.6	17.9	51.4
	16.96666667	
980.7	17.1	53.2
980.8	17.7	53.1
980.9	17.7	53
	17.5	

Samples	**Freq. of CD4+**	**CD4 Proliferation**
700.1	7.02	22.9
700.2	7.43	26.3
700.3	7.77	25.5
	7.406666667	
700.4	6.88	25.1
700.5	7.49	28.4
700.6	6.56	24
	6.976666667	
700.7	6.67	24.2
700.8	6.94	25.2

700.9	5.66	22
	6.423333333	
730.1	4	26.7
730.2	3.9	37.5
	3.95	
730.4	5.84	34.8
730.5	2.3	20
	4.07	
730.7	4.64	32.4
730.8	6.25	27.7
	5.445	
732.1	1.53	8.7
732.2	1.5	12.5
	1.515	
732.4	**4.2**	**26.3**
732.7	1.7	13
732.8	5.43	27.8
	3.565	
737.1	3.08	25
737.2	0	0
	1.54	
737.4	0	0
737.5	1.59	10
	0.795	
737.7	0	0
737.8	0	0
	0	
739.1	2.24	11.2
739.2	2.62	12.7
739.3	2.58	12.3
	2.48	
739.4	3.64	17.2
739.5	2.78	13.8
739.6	3.03	14.1
	3.15	
739.7	2.96	13.8
739.8	2.99	13.5
739.9	2.66	12.7
	2.87	
740.1	1.94	10.4
740.2	1.98	13.2
740.3	2.17	13.7

	2.03	
740.4	2.67	16.2
740.5	2.59	14.5
740.6	2.63	13.6
	2.63	
740.7	2.14	13.7
740.8	2.2	13.9
740.9	3	17.2
	2.446666667	
882.1	4.37	16.6
882.2	3.53	14.4
882.3	4.47	16.3
	4.123333333	
882.4	4.77	17.9
882.5	4.51	18.2
882.6	4.75	18.1
	4.676666667	
882.7	4.9	19.4
882.8	3.5	14.4
882.9	5.77	22.8
	4.723333333	
884.1	0.23	3.96
884.2	4.46	17.2
884.3	5.28	20.3
	3.323333333	
884.4	4.97	20
884.5	5.84	21.6
884.6	5.12	20.6
	5.31	
884.7	4.71	19.5
884.8	4.34	17.8
884.9	4.99	20.3
	4.68	
885.1	7.36	27.9
885.2	6.39	25.4
885.3	6.17	21.4
	6.64	
885.4	8.19	31
885.5	6.97	26.2
885.6	8.32	29.9
	7.826666667	
885.7	7.71	26.5
885.8	6.86	27

885.9	6.64	24.6
	7.07	
971.1	0	0
971.2	0	0
	0	
971.4	0	0
971.5	0	0
	0	
971.7	0	0
971.8	0	0
	0	

Samples	**Freq. of CD4+**	**CD4 Proliferation**
380.1	6.29	20.2
380.2	6.52	21.5
380.3	5.95	19.7
	6.253333333	
380.4	5.11	18.2
380.5	6.33	20.9
380.6	5.65	18.6
	5.696666667	
380.7	6.39	21.1
380.8	5.02	16.1
380.9	5.89	20.2
	5.766666667	
387.1	3.6	16
387.2	4.71	18.6
387.3	2.11	14.3
	3.473333333	
387.4	4.55	26.7
387.5	2.99	13.3
387.6	3.9	16.7
	3.813333333	
387.7	2.33	15.8
387.8	1.31	9.3
387.9	4.44	25
	2.693333333	
411.1	4.19	14
411.2	4.35	13.7
411.3	4.57	14.8
	4.37	
411.4	4.93	16.6

411.5	4.54	15.2
411.6	6.13	19.9
	5.2	
411.7	4.72	15.6
411.8	4.99	16.7
411.9	5.2	16.9
	4.97	
417.1	8.85	22.8
417.2	9.67	23.5
417.3	11.5	25.6
	10.00666667	
417.4	10.7	25
417.5	13.6	31
417.6	10.1	26.3
	11.46666667	
417.7	9.49	25.7
417.8	9.45	22.9
417.9	9.84	21.6
	9.593333333	
641.1	7.11	26.9
641.2	6.5	22.1
641.3	6.84	25.9
	6.816666667	
641.4	7.41	25.2
641.5	7.44	26.3
641.6	7.3	24.6
	7.383333333	
641.7	7.02	26.6
641.8	6.82	24.7
641.9	6.69	26.3
	6.843333333	
642.1	9.04	27.4
642.2	8.14	27.1
642.3	8.65	28.5
	8.61	
642.4	9.94	29.8
642.5	9.54	30.3
642.6	9.56	29.8
	9.68	
642.7	8.7	29.3
642.8	8.7	28
642.9	8.07	27
	8.49	

643.1	17.2	41.6
643.2	19	41
643.3	18.7	38
	18.3	
643.4	18.8	44.9
643.5	17.7	43.7
643.6	18.2	44.3
	18.23333333	
643.7	15.7	41.3
643.8	14.9	40.8
643.9	15.5	41.1
	15.36666667	
644.1	13.4	30.1
644.2	15	30.2
644.3	14.8	29.6
	14.4	
644.4	15.3	26.8
644.5	12.4	25.5
644.6	12.2	25.5
	13.3	
644.7	14	31.4
644.8	13.2	30
644.9	14.4	29.8
	13.86666667	
780.1	5.51	24.5
780.2	6.45	37.2
780.3	6.36	27.7
	6.106666667	
780.4	0	0
780.5	6.33	21.7
	3.165	
932.1	6.19	21.1
932.2	4.86	18.7
932.3	6.11	24.2
	5.72	
932.4	6.39	21.9
932.5	6	22.2
932.6	6.08	20
	6.156666667	
932.7	6.51	22.3
932.8	5.25	20
932.9	4.29	14.7
	5.35	

Samples	Freq. of CD4+	CD4 Proliferation
384.1	19.4	50
384.2	33.3	80
384.3	0	0
	17.56666667	
384.4	27.3	85.7
384.5	22.2	80
384.6	21.9	66.7
	23.8	
384.7	10.5	22.2
384.8	23.1	50
384.9	11.8	66.7
	15.13333333	
394.1	6.67	16.7
394.2	0	0
394.3	3.12	12.5
	3.263333333	
394.4	11.8	50
394.5	0	0
394.6	5.56	20
	5.786666667	
394.7	5.17	33.3
394.8	11.9	46.7
394.9	7.69	25
	8.253333333	
395.1	9.79	27.1
395.2	8.95	24.5
395.3	9.22	25.6
	9.32	
395.4	8.82	22.8
395.5	8.7	21.9
395.6	10.5	25.4
	9.34	
395.7	11.6	29.8
395.8	11.3	29.3
395.9	10.1	26.6
	11	
396.1	8.16	36.4
396.2	9.88	34.8
396.3	8.04	34.6
	8.693333333	
396.4	3.16	16.7
396.5	5.93	33.3

396.6	7.69	25
	5.593333333	
396.7	10.9	50
396.8	9.68	42.9
396.9	0	0
	6.86	
397.1	7.54	22.1
397.2	7.17	22.8
397.3	7.39	21.7
	7.366666667	
397.4	9.02	24.9
397.5	7.6	22.5
397.6	10.2	27.8
	8.94	
397.7	8.39	29.2
397.8	6.93	19.8
397.9	7.22	23.6
	7.513333333	
402.1	11.2	51.2
402.2	14.8	63.9
402.3	13.9	55.8
	13.3	
402.4	22.5	57.4
402.5	15	63.2
402.6	13.2	50
	16.9	
402.7	15.2	55.9
402.8	14.6	56.4
402.9	17.7	65.4
	15.83333333	
407.1	6.91	26.4
407.2	7.47	28.8
407.3	9.13	36.9
	7.836666667	
407.4	7.67	25.5
407.5	6.54	20.3
407.6	13.1	40.7
	9.103333333	
407.7	6.09	22.6
407.8	8.29	26.8
407.9	6.82	27.6
	7.066666667	
408.1	5.71	16.3

408.2	**7.74**	**21.2**
408.3	**7.25**	**19.2**
	6.9	
408.4	**10**	**24.7**
408.5	**6.34**	**15.4**
408.6	**7.61**	**19.5**
	7.983333333	
408.7	**13.3**	**33**
408.8	**10.3**	**26.7**
408.9	**9.71**	**25.2**
	11.10333333	
412.1	**8.05**	**21.5**
412.2	**9.13**	**24.4**
412.3	**8.06**	**22.8**
	8.413333333	
412.4	**9.26**	**24.6**
412.5	**8.53**	**23.9**
412.6	**9.19**	**24.7**
	8.993333333	
412.7	**10.8**	**29.2**
412.8	**16.8**	**42.8**
412.9	**8.86**	**24.7**
	12.15333333	
418.1	**6**	**27.8**
418.2	**5.65**	**28.9**
418.3	**7.53**	**27.3**
	6.393333333	
418.4	**4.13**	**15.2**
418.5	**8.16**	**32**
418.6	**5.88**	**24.3**
	6.056666667	
418.7	**4.84**	**21.4**
418.8	**3.78**	**19.1**
418.9	**4.01**	**19.4**
	4.21	

Samples	**Freq. of CD4+**	**CD4 Proliferation**
381.1	4.77	15.7
381.2	5.06	16.1
381.3	5.09	15.4
	4.973333333	

381.4	5.49	16.6
381.5	5.2	16.4
381.6	5.47	16.4
	5.386666667	
381.7	4.36	13.9
381.8	4.51	14.1
381.9	5.14	16.4
	4.67	
382.1	3.87	29.6
382.2	4.47	34.6
382.33	2.1	5.52
	3.48	
382.4	2.25	22.1
382.5	3.38	25.4
382.6	2.34	20.8
	2.656666667	
382.7	2.85	33.3
382.8	1.24	16.7
382.9	1.75	24
	1.946666667	
383.1	2.53	6.74
383.2	3.25	8.73
	2.89	
383.4	2.31	6.03
383.5	3.28	9.06
383.6	3.22	8.86
	2.936666667	
383.7	2.48	7.05
383.8	1.91	5.41
383.9	2.82	8.49
	2.403333333	
385.1	3.51	11.5
385.2	3.98	12.8
385.3	6.83	31.8
	4.773333333	
385.4	2.69	10.1
385.5	3.47	12.1
385.6	3.75	11.7
	3.303333333	
385.7	2.85	9.41
385.8	4.03	13.9
385.9	2.47	8.8
	3.116666667	

386.1	6.71	20.1
386.2	7.01	21.8
386.3	6.34	20.2
	6.686666667	
386.4	6.5	20
386.5	8.35	23.2
386.6	6.71	18.6
	7.186666667	
386.7	6.91	20.1
386.8	6.96	20.6
386.9	7.42	21.2
	7.096666667	
391.1	3.23	14.3
391.2	0.94	4.35
391.3	4.23	13
	2.8	
391.4	5.26	25
391.5	3.85	20
391.6	0	0
	3.036666667	
391.7	0	0
391.8	3.14	17.2
391.9	2.27	10
	1.803333333	
392.1	0	0
392.2	4	20
392.3	0	0
	1.333333333	
392.4	7.69	50
392.5	5.88	28.6
392.6	0	0
	4.523333333	
392.7	0	0
392.8	0	0
392.9	0	0
	0	
403.1	4.11	19.5
403.2	3.45	14.2
403.3	10.7	50
	6.086666667	
403.4	5.82	23.6
403.5	3.14	12.5
403.6	3.83	18.9

	4.263333333	
403.7	3.85	15.7
403.8	5.73	19.7
403.9	5.51	19.7
	5.03	
405.1	2.86	10.6
405.2	2.68	9.76
405.3	3.57	100
	3.036666667	
405.4	3.54	13.3
405.5	2.13	7.99
405.6	1.51	5.63
	2.393333333	
405.7	3.51	12.6
405.8	3.18	11.6
405.9	3.96	14.8
	3.55	
406.1	1.52	4.92
406.2	0	0
406.3	2.94	12.5
	1.486666667	
406.4	2.13	7.69
406.5	3.12	20
406.6	0	0
	1.75	
406.7	2.27	12.5
406.8	0	0
406.9	2.97	10.3
	1.746666667	

Samples	**Freq. of CD4+**	**CD4 Proliferation**
390.1	0	0
390.2	0	0
	0	
390.4	0	0
	0	
390.7	1.37	11.1
390.8	0	0
	0.685	
393.1	3.49	20.7
393.2	3.21	14.7

393.3	2.1	10.9
	2.933333333	
393.4	3.91	15.2
393.5	6.32	28.2
393.6	1.86	8.11
	4.03	
393.7	3.23	13.6
393.8	2.13	9.09
393.9	3.4	18.5
	2.92	
413.1	2.21	8.11
413.2	5.38	22.2
413.3	2.68	11.1
	3.423333333	
413.4	2.82	13.3
413.5	8.82	26.1
413.6	5.45	21.6
	5.696666667	
413.7	3.15	13.7
413.8	4.23	17.4
413.9	6.06	24.4
	4.48	
419.1	4.36	16.9
419.2	7.55	25.7
419.3	5.14	19.2
	5.683333333	
419.4	4.99	17.7
419.5	4.26	15
419.6	5.4	18.7
	4.883333333	
419.7	6.88	24.5
419.8	7.74	27.7
419.9	3.79	13.7
	6.136666667	
926.1	0	0
926.2	0	0
926.3	0	0
	0	
926.4	0	0
926.5	0	0
926.6	0	0
	0	
926.7	16.7	50

926.8	0	0
926.9	14.3	100
	10.33333333	

Samples	Freq. of CD4+	CD4 Proliferation
345.1	1.49	7.43
345.2	2.95	11.6
345.3	1.03	4.66
	1.823333333	
345.4	1.22	5.68
345.5	1.18	7.07
345.6	1.4	6.87
	1.266666667	
345.7	0.61	2.89
345.8	1.09	5.39
345.9	1.6	7.99
	1.1	
347.1	0.8	4.27
347.2	0.92	4.88
347.3	0.95	5.49
	0.89	
347.4	0.48	2.77
347.5	0.59	2.7
347.6	0.44	2.01
	0.503333333	
347.7	1.67	12.6
347.8	0.55	2.66
347.9	0.67	3.14
	0.963333333	
363.1	0.45	3.1
363.2	0.12	0.78
363.3	0.46	2.77
	0.343333333	
363.4	0.14	0.92
363.5	0.33	2.19
363.6	0.087	0.64
	0.185666667	
363.7	0.14	0.91
363.8	0.096	0.59
363.9	0.15	0.99
	0.128666667	

364.1	0.32	1.79
364.2	0.21	1.31
364.3	0.37	2.1
	0.3	
364.4	0	0
364.5	0	0
364.6	0	0
	0	
364.7	0.079	0.55
364.8	0.031	0.22
364.9	0	0
	0.036666667	
365.1	0.34	2.78
365.2	0.48	3.64
365.3	0	0
	0.273333333	
365.4	0	0
365.5	0	0
365.6	0.44	2.56
	0.146666667	
365.7	0	0
365.8	0	0
365.9	0.79	8
	0.263333333	
366.1	0	0
366.2	0	0
366.3	3.36	21.1
	1.12	
366.4	0	0
366.5	0	0
366.6	0	0
	0	
366.7	0	0
366.8	0	0
366.9	0	0
	0	
374.1	0.36	1.63
374.2	0.44	1.87
374.3	0.61	2.54
	0.47	
374.4	0.27	1.05
374.5	0.26	1.21
374.6	0.14	0.5

	0.223333333	
374.7	1.11	5.37
374.8	0.64	3.22
374.9	1.08	4.83
	0.943333333	
375.1	0.77	3.43
375.2	1.09	4.57
375.3	0.77	3.46
	0.876666667	
375.4	0.65	2.4
375.5	1.16	4.62
375.6	0.96	3.72
	0.923333333	
375.7	0.59	2.15
375.8	0.79	3.42
375.9	0.78	2.74
	0.72	

Samples	**Freq. of CD4+**	**CD4 Proliferation**
331.1	5.3	25.4
331.2	5.03	22
	5.165	
331.4	5.81	26.2
331.5	0.64	10.9
	3.225	
331.7	4.81	23.1
331.8	4.88	22.7
	4.845	
336.1	5.47	21.6
336.2	6.21	25.2
336.3	6.48	25.6
	6.053333333	
336.4	6.57	24.8
336.5	6.85	26.5
336.6	7.62	28.4
	7.013333333	
336.7	5.71	24.9
336.8	5.33	23.4
336.9	10.6	40.3
	7.213333333	
337.1	13.3	36.4

337.2	3.86	15.9
337.3	3.8	18.8
	6.986666667	
337.4	5.04	22.8
337.5	3.58	17.8
337.6	4.84	22.1
	4.486666667	
337.7	9.02	35.2
337.8	4.37	19.7
337.9	4.38	20
	5.923333333	
340.1	5.62	30.8
340.2	5.84	28.1
340.3	5.92	30.4
	5.793333333	
340.4	5.42	27.2
340.5	4.83	28.1
340.6	5.66	29.1
	5.303333333	
340.7	4.62	27.4
340.8	5.36	28.1
340.9	5.51	27.4
	5.163333333	
344.1	4.76	24.6
344.2	4.33	23.7
344.3	3.27	18
	4.12	
344.4	3.9	21.8
344.5	4.43	26.5
344.6	2.85	17.1
	3.726666667	
344.7	4.43	24.4
344.8	4.51	26.1
344.9	3.8	20
	4.246666667	
346.1	4.12	20.9
346.2	7.35	27.9
346.3	3.35	16.7
	4.94	
346.4	3.74	18.5
346.5	4.35	20.8
346.6	4.22	20.3
	4.103333333	

346.7	4.9	22.2
346.8	4.15	20.9
346.9	4.1	20.6
	4.383333333	
367.1	7.01	24.5
367.2	7.9	27.4
367.3	7.31	25.9
	7.406666667	
367.4	7.37	26.9
367.5	6.55	22.8
367.6	5.56	20.2
	6.493333333	
367.7	7.19	24.8
367.8	6.31	22.8
367.9	8.18	30.3
	7.226666667	
414.1	10.9	42.6
414.2	11.1	42.3
414.3	10.6	41.7
	10.86666667	
414.4	5.4	25.7
414.5	9.39	37.1
414.6	12.2	48.1
	8.996666667	
414.7	9.94	42.3
414.8	9.2	37.5
414.9	9.26	35.8
	9.466666667	

Samples	**Freq. of CD4+**	**CD4 Proliferation**
330.1	5.26	19.7
330.2	9.2	38.7
330.3	4.27	16
	6.243333333	
330.4	9.73	33.1
330.5	11.4	35.8
330.6	4.68	16.5
	8.603333333	
330.7	2.4	8.35
330.8	3.39	11.6
330.9	1.78	9.03
	2.523333333	

332.1	2.75	11.7
332.2	2.17	9.66
332.3	1.89	8.1
	2.27	
332.4	2.28	9.22
332.5	1.69	8.38
332.6	2.22	8.96
	2.063333333	
332.7	2.83	13.3
332.8	2.33	11.6
332.9	0.084	0.64
	1.748	
333.1	3.26	11.1
333.2	6.38	23.2
333.3	4.39	16.2
	4.676666667	
333.4	0.45	10
333.5	4.66	15.3
333.6	3.44	11.6
	2.85	
333.7	3.35	11.6
333.8	3.99	15.7
333.9	3.51	14.5
	3.616666667	
334.1	2.96	11.9
334.2	6.27	23.6
334.3	6.66	24.6
	5.296666667	
334.4	3.94	15.3
334.5	7.41	28
334.6	8.01	29.9
	6.453333333	
334.7	7.11	25.7
334.8	10.2	40.7
334.9	10.9	43
	9.403333333	
335.1	11.8	39.3
335.2	10.7	36.1
335.3	10.9	33.5
	11.13333333	
335.4	15.9	47.7
335.5	13.6	45.3
335.6	19.4	58

	16.3	
335.7	2.48	32.5
335.8	9.98	32.7
335.9	13.7	45
	8.72	
338.1	4.19	22.2
338.2	6.32	33.8
338.3	9.03	44.4
	6.513333333	
338.4	8.34	39.4
338.5	0.89	5.86
338.6	2.99	15.5
	4.073333333	
338.7	3.83	21.1
338.8	3.12	17.1
338.9	3.58	18.8
	3.51	
339.1	11.1	33.6
339.2	8.42	28.5
339.3	8.21	26.1
	9.243333333	
339.4	9.29	27.7
339.5	11.9	32.1
339.6	10.8	32.1
	10.66333333	
339.7	12.1	36.5
339.8	9.01	28.5
339.9	11	33.3
	10.70333333	
343.1	7.73	34.1
343.2	9.03	38
343.3	7.93	34.1
	8.23	
343.4	10.6	44.1
343.5	11	44.1
343.6	10.4	37.7
	10.66666667	
343.7	6.18	29.9
343.8	9.01	36.3
343.9	1.47	35.9
	5.553333333	
350.1	17.3	47.5
350.2	14.8	49.1

350.3	12	44.2
	14.7	
350.4	13.3	47.6
350.5	13.1	42.7
350.6	11.2	39.1
	12.53333333	
350.7	11.8	42.9
350.8	12.2	38.6
350.9	9.15	35
	11.05	
357.1	9	41
357.2	4.54	27.6
357.3	17.1	50.4
	10.21333333	
357.4	13	45.8
357.5	13	45.6
357.6	13.5	45.4
	13.16666667	
357.7	15.5	47.7
357.8	14.8	47.9
357.9	13.8	47
	14.7	
358.1	4.08	23
358.2	4.09	22.3
358.3	5.97	28.8
	4.713333333	
358.4	3.53	20.6
358.5	4.52	22
358.6	2.79	16
	3.613333333	
358.7	3.43	20.3
358.8	0.98	6.71
358.9	0.17	2.14
	1.526666667	
359.1	7.94	31.1
359.2	3.86	16.9
359.3	6.15	25.1
	5.983333333	
359.4	5.6	23.6
359.5	9.97	36.6
359.6	9.02	34.8
	8.196666667	
359.7	4.54	20

359.8	5.22	24.1
359.9	4.53	20.3
	4.763333333	
361.1	0.92	7.49
361.2	0.5	5.01
361.3	0.22	2.73
	0.546666667	
361.4	0.19	1.82
361.5	0.2	2.38
361.6	5.79	29.7
	2.06	
361.7	4.51	23.4
361.8	4.99	25.6
361.9	4.58	25
	4.693333333	
368.1	12.3	44
368.2	9.63	36.1
368.3	11.6	41
	11.17666667	
368.4	8.86	31.3
368.5	7.38	24.5
368.6	9.42	33.9
	8.553333333	
368.7	5.95	23.6
368.8	10.8	41
368.9	5.41	21.3
	7.386666667	
369.1	4.88	19.2
369.2	6.17	23.6
369.3	4.55	19.4
	5.2	
369.4	8.47	33.5
369.5	7.52	27.2
369.6	7.5	28.2
	7.83	
369.7	6.51	27.9
369.8	8.09	33.4
369.9	6.33	27.4
	6.976666667	
370.1	0.25	3.18
370.2	0.2	2.61
370.3	0.3	4.6
	0.25	

370.4	0.11	1.12
370.5	2.33	25.2
370.6	0.28	4.27
	0.906666667	
370.7	0	0
370.8	0.13	4.42
370.9	0.34	4.43
	0.156666667	
420.1	12.2	38
420.2	18	55.8
420.3	13.1	41.9
	14.43333333	
420.4	9.28	32
420.5	10.4	37.2
420.6	12.6	41.3
	10.76	
420.7	14.3	42.1
420.8	11.1	37.1
420.9	9.35	32.6
	11.58333333	
421.1	13.7	51
421.2	9.47	40.4
421.3	8.55	41
	10.57333333	
421.4	8.5	37.9
421.5	15	57.5
421.6	10.8	47.8
	11.43333333	
421.7	8.43	38.3
421.8	8.88	35.8
	8.655	

Samples	**Freq. of CD8+**	**CD8 Proliferation**
292.1	9.68	8.06
292.2	0	0
292.3	0	0
	3.226666667	**2.686666667**
292.4	3.85	0
292.5	1.22	0.46
	2.535	**0.23**
292.7	11.2	4.41

292.8	6.56	2.49
292.9	0	0
	5.92	**2.3**
293.1	**6.45**	**6.45**
293.4	**6.64**	**3.39**
293.7	**0**	**0**
296.1	**0**	**0**
296.4	**5.19**	**3.36**
296.7	**2.78**	**2.78**
721.1	2.33	1.55
721.2	5.18	2.91
721.3	7.82	3.63
	5.11	**2.696666667**
721.4	8.19	3.2
721.5	7.53	3
721.6	7.83	3.09
	7.85	**3.096666667**
721.7	6.14	3.17
721.8	1.35	1.35
721.9	4.55	0
	4.013333333	**1.506666667**
722.1	6.08	0.68
722.2	13.6	4.55
722.3	8.65	5.77
	9.443333333	**3.666666667**
722.4	10.5	10.5
722.5	4.69	4.69
722.6	0	0
	5.063333333	**5.063333333**
722.7	0	0
722.8	23.5	17.6
722.9	50	37.5
	24.5	**18.36666667**
756.1	1.28	1.28
756.2	0	0
	0.64	**0.64**
756.4	**0**	**0**

756.7	**0**	**0**
765.1	0	0
765.2	3.76	1.57
765.3	0	0
	1.253333333	**0.523333333**
765.4	2.66	1.14
765.5	1.57	1.57
	2.115	**1.355**
765.7	0	0
765.8	0	0
765.9	1.94	0
	0.646666667	**0**
775.1	**5.05**	**1.44**
775.7	**4**	**4**

Samples	Freq. of CD8+	CD8 Proliferation
297.1	**0**	**n/a**
297.4	**0**	**n/a**
297.7	**0**	**n/a**
298.1	**0**	**n/a**
298.4	**33.3**	**n/a**
298.7	**50**	**n/a**
723.1	**0**	**n/a**
723.4	**12.5**	**n/a**
723.7	**16.4**	**n/a**
758.1	**0**	**n/a**
758.7	**0**	**n/a**

761.1	50	n/a
761.2	0	n/a
	25	
761.4	**0**	**n/a**
761.7	0	n/a
761.8	0	n/a
	0	
770.1	0	n/a
770.2	0	n/a
770.3	0	n/a
	0	
770.4	7.84	n/a
770.5	12.1	n/a
770.6	29.5	n/a
	16.48	
770.7	25	n/a
770.8	0	n/a
770.9	0	n/a
	8.333333333	
772.1	**13.5**	**n/a**
772.4	**29.7**	**n/a**
772.7	0	n/a
772.8	0	n/a
772.9	0	n/a
	0	
781.2	35.3	n/a
782.1	30.6	n/a
782.3	34.8	n/a
	33.56666667	
782.4	31.9	n/a
782.5	26	n/a
782.6	5.85	n/a
	21.25	
782.7	33.9	n/a
782.8	35.2	n/a
782.9	50	n/a
	39.7	

Samples	**Freq. of CD8+**	**CD8 Proliferation**

751.1	0	0
751.2	0	0
751.3	0	0
	0	
751.4	0	0
751.5	0	0
	0	
752.1	0	0
752.2	0	0
	0	
752.4	0	0
752.5	0	0
	0	
753.1	0	0
753.2	0	0
753.3	0	0
	0	
753.4	0	0
753.5	0	0
753.6	0	0
	0	
754.1	0	0
754.2	0	0
754.3	0	0
	0	
754.4	0	0
754.5	0	0
	0	
756.2	0	0
756.3	0	0
	0	
756.4	0	0
756.5	0	0
756.6	0	0
	0	
757.1	0	0
757.2	0	0
757.3	0	0
	0	
757.4	0	0
757.5	0	0
757.6	0	0
	0	

760.1	0	0
760.2	0	0
760.3	0	0
	0	
760.4	0	0
760.5	0	0
760.6	0	0
	0	
761.1	0	0
761.2	0	0
761.3	0	0
	0	
761.4	0	0
761.5	0	0
761.6	0	0
	0	
764.1	0	0
764.2	0	0
764.3	0	0
	0	
764.4	0	0
764.5	0	0
764.6	0	0
	0	
951.1	0	0
951.2	0	0
	0	
951.4	0	0
951.5	0	0
	0	
959.1	0	0
959.2	0	0
959.3	0	0
	0	
959.4	0	0
959.5	0	0
959.6	0	0
	0	
972.1	0	0
972.2	0	0
972.3	0	0
	0	
972.4	0	0

972.5	0	0
	0	
981.1	0	0
981.2	0	0
981.3	0	0
	0	
981.5	0	0
981.6	0	0
	0	
982.1	0	0
982.2	0	0
982.3	0	0
	0	
982.4	0	0
982.5	0	0
982.6	0	0
	0	
985.1	0	0
985.2	0	0
985.3	0	0
	0	
985.4	0	0
985.5	0	0
985.6	0.014	100
	0.004666667	

Samples	**Freq. of CD8+**	**CD8 Proliferation**
726.1	10	3.33
726.2	10.3	7.69
762.3	13.8	13.8
	11.36666667	
726.4	12.3	3.08
726.5	10.5	0
	11.4	
726.7	5	0
726.8	6.67	6.67
	5.835	
728.1	10.7	1.3
728.2	11.3	1.8
728.3	10.8	1.25
	10.93333333	

728.4	11.2	1.46
728.5	12.1	1.36
728.6	10.6	1.36
	11.3	
728.7	10.4	1.69
728.8	10.2	2.13
728.9	11.5	1.92
	10.7	
886.1	11	1.26
886.2	12	1.47
886.3	10.9	1.42
	11.3	
886.4	11.3	1.2
886.5	10.9	1.41
886.6	11.1	1.31
	11.1	
886.7	11	1.4
886.8	10.5	1.15
886.9	10.8	0.61
	10.76666667	
887.1	10.8	0.21
887.2	11.9	0.37
887.3	11.1	0.37
	11.26666667	
887.4	11.9	0.57
887.55	11.4	0.37
887.66	12.2	0.26
	11.83333333	
887.7	11.5	0.15
887.8	10.4	0.18
887.9	10.9	0.28
	10.93333333	
926.1	1.45	0.29
926.2	4.15	0.46
962.3	3.54	2.02
	3.046666667	
926.4	2.02	0.51
926.5	4.23	2.82
926.6	1.83	0
	2.693333333	
926.7	3.22	2.34
926.8	2.44	1.83
926.9	2.13	2.13

	2.596666667	
927.1	10.1	2.53
927.2	9.78	2.85
927.3	9.39	3.31
	9.756666667	
927.4	9.69	2.92
927.5	9.45	2.76
927.6	9.47	2.47
	9.536666667	
927.7	9.92	2.18
927.8	7.31	2.95
928.9	9.13	2.52
	8.786666667	
948.1	2.89	0.24
948.2	2.17	0.62
	2.53	
948.4	1.56	0.67
948.5	2.12	0.96
	1.84	
948.7	0.79	0.79
948.8	1.78	0.4
	1.285	
954.1	7.45	1.29
954.2	7.17	1.28
954.3	6.58	1.16
	7.066666667	
954.4	7.13	1.41
954.5	6.4	1.23
954.6	6.84	1.37
	6.79	
954.7	4.07	3.66
954.8	6.64	0.12
954.9	7.49	0.72
	6.066666667	
976.1	10.1	0.27
976.2	9.48	0.27
976.3	9	0.26
	9.526666667	
976.4	9.08	0.24
976.5	10.2	0.28
976.6	10.4	0.41
	9.893333333	
976.7	9.96	0.37

976.8	10.1	0.83
976.9	10.1	1.05
	10.05333333	
977.1	14.6	1.84
977.2	11.6	1.28
977.3	10.7	1.43
	12.3	
977.4	12.3	0.99
977.5	11.9	1.22
977.6	11.4	1.01
	11.86666667	
977.7	10.4	1
977.8	11.2	1.13
977.9	10.8	0.92
	10.8	

Samples	**Freq. of CD8+**	**CD8 Proliferation**
692.1	1.53	14.8
692.2	1.21	11.8
692.3	1.28	13
	1.34	
692.4	0.64	6.36
692.5	1.19	11.2
692.6	1.29	12.5
	1.04	
692.7	1.25	12.2
692.8	1.33	12.1
692.9	1.62	14.5
	1.4	
693.1	1.53	15.8
693.2	1.57	18.5
693.3	1.47	16.2
	1.523333333	
693.4	1.51	16.3
693.5	0.78	10.1
693.6	1.13	14.9
	1.14	
693.7	1.47	17.9
693.8	1.38	17.1
693.9	1.24	15.2
	1.363333333	

694.1	1.09	13.2
694.2	1.18	16.9
694.3	1.03	13.4
	1.1	
694.4	1.09	13
694.5	1.45	16.9
694.6	1.11	13.6
	1.216666667	
694.7	0.92	11.1
694.8	1.11	14.5
694.9	0.9	11.6
	0.976666667	
729.1	1.49	13
729.2	2.54	19.7
	2.015	
729.4	2.78	27.7
729.5	0	0
	1.39	
729.7	2.73	20.7
729.9	2.72	19.7
	2.725	
738.1	0.9	16
738.2	1.33	23.6
738.3	1.04	21.1
	1.09	
738.4	1.64	24.4
738.5	1.42	19.3
738.6	1.22	18.2
	1.426666667	
738.7	0.92	15.5
738.8	1.58	25.1
738.9	1.31	20.2
	1.27	
758.1	1.11	15.1
758.2	1.03	16.3
758.3	1.13	17.5
	1.09	
758.4	1.21	13.8
758.5	1.45	14.5
758.6	1.73	18.2
	1.463333333	
762.1	2.15	22.9
762.2	2.74	26.4

762.3	2.5	25.7
	2.463333333	
762.4	2.12	19.9
762.5	2.16	20.4
762.6	2.36	21.9
	2.213333333	
881.1	2.78	30.5
881.2	2.5	32.1
881.3	3.18	38.3
	2.82	
881.4	3.18	36.1
881.5	2.85	34.1
881.6	2.83	33.5
	2.953333333	
881.7	3.47	36.9
881.8	2.93	33.5
881.9	2.7	31.1
	3.033333333	
883.1	1.79	20.6
883.2	2.07	23.1
883.3	2.28	22.9
	2.046666667	
883.4	2.03	23.4
883.5	1.9	22.3
883.6	2.78	28.8
	2.236666667	
883.7	2.39	25.1
883.8	2.17	21.8
883.9	2.72	27.8
	2.426666667	
888.1	2.2	21.2
888.2	2.25	22.8
888.3	1.96	21.3
	2.136666667	
888.4	2.47	26.4
888.5	2.1	22.7
888.6	1.88	20.3
	2.15	
888.7	2.21	22.1
888.8	2.09	18.9
888.9	1.82	18.1
	2.04	
931.1	4.99	27.7

931.2	5.06	28.2
	5.025	
931.4	5.13	28.6
931.5	5.97	32.4
	5.55	
931.7	5.19	28.4
931.8	5.22	29.8
	5.205	
933.1	3.82	24
933.2	3.02	20.4
933.3	2.57	17.6
	3.136666667	
933.4	3.51	21.7
933.5	3.52	22.3
933.6	3.44	21.3
	3.49	
933.7	4.06	27.2
933.8	3	19.3
933.9	2.88	20.1
	3.313333333	
949.1	0.96	50
949.2	0.94	66.7
949.3	0.48	100
	0.793333333	
949.4	1.35	66.7
949.5	0.4	25
	0.875	
952.1	3.71	42.7
952.2	3.99	44.1
952.3	4.58	48.3
	4.093333333	
952.4	5.14	47.8
952.5	4.41	46.8
952.6	4.87	44.7
	4.806666667	
952.7	0	0
952.8	4.51	42.9
952.9	5.71	47.4
	3.406666667	
953.1	1.3	20.3
953.2	1.42	19.2
953.3	1.78	25
	1.5	

953.4	1.31	21.7
953.5	1.61	23.8
953.6	1.05	18.7
	1.323333333	
953.7	1.73	23.2
953.8	1.24	19.8
953.9	1.17	19.4
	1.38	
956.1	1.17	31.5
956.2	2.54	30
956.3	1.33	34.2
	1.68	
956.4	1.57	37.2
956.5	1.08	26.4
956.6	1.3	28.2
	1.316666667	
956.7	1.36	36.8
956.8	1.47	35.1
956.9	1.1	26.7
	1.31	
957.1	0	0
957.2	0	0
957.3	1.96	50
	0.653333333	
957.4	1.14	100
957.5	1.15	50
	1.145	
957.7	4.17	100
957.8	0	0
957.9	0	0
	1.39	
969.1	1.33	18.4
969.2	1.52	20.9
969.3	1.48	21.7
	1.443333333	
969.4	1.61	23.3
969.5	1.58	20.9
969.6	1.24	18.2
	1.476666667	
969.7	1.61	21.6
969.8	1.82	22.3
969.9	1.66	21.5
	1.696666667	

978.1	0.69	27.3
978.2	0.52	22.2
978.3	0.81	23.1
	0.673333333	
978.4	0.84	37.5
978.5	0.18	7.14
	0.51	
978.7	0.34	7.14
978.8	1.19	55.6
978.9	0	0
	0.51	
980.1	4.16	42.5
980.2	4.35	42.5
980.3	4.35	41.2
	4.286666667	
980.4	3.09	33.1
980.5	3.41	37.4
980.6	4.13	40
	3.543333333	
980.7	3.69	39.8
980.8	4.48	40.1
980.9	4.14	38.8
	4.103333333	

Samples	**Freq. of CD8+**	**CD8 Proliferation**
700.1	3.46	28.4
700.2	3.83	30.4
700.3	4	29.5
	3.763333333	
700.4	3.34	30.4
700.5	3.61	32.7
700.6	3.18	29.4
	3.376666667	
700.7	3.83	34.4
700.8	3.63	30
700.9	3.43	28.1
	3.63	
730.1	1	33.3
730.2	3.9	75
	2.45	
730.4	0	0

730.5	1.72	23.1
	0.86	
730.7	1.69	22.2
730.8	2.4	38.5
	2.045	
732.1	0	0
732.2	0.75	14.3
	0.375	
732.4	**1.68**	**22.2**
732.7	1.14	50
732.8	3.26	42.9
	2.2	
737.1	1.54	33.3
737.2	0	0
	0.77	
737.4	0	0
737.5	0	0
	0	
737.7	0	0
737.8	11.1	100
	5.55	
739.1	1.7	16.3
739.2	1.8	17.5
739.3	1.81	17
	1.77	
739.4	2.38	23.3
739.5	2.03	19.3
739.6	1.36	14
	1.923333333	
739.7	2.32	19.5
739.8	1.99	18.2
739.9	2.11	17.6
	2.14	
740.1	0.51	9.23
740.2	1.25	21.4
740.3	1.32	24
	1.026666667	
740.4	1.6	24.6
740.5	1.21	19.5
740.6	1.42	22.5
	1.41	
740.7	1.04	18.6

740.8	1.61	26.4
740.9	1.32	22
	1.323333333	
882.1	3.25	22.1
882.2	2.81	18.7
882.3	2.94	20.1
	3	
882.4	3.61	23.5
882.5	2.9	20.4
882.6	3.85	24
	3.453333333	
882.7	3.48	25.1
882.8	3.19	20.8
882.9	4.04	28.3
	3.57	
884.1	0.33	6.07
884.2	2.05	21.5
884.3	2.18	24.4
	1.52	
884.4	2.05	21.9
884.5	2.09	22
884.6	2.33	23.8
	2.156666667	
884.7	2.21	21.5
884.8	2.44	24
884.9	2.21	23
	2.286666667	
885.1	2.54	28.8
885.2	2.86	30.2
885.3	2.07	24
	2.49	
885.4	2.98	33.5
885.5	2.13	23.3
885.6	2.25	25.8
	2.453333333	
885.7	2.71	28.6
885.8	3.09	32.7
885.9	2.34	23.9
	2.713333333	
971.1	0	0
971.2	0	0
	0	
971.4	0	0

971.5	0	0
	0	
971.7	0	0
971.8	0	0
	0	

Samples	Freq. of CD8+	CD8 Proliferation
380.1	2.5	18.2
380.2	3.42	22.9
380.3	3.24	20.8
	3.053333333	
380.4	3.12	24.5
380.5	2.39	19.7
380.6	2.19	16.6
	2.566666667	
380.7	3.74	24.5
380.8	2.85	20.8
380.9	2.65	18.3
	3.08	
387.1	0.9	28.6
387.2	0.36	9.09
387.3	0.84	13.3
	0.7	
387.4	1.14	25
387.5	0	0
387.6	0	0
	0.38	
387.7	0	0
387.8	0.66	13.3
387.9	0	0
	0.22	
411.1	1.64	23.9
411.2	1.73	26.1
411.3	1.51	22.7
	1.626666667	
411.4	1.57	26
411.5	1.85	28.1
411.6	1.71	28.8
	1.71	
411.7	1.57	25.4
411.8	2.12	27.8

411.9	1.86	29.5
	1.85	
417.1	3.94	37.4
417.2	3.67	40
417.3	3.13	31.1
	3.58	
417.4	3.35	33.1
417.5	3.63	36.6
417.6	3.8	38.2
	3.593333333	
417.7	3.04	32.1
417.8	2.68	28.6
417.9	3.37	30.1
	3.03	
641.1	3.03	31.6
641.2	2.4	25.8
641.3	2.56	26.4
	2.663333333	
641.4	2.82	26.2
641.5	2.76	26.3
641.6	2.5	27.4
	2.693333333	
641.7	2.77	29.1
641.8	2.36	25.2
641.9	2.57	28.5
	2.566666667	
642.1	2.56	26.4
642.2	3.6	31.9
642.3	2.7	25.6
	2.953333333	
642.4	2.96	30.9
642.5	3.31	30.8
642.6	2.68	28.3
	2.983333333	
642.7	3.39	31.2
642.8	3.57	31.5
642.9	3.38	33.7
	3.446666667	
643.1	3.78	38.5
643.2	4.57	40.4
643.3	4.5	39.3
	4.283333333	
643.4	4.06	45

643.5	4.34	43.9
643.6	4.69	44.1
	4.363333333	
643.7	4.11	40.5
643.8	4.09	41.9
643.9	4.53	42.3
	4.243333333	
644.1	3.09	35
644.2	3.23	33.5
644.3	3.21	33.8
	3.176666667	
644.4	2.65	28.1
644.5	2.53	29.8
644.6	2.58	31.7
	2.586666667	
644.7	3.61	39
644.8	2.82	34
644.9	2.71	33.6
	3.046666667	
780.1	2.54	35.3
780.2	1.21	18.8
780.3	2.12	33.3
	1.956666667	
780.4	3.45	33.3
780.5	1.27	16.7
	2.36	
932.1	3.05	28.3
932.2	2.95	26.1
932.3	3.01	27.9
	3.003333333	
932.4	2.87	25.7
932.5	2.9	24.6
932.6	1.27	10.2
	2.346666667	
932.7	3.03	26.6
932.8	2.79	21.2
932.9	2.73	25.6
	2.85	

Samples	**Freq. of CD8+**	**CD8 Proliferation**
384.1	0	0

384.2	0	0
384.3	0	0
	0	
384.4	0	0
384.5	0	0
384.6	3.12	40
	1.04	
384.7	0	0
384.8	0	0
384.9	17.6	75
	5.866666667	
394.1	0	0
394.2	7.41	40
394.3	3.12	50
	3.51	
394.4	0	0
394.5	0	0
394.6	0	0
	0	
394.7	0	0
394.8	0	0
394.9	0	0
	0	
395.1	3.87	23.1
395.2	3.93	24.4
395.3	3.41	21.5
	3.736666667	
395.4	2.03	14.1
395.5	2.61	20.9
395.6	2.85	22.5
	2.496666667	
395.7	4.63	29.6
395.8	3.55	19.4
395.9	3.95	25.9
	4.043333333	
396.1	2.04	28.6
396.2	0	0
396.3	3.57	40
	1.87	
396.4	2.11	33.3
396.5	1.48	40
396.6	1.28	25
	1.623333333	

396.7	0	0
396.8	0	0
396.9	0	0
	0	
397.1	1.73	15.2
397.2	2.16	19
397.3	2.23	17.9
	2.04	
397.4	0.93	11.1
397.5	1.66	14.9
397.6	1.56	16.7
	1.383333333	
397.7	2.05	20.3
397.8	2.57	20
397.9	2.18	19
	2.266666667	
402.1	2.6	47.6
402.2	1.29	40
402.3	2.89	47.6
	2.26	
402.4	1.16	33.3
402.5	1.25	28.6
402.6	0.88	33.3
	1.096666667	
402.7	3.2	50
402.8	5.96	47.4
402.9	1.04	20
	3.4	
407.1	3.27	42.9
407.2	2.9	28
407.3	1.14	23.1
	2.436666667	
407.4	1.6	20.8
407.5	1.87	22.2
407.6	3.18	50
	2.216666667	
407.7	2.32	23.5
407.8	1.69	21.4
407.9	3.28	29.5
	2.43	
408.1	1.47	10.7
408.2	2.3	19.6
408.3	2.86	19.3

	2.21	
408.4	0.93	8.7
408.5	1.73	11.1
408.6	1.95	13.8
	1.536666667	
408.7	3.01	21.6
408.8	2.73	18.1
408.9	3.27	23.7
	3.003333333	
412.1	4.56	22.4
412.2	2.98	16.3
412.3	4.3	21.8
	3.946666667	
412.4	4.17	21.5
412.5	4.87	24.1
412.6	5.14	26.4
	4.726666667	
412.7	5.17	24.2
412.8	9.21	41.9
412.9	3.4	18.1
	5.926666667	
418.1	0	0
418.2	1.3	15.8
418.3	0.42	4.55
	0.573333333	
418.4	0.83	20
418.5	1.02	16.7
418.6	0.65	9.09
	0.833333333	
418.7	0	0
418.8	1.68	16
418.9	1.43	16.7
	1.036666667	

Samples	**Freq. of CD8+**	**CD8 Proliferation**
381.1	2.68	15.8
381.2	3.22	20.3
381.3	2.62	18.9
	2.84	
381.4	2.08	13.9
381.5	2.04	12.8
381.6	2.44	15.6

	2.186666667	
381.7	2.37	15.1
381.8	2.62	16.1
381.9	2.13	13.7
	2.373333333	
382.1	0	0
382.2	0.25	50
382.33	0.97	5.38
	0.406666667	
382.4	0.15	25
382.5	0.21	20
382.6	0.16	50
	0.173333333	
382.7	0.15	12.5
382.8	0	0
382.9	0.29	33.3
	0.146666667	
383.1	1.27	6.93
383.2	1.23	6.97
	1.25	
383.4	0.66	4.57
383.5	0.83	5.84
383.6	0.93	5.95
	0.806666667	
383.7	0.73	4.76
383.8	0.78	4.98
383.9	1	6.41
	0.836666667	
385.1	0.73	5.29
385.2	1.89	11.8
385.3	3.41	40
	2.01	
385.4	0.82	6.19
385.5	1.73	13.6
385.6	0.35	2.73
	0.966666667	
385.7	1.25	8.64
385.8	1.51	12.5
385.9	0.22	1.72
	0.993333333	
386.1	1.7	14.5
386.2	2	17.6
386.3	2.22	18.8

	1.973333333	
386.4	1.55	16.3
386.5	2.33	22.3
386.6	1.93	18.4
	1.936666667	
386.7	2.35	19.5
386.8	3.08	25.4
386.9	2.46	21.6
	2.63	
391.1	0	0
391.2	0.94	8.33
391.3	0	0
	0.313333333	
391.4	0	0
391.5	3.85	50
391.6	0	0
	1.283333333	
391.7	2	33.3
391.8	0.63	8.33
391.9	0	0
	0.876666667	
392.1	0	0
392.2	0	0
392.3	0	0
	0	
392.4	0	0
392.5	0	0
392.6	0	0
	0	
392.7	0	0
392.8	0	0
392.9	0	0
	0	
403.1	1.64	16.7
403.2	0.66	8.51
403.3	2.29	37.5
	1.53	
403.4	1.39	17.9
403.5	0.63	7.14
403.6	2.73	26.3
	1.583333333	
403.7	2.45	21.2
403.8	1.54	18.4

403.9	0.79	8
	1.593333333	
405.1	0.46	6.17
405.2	0.77	10.5
405.3	0	0
	0.41	
405.4	0.52	7.81
405.5	0.37	7.84
405.6	0.28	4.48
	0.39	
405.7	0.32	6.67
405.8	0.66	12
405.9	1.1	16.7
	0.693333333	
406.1	0.51	4.76
406.2	0	0
406.3	0	0
	0.17	
406.4	0	0
406.5	0	0
406.6	0	0
	0	
406.7	0	0
406.8	0	0
406.9	0	0
	0	

Samples	**Freq. of CD8+**	**CD8 Proliferation**
390.1	0	0
390.2	0	0
	0	
390.4	0	0
	0	
390.7	0	0
390.8	0	0
	0	
393.1	3.49	40
393.2	0.64	14.3
393.3	2.52	30
	2.216666667	
393.4	0.56	12.5
393.5	2.87	55.6

393.6	1.24	22.2
	1.556666667	
393.7	5.91	68.8
393.8	2.13	37.5
393.9	2.04	50
	3.36	
413.1	0	0
413.2	2.69	26.3
413.3	3.36	33.3
	2.016666667	
413.4	2.11	42.9
413.5	4.41	85.7
413.6	3.47	58.3
	3.33	
413.7	2.25	29.4
413.8	2.46	41.2
413.9	2.75	33.3
	2.486666667	
419.1	4.02	33.3
419.2	4.42	36.6
419.3	4.66	42.4
	4.366666667	
419.4	3.84	34.2
419.5	4.93	40.7
419.6	2.79	32.4
	3.853333333	
419.7	3.54	32.4
419.8	6.06	50.9
419.9	3.05	30.7
	4.216666667	
926.1	0	0
926.2	0	0
926.3	0	0
	0	
926.4	0	0
926.5	4.35	100
926.6	0	0
	1.45	
926.7	0	0
926.8	3.7	50
926.9	0	0
	1.233333333	

Samples	Freq. of CD8+	CD8 Proliferation
345.1	0.4	6.37
345.2	0.58	15.1
345.3	0.44	10.9
	0.473333333	
345.4	0.37	10.4
345.5	0.21	4.81
345.6	0.47	7.69
	0.35	
345.7	0.64	13.1
345.8	0.42	8.43
345.9	0.3	5.77
	0.453333333	
347.1	0.18	3.42
347.2	0.28	6.44
347.3	0.33	7.1
	0.263333333	
347.4	0.18	3.29
347.5	0.15	3.03
347.6	0.2	3.7
	0.176666667	
347.7	0.055	3.64
347.8	0.36	5.8
347.9	0.22	6.02
	0.211666667	
363.1	0.23	4.49
363.2	0.24	3.97
363.3	0.47	8.1
	0.313333333	
363.4	0.25	4.03
363.5	0.25	5.73
363.6	0.14	2.14
	0.213333333	
363.7	0.39	5.71
363.8	0.37	5.61
363.9	0.25	3.75
	0.336666667	
364.1	0.37	5.3
364.2	0.41	4.78
364.3	0.32	4.21
	0.366666667	

364.4	0.38	3.27
364.5	0.23	2.07
364.6	0.38	3.15
	0.33	
364.7	0.63	5.88
364.8	0.44	3.51
364.9	0.45	3.51
	0.506666667	
365.1	0	0
365.2	0	0
365.3	0	0
	0	
365.4	0	0
365.5	0.27	5.88
365.6	0.44	16.7
	0.236666667	
365.7	0	0
365.8	0	0
365.9	0	0
	0	
366.1	0	0
366.2	0	0
366.3	0	0
	0	
366.4	0	0
366.5	0	0
366.6	0.11	3.45
	0.036666667	
366.7	0.11	5.88
366.8	0	0
366.9	0	0
	0.036666667	
374.1	0.28	2.3
374.2	0.26	2.33
374.3	0.35	3.34
	0.296666667	
374.4	0.47	5.24
374.5	0.18	1.48
374.6	0.49	5.52
	0.38	
374.7	0.52	5.3
374.8	0.34	3.94
374.9	0.21	2.14

	0.356666667	
375.1	0.2	1.83
375.2	0.31	2.85
375.3	0.1	1
	0.203333333	
375.4	0.22	2.39
375.5	0.21	2.37
375.6	0.094	1.16
	0.174666667	
375.7	0.48	5.41
375.8	0.071	0.63
375.9	0.22	3.05
	0.257	

Samples	**Freq. of CD8+**	**CD8 Proliferation**
331.1	3.24	36.6
331.2	2.55	35.4
	2.895	
331.4	2.95	36.3
331.5	2.46	32.2
	2.705	
331.7	3.26	37
331.8	2.63	31.8
	2.945	
336.1	3.94	35.5
336.2	4.3	42.2
336.3	4.39	41.6
	4.21	
336.4	3.57	33.2
336.5	3.55	34.4
336.6	3.75	41.7
	3.623333333	
336.7	3.62	34.9
336.8	4.43	40
336.9	4.71	52.3
	4.253333333	
337.1	3.33	33.3
337.2	2.53	23.8
337.3	2.44	26.3
	2.766666667	
337.4	2.42	24.1
337.5	2.18	22.3

337.6	1.96	22.1
	2.186666667	
337.7	3.51	58.6
337.8	2.99	26
337.9	2.17	27.3
	2.89	
340.1	2.31	36.6
340.2	2.81	43.7
340.3	1.81	29.3
	2.31	
340.4	1.96	29.4
340.5	2.23	34.5
340.6	1.35	29.7
	1.846666667	
340.7	2.6	45.8
340.8	1.44	33.3
340.9	1.24	23
	1.76	
344.1	3.21	42.5
344.2	2.88	50
344.3	2.37	28.4
	2.82	
344.4	1.83	25.9
344.5	2.82	38.9
344.6	2.16	37.9
	2.27	
344.7	1.8	31
344.8	1.38	23.4
344.9	2.28	36
	1.82	
346.1	3.76	45.7
346.2	3.74	42.6
346.3	3.38	38.3
	3.626666667	
346.4	3.28	34.4
346.5	2.83	32.1
346.6	2.46	32.6
	2.856666667	
346.7	3.05	38.8
346.8	3.36	38.6
346.9	3.03	34.8
	3.146666667	
367.1	6.25	34.1

367.2	6.16	35.9
367.3	8.32	47.7
	6.91	
367.4	6.5	37.9
367.5	6.1	35.6
367.6	6.48	38.5
	6.36	
367.7	7.6	42.5
367.8	6.76	38.5
367.9	6.75	44.7
	7.036666667	
414.1	7.85	69.7
414.2	6.68	68.6
414.3	6.83	67.9
	7.12	
414.4	6.52	49
414.5	7	70.4
414.6	6.42	74.8
	6.646666667	
414.7	7.82	72.8
414.8	7.19	70.3
414.9	5.88	67.7
	6.963333333	

Samples	**Freq. of CD8+**	**CD8 Proliferation**
330.1	3.99	48
330.2	1.65	25.3
330.3	3.01	35.8
	2.883333333	
330.4	2.78	43.3
330.5	3.51	59.4
330.6	3.09	35.5
	3.126666667	
330.7	1.71	16.3
330.8	2.5	24.8
330.9	1.78	17.7
	1.996666667	
332.1	2.25	19.3
332.2	2.37	20.9
332.3	2.22	22.6
	2.28	
332.4	2.11	23.4

332.5	1.79	22.9
332.6	2.28	22.7
	2.06	
332.7	2.54	29.7
332.8	2.9	26.8
332.9	0.22	2.06
	1.886666667	
333.1	3.07	35.4
333.2	1.76	32
333.3	2.04	26.6
	2.29	
333.4	0.27	5.08
333.5	2.33	31.2
333.6	1.97	25.2
	1.523333333	
333.7	2.96	33.8
333.8	2.2	27.1
333.9	2.81	41.6
	2.656666667	
334.1	2.51	25.4
334.2	4.55	51.4
334.3	5.61	53.1
	4.223333333	
334.4	2.86	28.9
334.5	3.95	47.4
334.6	3.29	41.1
	3.366666667	
334.7	4.39	48.4
334.8	3.76	50.2
334.9	3.82	46.8
	3.99	
335.1	8.18	68.4
335.2	5.48	53.2
335.3	7.18	69.3
	6.946666667	
335.4	7.75	68.1
335.5	6.23	59.4
335.6	8.96	74.9
	7.646666667	
335.7	2.67	56.6
335.8	6.57	61.5
335.9	7.36	73.6
	5.533333333	

338.1	2.61	35.1
338.2	2.49	37.8
338.3	2.84	50.2
	2.646666667	
338.4	2.8	46.4
338.5	0.89	11.7
338.6	2.96	37.9
	2.216666667	
338.7	3.33	39.6
338.8	2.63	31.4
338.9	2.63	31.6
	2.863333333	
339.1	5.8	48.8
339.2	5.58	40.6
339.3	5.61	44.4
	5.663333333	
339.4	5.36	48.6
339.5	7.58	56.1
339.6	6.15	51
	6.363333333	
339.7	7.47	57.6
339.8	6.26	53
339.9	6.08	49.8
	6.603333333	
343.1	3.81	52.1
343.2	3.13	51.5
343.3	2.25	42.5
	3.063333333	
343.4	3.39	63.2
343.5	2.88	50.6
343.6	3.56	58.3
	3.276666667	
343.7	2.55	35.6
343.8	2.11	36.3
343.9	5.03	68.9
	3.23	
350.1	3.4	77.8
350.2	4.75	80.6
350.3	3.67	68.1
	3.94	
350.4	3.58	77.3
350.5	3.87	80.3
350.6	3.2	71.4

	3.55	
350.7	3.93	75.9
350.8	4.9	71.3
350.9	3.12	64.1
	3.983333333	
357.1	3.26	57.1
357.2	4.14	39.8
357.3	8	74.3
	5.133333333	
357.4	6.41	70.4
357.5	6.3	71.1
357.6	5.46	69.2
	6.056666667	
357.7	7.53	75.9
357.8	9.01	79.9
357.9	6.87	71.7
	7.803333333	
358.1	2.91	36.9
358.2	2.39	33
358.3	2.65	33.8
	2.65	
358.4	2.44	34.1
358.5	3.18	37.8
358.6	2.52	28.7
	2.713333333	
358.7	3.5	36.6
358.8	1.14	10.4
358.9	0.37	4.89
	1.67	
359.1	2.64	38.8
359.2	1.47	22.9
359.3	2.1	31.7
	2.07	
359.4	2.1	32.9
359.5	3.71	56.9
359.6	2.68	45.7
	2.83	
359.7	1.55	21.6
359.8	1.82	26
359.9	1.96	27.7
	1.776666667	
361.1	0.61	8.6
361.2	0.5	7.6

361.3	0.24	3.74
	0.45	
361.4	0.39	5.43
361.5	0.36	5.1
361.6	3.88	50.2
	1.543333333	
361.7	3.69	45.2
361.8	3.37	41.6
361.9	3.14	39.7
	3.4	
368.1	7.28	55.2
368.2	6.87	50.9
368.3	6.44	51.3
	6.863333333	
368.4	6.16	51.3
368.5	5.74	41.7
368.6	5.26	47.3
	5.72	
368.7	3.52	28.1
368.8	6.75	50.6
368.9	4.14	31.8
	4.803333333	
369.1	5.64	43.9
369.2	5.86	47.1
369.3	4.94	42.1
	5.48	
369.4	6.19	57
369.5	7.29	62.1
369.6	6.99	59
	6.823333333	
369.7	5.3	48.6
369.8	5.64	51.3
369.9	5.82	47
	5.586666667	
370.1	0.39	7.73
370.2	0.23	6.6
370.3	0.19	4.1
	0.27	
370.4	0.17	4.08
370.5	0.58	17.3
370.6	0.14	3.5
	0.296666667	
370.7	0.3	6.82

370.8	0.31	8.28
370.9	0.29	6.99
	0.3	
420.1	7.8	68.2
420.2	9.06	71.9
420.3	7.91	62.7
	8.256666667	
420.4	4.44	47
420.5	5.81	52
420.6	5.62	50
	5.29	
420.7	6.69	63.9
420.8	5.48	57.3
420.9	6.07	50.8
	6.08	
421.1	5.92	65.9
421.2	3.64	54.7
421.3	4.09	66.7
	4.55	
421.4	4.98	68.4
421.5	5.35	72.1
421.6	3.21	62.6
	4.513333333	
421.7	4.91	62.3
421.8	4.03	54.4
	4.47	

APPENDIX V: WESTERN BLOT DATA AND K7M2 CULTURE DATA

Western Blot Pictures

Loading Gel

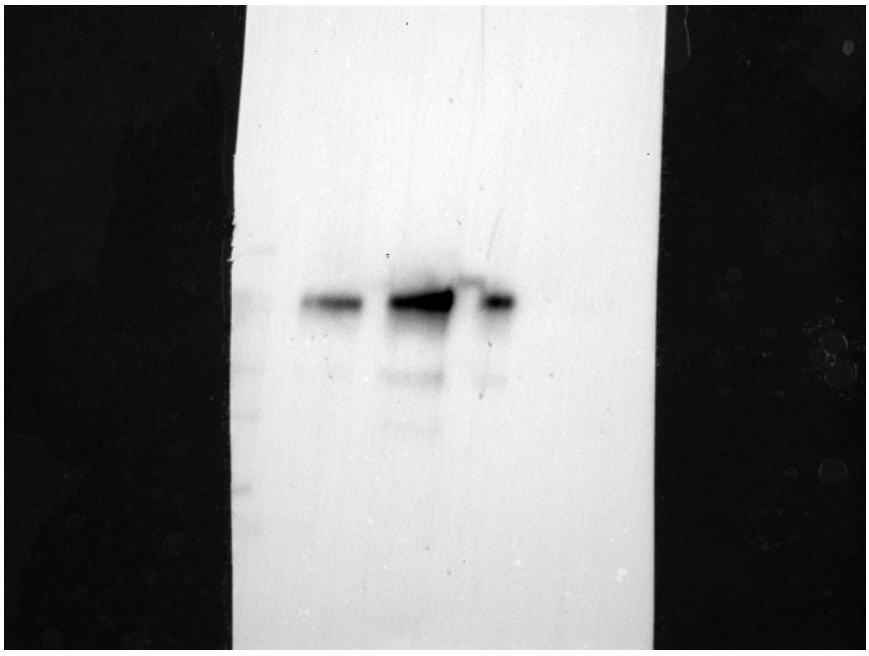

Allograft Serum

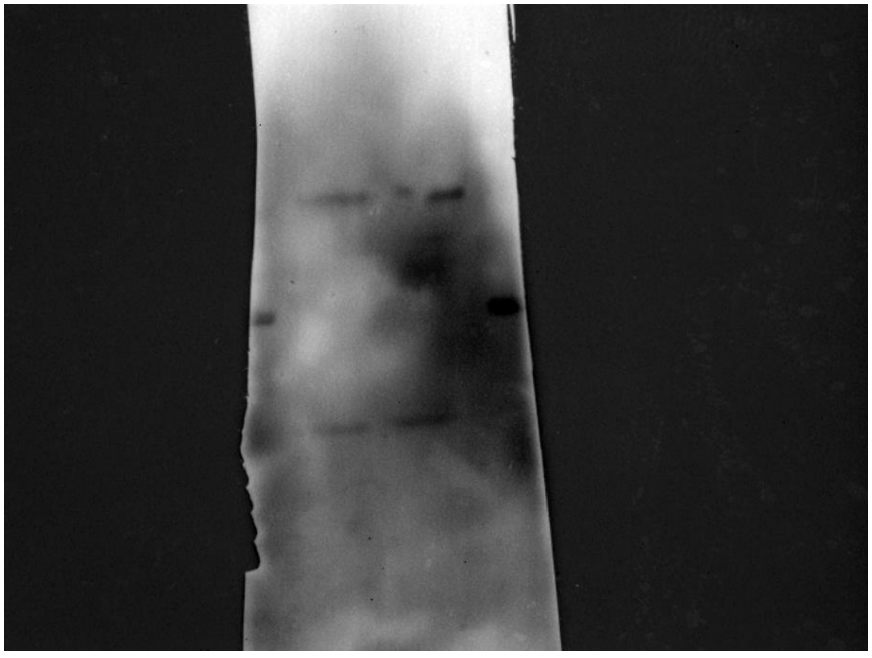

Autograft Serum

K7M2 Cell Culture

Cells + Allo Serum 1_100.fcs	197	15.1
Cells + Allo 1_50.fcs	229	18
Cells + Auto 1_50.fcs	80.9	6.69
Cells + Auto 1_100.fcs	92.8	6.58
Cells+ CTL Serum 1_100.fcs	70	9.22
Cells.fcs	12.7	1.02
Mean	114	9.44
SD	82.3	6.2

	Mean FITC Intensity	Antibody Bound
Cells.fcs	12.7	1.02
Cells+ CTL Serum 1_100.fcs	70	9.22
Cells + Allo Serum 1_100.fcs	197	15.1
Cells + Auto 1_100.fcs	92.8	6.58

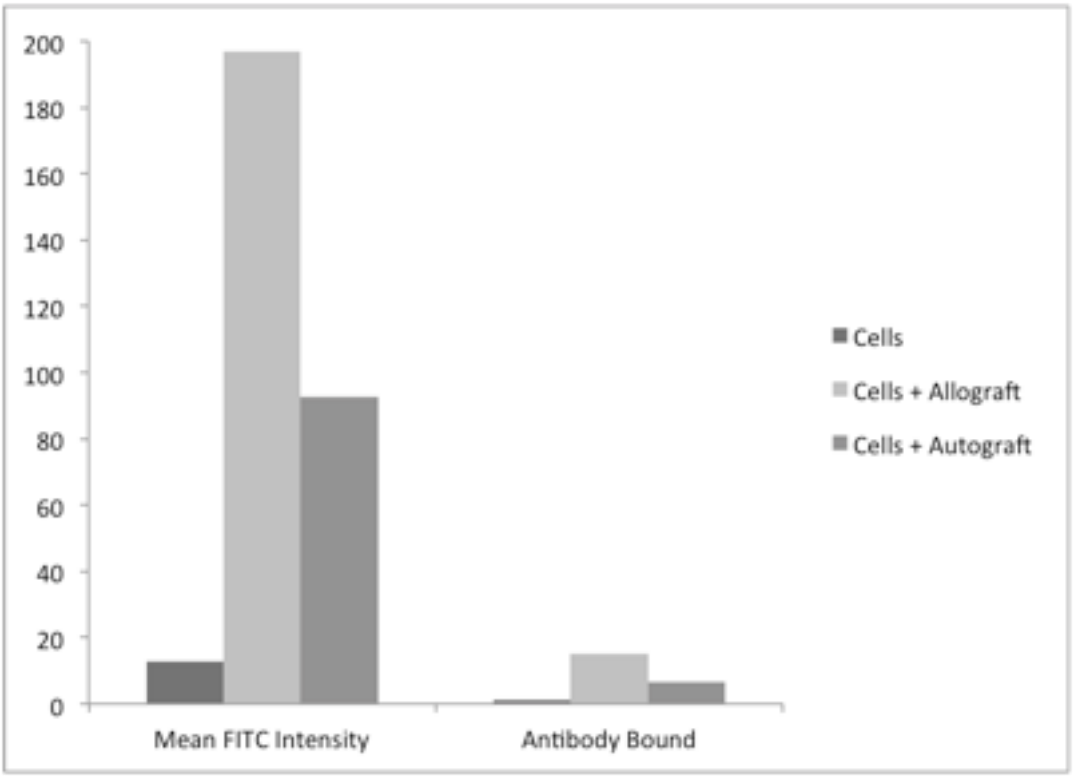
200
180
160
140
120
100
80
60
40
20
0
Mean FITC Intensity
Antibody Bound
Cells
Cells + Allograft
Cells + Autograft